THE EFFECTIVE INTERACTIONS AND DEFORMATIONS IN 1d-2s AND 1f-2p SHELLS

A thesis

submitted to

THE MAHARAJA SAYAJIRAO UNIVERSITY OF BARODA

for the degree of DOCTOR OF PHILOSOPHY in PHYSICS

by

D.R. KULKARNI,

Physical Research Laboratory,

Navrangpura, Ahmedabad-9

APRIL 1972

PREFACE

There are two major problems in nuclear structure calculations. One concerns the knowledge of the two-body interaction operating between the nucleons inside the nucleus. Other relates to the solution of the many-body Schrodinger equation. In a way, both the problems are mutually dependent in the sense that the knowledge of the two-body interaction will pave the way for the solution of the many-body problem. In fact various schemes and methods for solving the many-body problem have been devised, each one stressing one or the other aspect of the two-body interaction. As we are interested in the deformation of nuclei, we mainly concentrate on the field-producing properties of the two-body interactions which cause these deformations and work in the formalisms based on these properties. The deformed Hartree-Fock (HF) formalism is one which met with considerable success in describing the properties of deformed nuclei. On the other hand there is a SU_3 group theoretical model due to Elliott which can give rise to rotational spectra which are so characteristic of all axially deformed nuclei. The success of this model should be explained in terms of the nature of real two-body effective interaction.

The success or failure of a particular interaction in any particular case cannot be explained easily unless one

makes a detailed study of the important constituents of the interaction. It is known that as the nuclear interactions are short-ranged, the interactions in the state of relative angular momentum l=0 of two nucleons form the dominant part of the interaction. These interactions are called 's' state interactions. Therefore it seems to be of great importance to study the properties of 's' state interactions.

The work presented in this thesis has been motivated by two different considerations. The first consideration deals with the understanding of the nature of the effective interaction. Second consideration tries to seek the proper formalism to describe the excited states which do not belong to the ground state band.

In the beginning we have briefly reviewed the most important and relevant developments in Nuclear Physics in the context of the work presented here and also described its scope and motivation at some length.

T Then we have studied the SU_3 properties of different radial matrix elements of the nuclear interaction in general and 's' state integrals in particular, both in the 1d-2s and 1f-2p shells. This study enables us to understand the success of the SU_3 scheme in the 1d-2s shell and it also clearly brings out the limitation of this scheme as we go to 1f-2p shell.

Later we have discussed the properties of 's' state interactions in HF formalism in the 1d-2s shell. Not only these properties can throw light on the behaviour of a particular interaction, but also they provide clues to use these model interactions to produce the desired effects.

We have also made the detailed analysis of the two-body effective interactions in the 1f-2p shell. The whole interaction is expressed in the basis of SU_3 scheme. This analysis reveals that the effective two-body interaction in the 1f-2p shell is dominantly q.q type and the absence of well-developed spectra in the 1f-2p shell is mainly due to the unfavourable sequence of single particle energies.

As a part of the study of the effective interactions, we have studied the effects of core-excitations in both HF and SU_3 formalisms. The study is made in the 1d-2s shell. The results are discussed in the light of the conclusions reached in the previous chapters.

Finally we have applied the generator coordinate method to calculate the ^{20}Ne spectrum by using the constrained HF states as basis. The results thus obtained compare quite well upto 18 MeV with those obtained from exact shell model calculations.

Later we have discussed the properties of 's' state interactions in HF formalism in the 1d-2s shell. Not only these properties can throw light on the behaviour of a particular interaction, but also they provide clues to use these model interactions to produce the desired effects.

We have also made the detailed analysis of the two-body effective interactions in the 1f-2p shell. The whole interaction is expressed in the basis of SU_3 scheme. This analysis reveals that the effective two-body interaction in the 1f-2p shell is dominantly q.q type and the absence of well-developed spectra in the 1f-2p shell is mainly due to the unfavourable sequence of single particle energies.

As a part of the study of the effective interactions, we have studied the effects of core-excitations in both HF and SU_3 formalisms. The study is made in the 1d-2s shell. The results are discussed in the light of the conclusions reached in the previous chapters.

Finally we have applied the generator coordinate method to calculate the ^{20}Ne spectrum by using the constrained HF states as basis. The results thus obtained compare quite well upto 18 MeV with those obtained from exact shell model calculations.

Acknowledgments

The author wishes to express with gratitude his sincere indebtedness to Professor S.P. Pandya for introducing him to the subject, for his inspiring and valuable guidance and for the constant encouragement throughout the course of this work. It is a great pleasure to thank Dr. K.H. Bhatt and Dr. S.B. Khadkikar for their fruitful collaboration and many stimulating and enlightening discussions which have always led him to better understanding of the results. He would like to thank Dr. J.C. Parikh for some useful discussions, comments and suggestions. Thanks are also due to Dr. (Miss) M.S. Shah for her interest in the work and for some discussions in the initial phase of this work.

He would like to express his thanks to Dr. E.C. Halbert and Dr. J.B. McGrory of Oak Ridge National Laboratory, for providing him the shell model results of ^{20}Ne for different interactions. Also he is thankful to Dr. M.R. Gunye of Tata Institute of Fundamental Research for few discussions and important suggestions in computer programming.

He would like to take this opportunity to thank Mr. S.R. Thakore, the Head of the Computer Division, PRL for providing him liberal computer facilities. Thanks are also due to all the members of the computer division, PRL,

especially the programmers Mr. P.S. Shah, Mr. I.V. Vayeda, Mr. C.J. Rathod and Mr. S.B. Barve for the help and cooperation they have extended to him during the course of this work.

The author would be failing in his duty if he fails to record his sincere thanks to Late Professor Vikram A. Sarabhai, the Director, PRL, not only for providing him the opportunity to work in this laboratory but also for partially financing his trip to Italy to attend the Nuclear Theory Course at International Centre for Theoretical Physics, Trieste. The financial support from the Ministry of Education, Government of India, is also gratefully acknowledged.

Finally he would like to thank Mr. K. Venugopalan for his careful and neat typing of this thesis.

CONTENTS

ooo

CHAPTER I

Introduction.

The theory of nuclear structure poses two major problems. One relates to the knowledge of the interaction operating between two nucleons inside the nucleus. The second problem is concerned with the solution of many-body Schrodinger equation. In a way, these two problems are inter-dependent. The solution of the first problem cannot be obtained unless one can solve the second problem at least approximately, if not exactly. On the other hand the nature of the interaction has a direct bearing on the possible solutions of the many-body system. The present thinking regarding the nature of the inter-particle interaction is based on the following arguments. The nuclear physics which is essentially a low-energy physics deals with non-relativistic systems and hence the mesonic degrees of freedom of inter-particle interactions can be suppressed leading to the concept of an inter-nucleon potential. The potential which can form a stable and strongly bound nuclear system is considered to be overall attractive and short-ranged. It is further assumed that this potential is a two-body potential. Apart from this, currently accepted models of the potential contain exchange terms, as well as non-central terms like tensor, spin-orbit etc. Such models are quite complex, and several of them seem equally acceptable for nuclear structure studies. Thus even though we have a good feeling for the qualitative aspects of nuclear interactions,

we do not have a unique knowledge of its form, strength etc. As far as the exact solution of the many-body system is concerned, one knows that it is a mathematically complex task and therefore needs to be solved through appropriate approximations about the behaviour of the system.

Historically these problems have been tackled in the following way. It was assumed that the nucleons in the bound nuclear system are moving approximately independently of each other in an average potential field created by the presence of all other particles. This assumption gives rise to what is called an 'independent particle model'. The development of shell model which essentially specifies the form of the average potential to be used in the independent particle picture has approximately solved the second problem. Mayer and Jensen[1] first suggested that the form of the average potential is that of a spherically symmetric harmonic oscillator well. The actual shell-model potential is generally written[2] as

$$H_0 = \left(\frac{p^2}{2m} + \frac{1}{2} m\omega^2 r^2 \right) + \kappa \vec{l} \cdot \vec{s} + \beta \vec{l} \cdot \vec{l}$$

The term in the bracket on r.h.s denotes the usual spherical harmonic oscillator potential. The second term corresponds to the single particle spin-orbit interaction and the third term corresponds to the interaction of the orbit

with itself, first introduced by Nilsson[3]. It can be shown that a proper choice of parameters of this Hamiltonian gives rise to the desired shell-structure which successfully explains the magic numbers corresponding to stable nuclei and can also predict correctly the spins and magnetic moments of nuclei with one valence particle. This initial success enhanced the faith in shell model. Later such shell model calculations were further extended to nuclei with more than one valence particles.

The philosophy of shell model calculations for nuclei with more than one valence particles is briefly stated as follows. The nucleons in the nucleus are divided into two groups, the core nucleons and the valence nucleons. The core is assumed to be inert so far as the properties of low-lying states of nuclei are concerned. In other words the assumption implies that the core has total angular momentum $J=0$, total isospin $T=0$ as well as zero magnetic moment, quadrupole moment etc. This means that the properties of low-lying states of nucleus emerge only from the interplay of valence particles interacting through the 'residual interaction'. The valence particles can occupy single particle states in a given 'configuration space'. The mixing of different configurations will be through residual interaction. The two-body matrix elements of the residual interaction which result in the coupling of two configurations enter as input information in shell model calculations. In brief, one may say that the procedure of shell model calculations

consists of constructing a Hamiltonian matrix for a given residual interaction in a given configuration space, which is subsequently diagonalised giving us various energy eigen values and corresponding eigen functions.

It will be noticed that the advent of shell model has modified the first problem slightly. What is now required in the framework of shell model is the residual interaction in a chosen configuration space and not the actual free nucleon-nucleon (N-N) interaction. In fact the shell model assumes that the main part of the total N-N interaction has been absorbed in the average shell model potential which generates the basis states required for complicated shell-model calculations. To find a residual interaction which is weak enough to justify a first order perturbation treatment over basis states is the new problem in the framework of shell model. Needless to say, the form and nature of this interaction would be a function of configuration space used for shell model calculations. It also presumably depends on the number of valence particles. Therefore the residual interaction is the 'effective interaction' between a number of active valence nucleons in a limited configuration space of single particle states.

In early years, various[2] shell model calculations were performed with simple residual interactions using different coupling schemes. The 'intermediate coupling' scheme is preferred to L-S or j-j coupling schemes. A pure central force

produces L-S coupling while a pure spin-orbit force produces j-j coupling. As the nuclear interaction contains both the ingredients, it is supposed to produce the 'intermediate coupling'. It should be pointed out however that there is no rule for constructing an 'intermediate coupled' state other than by the full diagonalisation of the energy matrix in L-S or j-j coupling basis states.

The form of residual interaction was still unknown in early days and hence a phenomenalogical approach was adopted. There are three ways of parameterising the effective interaction. One[4] is to assume some analytical form of the interaction (shape, range, depth, exchange nature etc.) and fit its parameters so as to get the best possible agreement with observed energy levels and other nuclear properties. The second way[5] is to treat all the two-body matrix elements of the effective interaction required in the calculations as parameters and fit them to get the observed energy level schemes. This method has a limited scope and can be used only when the number of two-body matrix elements involved is small. Alternatively the third method[6] is very useful. In this method the number of two-body matrix elements (to be treated as free parameters) is reduced by expressing them in terms of a small set of radial matrix elements. This expression is simple and practical if the nuclear interaction is assumed to be central. Another advantage of this method is that no explicit radial dependence of

the interaction needs to be assumed. These parameters or radial matrix elements are again fitted to get the best possible agreement with observed nuclear energy levels. The shell model calculations have been usually performed using a j-j coupling scheme and all the three methods for the residual interactions. The dramatic success of such calculations revealed two major points. Firstly the assumption of an independent particle model and the consequent existance of a single-particle potential seem to have been amply justified. Secondly, with a suitable degree of configuration mixing and an appropriate choice of two-body effective interactions, it is possible to explain and predict a large body of experimental information on nuclei.

Apart from the phenomenological approach there are other fundamental approaches to understand the two-body effective interactions. It can be argued that microscopic considerations should lead to this effective interaction from the observed N-N interaction, as abstracted from N-N scattering data and the deuteron data. The interactions derived by analysing scattering data are called the 'realistic interactions'. Many such potentials are now available in the literature[7]. Usually such interactions are singular in nature (i.e. contain infinite repulsion at short distance). Therefore they cannot be used in the shell model calculations directly. An effective interaction can however be extracted from these singular realistic potentials using Brueckner-Bethe-Goldstone[8] formalism.

Several such calculations are available in the literature[9].

Some attempts[10] have also been made to derive the 'realistic interactions' from field theoretical point of view. Although there does not exist a completely satisfactory field theoretical derivation of nuclear interactions, some semi-field theoretical considerations have been used in deriving such interactions. The long-ranged part of the interaction which is relatively weak is now known to result from exchange of the well known π meson, while the short-ranged part of the interaction for which multiple meson exchange effects become important is treated phenominologically. The one boson exchange potentials (OBEP) are the results of such phenomenological calculations in which the effects of multiple meson exchange at short distances are simulated by the exchange of different types of heavy bosons.

Soon it was realised that the shell model calculations for nuclei with more than two valence nucleons is a prohibitively complicated job. The size of the Hamiltonian matrix to be constructed increases very rapidly as the number of valence nucleons and the configuration space become larger and larger and even big computers cannot handle the situation beyond a certain limit. Shell model calculations with six valence particles in the configuration space containing three single particle levels (for example in 1d-2s shell) have been reported[11]. Similar calculations[12] for nuclei with more than

6 particles could be done only using some scheme for truncating the configuration space. All these calculations however reveal a very important fact that the relatively simple shell model whenever practicable reproduces all the features of the nuclear level schemes and other properties reasonably well.

As stated above, the shell model calculations are not feasible when the number of valence nucleons and the configuration space are both large. Therefore one has to find out some other methods of solving the many-body problem in nuclear physics. Many schemes and methods have been proposed stressing one or the other important characteristic of two-body interactions. The importance of pairing interaction is stressed in the 'seniority scheme'[13]. The later development of Bardeen-Cooper-Schriffer (BCS) formalism[14] which is essentially a variational formalism is also based on the dominance of pairing in two-body interaction. The more sophisticated development in this direction is the self-consistent formalism generally known as Hartree-Fock-Bogolyubov (HFB) formalism[14].

On the other hand, the success of the collective model of Bohr and Mottelson indicated the dominance of the field-producing components in the two-body interaction. The self-consistent way of taking into account the field-producing part of the interaction is the well-known 'deformed Hartree-Fock' formalism[15] Further, the symmetry considerations of the nuclear Hamiltonian introduced the use of group theoretical methods in nuclear

structure calculations. The 'SU_3' scheme[16] of Elliott, which essentially diagonalises the dominant field-producing component Q.Q of the interaction, has been quite successful in study of the deformed nuclei in 1d-2s shell. Since the work we will be presenting here concerns mainly with the study of the deformed nuclei, we will describe the 'SU_3 scheme' of Elliott and 'deformed Hartree-Fock' formalism a little more elaborately in the following paragraphs.

1. SU_3 Scheme

The SU_3 scheme is devised to find the eigenfunctions and eigenvalues of the many-body system in the frame work of shell model. This job can be very well simplified, if we study the symmetry properties of the nuclear Hamiltonian under consideration. In other words, if the Hamiltonian itself is invariant under some group, the eigen functions of such a Hamiltonian belong to one of the irreducible representations of that group and the eigen values can be found analytically. The nuclear many-body problem has been tackled using such group theoretical methods. The SU_3 scheme developed by Elliott is one of such methods based on the invariance of nuclear Hamiltonian under SU_3 transformation group.

The nucleons are fermions and hence the nuclear wave functions must be antisymmetric with respect to exchange of all coordinates of any two nucleons. That is to say that the

nuclear many-body wave functions belong to the antisymmetric representation of the permutation symmetry group. The SU_3 scheme assumes that the nuclear forces are independent of spin and isospin states of nucleons. Therefore the nuclear wave functions are characterized by space coordinates only. These wave functions, therefore, can be classified according to the irreducible representations of permutation group S_k(k = no. of particles). It is well known that the classification according to irreducible representations of S_k is equivalent to that according to the irreducible representations of the group of all the unitary transformations between 's' single-particle bases i.e. the group U_s. Further it was shown by Jouch and Hill[17] that a spherical harmonic oscillator Hamiltonian in three dimensions commutes with the operators of the group U_3. Therefore the eigen functions of harmonic oscillator are labelled by the irreducible representation of U_3 and there is a degeneracy of functions belonging to the same representations. The functions which transform according to an irreducible representation of U_3 also transform according to an irreducible representation of SU_3. Thus the spatial many-body wave functions in a given major oscillator shell transform according to a definite irreducible representation of permutation and SU_3 groups. Further it was shown that R_3 is a subgroup of SU_3. This implies that the wave functions can be further classified according to the irreducible representations of R_3. Thus the wave function in this scheme can be written as

$|[f](\lambda\mu)\ L\rangle$ where $[f]$ denotes the permutation symmetry, $(\lambda\mu)$, SU_3 symmetry and L, R_3 symmetry. The details of this scheme are given by Elliott[16] and Banerjee and Levinson[18]. The next task is to show that this many-body SU_3 wave function is an eigen function of the Hamiltonian. In other words we must find out the Hamiltonian which can be diagonalised by SU_3 wave functions. Elliott[16] has shown that the two-body interaction

$$V = (1/4)\ (Q.Q) + 3(L.L) \qquad \text{where } Q = \sum_{i=1}^{N} q_i$$

will be diagonalised by the SU_3 wave functions. In other words V will not mix states of different SU_3 symmetry $(\lambda\mu)$. But the wave functions have also good angular momentum L. Therefore they will diagonalise the term (L.L) and hence the term Q.Q is also diagonal with the eigen values

$$Q.Q \quad = C\ (\lambda\mu) - 3\ L\ (L + 1)$$

where $C(\lambda\mu)$ is the eigen value of the Casimir operator for the SU_3 representation $(\lambda\mu)$. Thus the energies of states of a given $(\lambda\mu)$ symmetry but with different L values will follow the rotational sequence $L(L + 1)$.

Elliott has done calculations in 1d-2s shell with this model. He could get good agreement with the observed spectra in 1d-2s shell by adjusting the strength of central interactions.

It was shown by Elliott that the 'L' states projected from SU_3 intrinsic states corresponding to maximum eigen value of Casimir operator give good agreement with the low-lying states of nuclei. Moreover it was also found convenient to use the state of 'maximum weight' of a given SU_3 representation for calculation of low-lying spectra of nuclei. The state of 'maximum weight' is defined as that state which has a maximum (or minimum) quadrupole moment. It was further observed that the SU_3 representation of highest eigen value of Casimir operator belongs to the highest space symmetric representation. This is expected as the nuclear forces are short ranged and consequently their contribution to the anti-symmetric states in space is much smaller compared to that of the symmetric states in space.

This scheme is somewhat rigid in the sense that it demands strict symmetry to be obeyed by the nuclear Hamiltonian. The assumption underlying this scheme is that the nuclear forces have Wigner's supermultiplet symmetry[19] and further that they are of q.q type. The success of this model implies that the two-body effective interaction indeed has dominantly such properties. However the two-body interaction also contains non-central parts like tensor and spin-orbit interactions and also various multipoles other than quadrupole. Further the model required complete degeneracy of single particle orbits of a major oscillator shell, whereas actually one requires a one-body spin-orbit interaction to explain the magic numbers observed in

the periodic table. All these terms will violate the SU_3 symmetry and will try to mix different irreducible representations of SU_3. As a result SU_3 scheme cannot be an exact scheme and very detailed and sophisticated nuclear structure calculations do show up departures from it; however, it can certainly provide a good guideline to such calculations.

To summarise we say that the SU_3 sehcme provides a basis in which a dominant part of the residual interaction is already diagonal. The natural extension of this scheme is to do the configuration mixing calculations in SU_3 basis. But such calculations are much more complicated than the usual shell model calculations. However the beauty of Elliott's SU_3 scheme lies in the fact that it has built-in rotation in its formalism and does not introduce the classical concepts like rotation, deformation etc.

2. HF formalism

Before the advent of Hartree-Fock formalism in nuclear physics, several collective models were in vogue. They owed their origin to collective features such as the rotational spectra, the enhanced E_2 transitions and the large quadrupole moments exhibited by nuclei especially in the rare earth region. Bohr and Mottelson[20] argued that these effects are caused by collective motions of many nucleons, since such features cannot be explained in terms of the single particle shell model. They

proposed that the nuclei can be deformed and execute some collective motions like vibrations and rotations. Their model could successfully explain the above collective features. Later they unified the collective model with the single particle model and gave a unified model of nucleus. They proposed that the nuclei have some deformed equilibrium shape and the valence nucleons move independently in this deformed potential well. In addition these nuclei also execute the collective motions. They further argued that the frequencies of the collective motions of nucleus are such that this motion can be easily decoupled from the motion of the single particles in the deformed field. This is what is called 'the adiabatic approximation'. This approximation enables us to write the total nuclear wave function as a product of the collective wave function and the intrinsic wave function of the particles. Later Nilsson[3] provided the intrinsic wave functions using the Q_o^2 deformation field. Though the unified model was successful in a large number of applications it has two inherent defects. It is a macroscopic model and does not involve the explicit use of the two-body interaction. Theoretically it is not satisfactory as it introduces 3 redundant collective coordinates for describing the nuclear system.

An alternative approach to study the collective features (which is not open to such criticism) is the HF theory of nuclear structure. This is a microscopic theory as it uses the two-body

interaction explicitly. The projection technique of Peierls and Yoccoz[21] has removed the second objection of redundant collective coordinates. The HF theory is essentially aimed at extracting the single particle potential and nuclear deformations from the two-body interaction. This is done usually by a variational method. The actual procedure involves finding out suitably deformed single particle wave functions by minimising the total energy in a given configuration space. The resultant deformation depends on the interaction that is employed and also on the number of particles in the intrinsic states. The good angular momentum states are then projected from such a deformed intrinsic state. The structure of these states has been found[22] to be in good agreement with the low-lying shell model states.

It should be remembered here that the shell model in its fullest generality (i.e. including configuration mixing in large space) contains in principle a full description of nuclear properties and therefore is theoretically capable of handling all collective features. But as the computational labour involved is tremendous, we have to invoke the HF approximation along with projection technique. Therefore the validity of HF approximation can be assessed by comparing the HF results with the exact shell model results. There is a reason to believe that the projected HF states would be in agreement with the low-lying shell model states. When we try to minimise the

energy of the intrinsic state, we are essentially increasing the proportion of low-lying states contained in the intrinsic states. At present the HF theory has been well established in nuclear structure calculations[22] of light nuclei. This theory provides an approximation to the shell model configuration mixing calculations and simplifies them to a great extent. This simplification comes essentially through the assumption that the intrinsic state of the nucleus is suitably described by a single determinantal wave function. The validity of this assumption is closely related to the largeness of the HF gap (i.e. gap between the highest occupied and the lowest unoccupied HF single particle states) in N=Z even nuclei. When the projected states of the nucleus from a single determinantal HF intrinsic state do not have a good overlap with the shell model states, it is quite likely that the above assumption is not valid for that particular nucleus. The next step in such cases is to perform the configuration mixing calculations in the basis of HF intrinsic states. These calculations as in SU_3 scheme are quite cumbersome and therefore may not be preferred to exact shell model calculations.

It may be noted that one to one correspondence between the collective model and the HF formalism seems as yet to be not very clear. But it can be shown that the adiabatic approximation in the collective model is the classical limit of the projection formulae of Peierls and Yoccoz when the

deformation is very large. Also the comparison of HF theory and SU_3 scheme will make a very interesting study. Both the theories give intrinsic states from which states of good angular momentum can be projected. Whereas the SU_3 scheme works only if the potential is spin-independent and central (Q.Q type) in character, the HF theory can work with any well behaved potential including spin-dependence. Thus HF theory seems to be extension to the SU_3 scheme. In fact Harvey[23] has shown that for spin-independent potentials both the approaches are equivalent. The above considerations lead us to assume that for central potentials the SU_3 scheme and HF scheme will lead to essentially the same collective states. With spin-dependent potentials however the two schemes will deviate in their prescriptions for generating the lowest collective states. One should not be surprised at the similarity of the HF and SU_3 schemes in the absence of spin-dependent forces. We know that the HF procedure picks out the field effects from a given potential and these are necessarily of a long range character. At the same time it should be noted that one of the dominant terms of a long-range potential has the Q.Q form which is closely associated with the Casimir operator SU_3. This explains the similarity of both the schemes in the absence of spin-dependent potentials.

Further the calculations of the nuclei in which there is excess of neutrons over protons showed that the HF is not a

good approximation for such nuclei and a single determinantal description does not hold good for them. The excess of neutrons gives rise to short-range correlations which can not be taken into account by HF formalism. Such pairing correlations in T=1 states can be well taken care of by HFB formalism. It was further shown[24] that T=0 pairing correlations are also equally strong and should be taken into account for better description of nuclei.

The HF formalism as now developed is meant only for the description of states belonging to ground state band and is therefore incapable of giving description of excited states that are not part of the ground band. The variational procedure of this theory cannot be applied to them. One often looks for other minima of HF calculations with different symmetries and takes them as intrinsic states for generating excited states. Therefore the study of excited states in the HF framework deserves special care. The excited states may also alternatively be projected from the excited bands which can be obtained by particle-hole excitations over the HF ground state. This is in fact the configuration mixing calculations in the basis of intrinsic states obtained by particle-hole excitations over the HF ground state. Such an approximation is known as Tamm-Dancoff approximation. It will be a good approximation provided the HF gap is large. This allows up to ignore the contributions from many particle-many hole excitations to the lowest excited bands.

A few such calculations[25] have been reported.

An alternative method to obtain excited levels in the nuclear spectra is the generator coordinate method, suggested by Hill and Wheeler[26]. They proposed that the wave function of a nucleus could be written as an integral over the collective variable (generator coordinate) of the collective wave function times the intrinsic part, which may be taken as an independent particle wave-function evaluated as a function of the collective variable. A simple illustration of this method is the projection formalism of obtaining states of good angular momentum from the HF intrinsic state. This formalism is just a particular case of the generator coordinate method with the angle of rotation of the symmetry axis as a generator coordinate. To obtain additional levels in the nuclear spectra, we generalise this method by using the deformation of intrinsic state itself as an additional generator coordinate. The intrinsic states of different deformations are obtained by driving the HF solution by an external quadrupole Q_0^2 field. Thus we get an improved ground band as well as the excited states not belonging to ground band. We have applied this method (for the first time)to obtain excited states not belonging to the ground state band. A comparison of the result with those of exact shell model calculations is satisfactory, thus vindicating this rather simple method and at the same time revealing the underlying collective nature of the shell model

spectra. The method of generator coordinate as explained above has much wider applicability than the complex shell model calculations due to its simplicity.

3. Scope of this thesis

The work that is presented in this thesis has been motivated by two considerations. The first consideration is that of the interparticle interactions. Various effective interactions have been used with HF models and they more or less yield similar results. The success or failure of an interaction in any particular case cannot be explained easily. To do this one needs to study the detailed structure of the effective interactions. That is to say that the important ingredients which constitute the two-body interaction should be isolated and their properties should be studied separately. It is well known that the two-body residual interaction is dominantly central in character. The two-body matrix elements of a central interaction can be expressed as linear combinations of diagonal radial integrals. These radial integrals in 1d-2s shells are fitted[27] to obtain the best possible agreement with the observed energy levels of Oxygen and Fluorine isotopes. It was observed that of all the radial integrals, the radial integrals corresponding to the state of relative angular momentum l=0, are dominant ones. The interaction that acts in the state of relative angular momentum l=0 is called 's' state interaction. Thus 's' state interactions

are the most important ingredients of the total interaction in 1d-2s shell. Therefore it seems meaningful to undertake a detailed study of 's' state interactions. This study will presumably threw some light on the behaviour of the nuclei.

With this view in mind we have investigated the properties of such interactions both in SU_3 scheme as well as in HF formalism. On the basis of the properties of these interactions, one can explain not only the success of the SU_3 scheme of Elliott but also show the limitations of the scope of this SU_3 model. We also explain the success of HF formalism, in general, in the beginning of 1d-2s shell. We can predict whether a HF approximation is good approximation in a given nucleus. In chapter two, we present the study of the properties of radial integrals in SU_3 scheme[28]. The results for both 1d-2s and 1f-2p shells are presented. In chapter three, we present the properties of 's' state interactions in HF formalism. The results are presented for 1d-2s shell in which the calculations are performed for several N=Z even nuclei by using different 's' state interactions. The results of HF calculations are compared with the shell model calculations wherever they are available. In chapter four we have analysed in detail the effective two-body interaction in 1f-2p shell given by Kuo and Brown[30]. The complete interaction has been analysed[31] in the SU_3 scheme. The absence of well-developed rotational character in 1f-2p shell can be explained on the basis of this analysis and the role of single-particle energies. In chapter five we studied the effects of core-

excitations both in SU_3 scheme and in HF formalism. The two-body effective interaction given by Kuo[32] in 1d-2s shell has been used. The calculations are performed using bare (without core-excitations) and renormalised (with core-excitation) interactions. The effect of core-excitations in 1f-2p shell are also studied and compared with those in 1d-2s shell.

The second part of this work deals with the description of excited bands of states. As the HF formalism is inadequate to study the excited bands of states, the Tamm-Dancoff approximation has been used to calculate the excited states of ^{20}Ne and ^{19}F. The renormalised interaction of Kuo[32] has been used for this purpose. The K=0 and K=2 bands of ^{20}Ne and the K=3/2 band of ^{19}F were calculated and the states of good angular momentum were projected from these bands. The results thus obtained show that a considerable band mixing is required before we can get a reasonably good agreement with shell model results. However due to limited computer facility available to us, we could not carry out these calculations completely and therefore these results are not included in the thesis.

In chapter six we have employed the generator coordinate method to obtain ^{20}Ne spectrum. The interaction used is again the renormalised interaction of Kuo[32]. The generator coordinate used is Q_0^2 which drives the solution of ^{20}Ne to different deformations. Three points are used for calculations. The

results thus obtained compare very well with those obtained by exact shell model calculations.

It is appropriate at this stage to mention that most of the programming part of these calculations, right from the simple Clebsch-Gordan coefficients to the projection of good angular momentum states is done by me. The preliminary work has been done on IBM 1620 computer at Physical Research Laboratory, Ahmedabad while most of the detailed calculations are done on CDC 3600/160A computer system installed at Tata Institute of Fundamental Research, Bombay.

REFERENCES

1) M.G. Mayer and J.H.D. Jensen, Elementary theory of Nuclear Shell Structure, John Wiley and Sons, New York, 1955.

2) J.P. Elliott and A.M. Lane, Handbuch der Physik, 39 (1957) and the references therein.

3) S.G. Nilsson, Mat. Fys. Medd. Dan. Vid. Selsk. 29, No.16 (1955).

4) i) J.P. Elliott and B.H. Flowers, Proc. Roy. Soc. A229 (1955) 536.

ii) L. Rosenfeld, Nuclear Forces, North-Holland Publishing Co., Amsterdam, 1948.

5) i) I. Talmi, Rev. Mod. Phys. 34 (1962) 704.

ii) P. Federman and I. Talmi, Phys. Lett. 19 (1965) 490.

6) S.P. Pandya, Nucl. Phys. 43 (1963) 636.

7) i) T. Hamada and T.D.Johnston, Nucl. Phys. 34 (1962) 383.

ii) Lassila, Hull, Ruppel, MacDonald and Breit, Phys. Rev. 126 (1962) 881.

iii) F. Tabakin, Ann. Phys. 30 (1964) 51.

8) i) H.A. Bethe and J. Goldstone, Proc. Roy. Soc. A238 (1957) 551.

ii) K.A. Brueckner, and J.L. Gammel, Phys. Rev. 109 (1958) 1023.

iii) H.A. Bethe, Phys. Rev. 103 (1956) 1353.

9) i) T.T.S. Kuo and G.E. Brown, Nucl. Phys. 85 (1966) 40.

ii) D.M. Clement and E.U. Baranger, Nucl. Phys. A108 (1968) 27.

iii) C.M. Shakin, Y.R. Waghmare and M.H. Hull, Phys. Rev. 161 (1967) 1006.

10) i) A.E.S. Green and T. Sawada, Rev. Mod. Phys. 39, (1967) 594.

ii) G. Breit, Proceedings of International Conference on properties of Nuclear States, Montreal, 1969, p.293.

11) E.C. Halbert, J.B. McGrory, B.H. Wildenthal and S.P. Pandya, "Advances in Nuclear Physics" Vol. 4, edited by M. Baranger and E. Vogt (Plenum Press, New York, 1971).

12) i) A. Arima, S. Cohen, R.D. Lawson and M.H. Macfarlane, Nucl. Phys. A 108 (1968) 94.

ii) J.B. McGrory and B.H. Wildenthal, Phys. Lett. 34 B (1971) 373.

iii) S.K.M. Wong and A.P. Zuker, Phys. Lett. 36 B (1971) 437.

13) De-Shalit and I. Talmi, Nuclear Shell Theory (Acadamic Press Inc., New York) 1963.

A.M. Lane Nuclear theory (W.A. Benjamin Inc. 1964).

14) M. Baranger, Cargese Lectures in theoretical physics, W.A. Benjamin, New York, 1962.

15) i) I. Kelson and C. Levinson, Phys. Rev. 134B (1964) 269.
ii) I. Kelson, Phys. Rev. 132 (1963) 2189.
See also reference 22.

16) i) J.P. Elliott, Proc. Roy. Soc. A245 (1958) 128, 562.
ii) M. Harrey and J.P. Elliott, Proc. Roy. Soc. A272 (1963) 557.

17) J.M. Jouch and E.L. Hill, Phys. Rev. 57 (1940) 641.

18) M.K. Banerjee and C.A. Levinson, Phys. Rev. 130 (1963) 1036.

19) E.U. Wigner, Phys. Rev. 51 (1937) 106.

20) A. Bohr and B.R. Mottelson, Mat. Fys. Medd. Dan. Vid. Selsk, 27 (1953) 16.

21) R.E. Peierls and J. Yoccoz, Proc. Roy. Soc. 70A (1957) 381.

22) G. Ripka, Advances in Nuclear Physics Vol. I edited by M. Baranger and E. Vogt (Plenum Press, 1968).

23) M. Harvey, Advances in Nuclear Physics, Vol. I edited by M. Baranger and E. Vogt (Plenum Press, 1968).

24) i) H.T. Chen and A. Goswami, Phys. Lett. 24B (1967) 257.
ii) J. Bar-Tauv, A. Goswami, A.L. Goodman and G.L. Struble, Phys. Rev. 178 (1969) 1670.

iii) H.H. Wolter, A. Faessler and P.U. Sauer, Phys. Lett. 31B (1970) 516.

25) S.N. Tewari, Phys. Lett. 29B (1969) 5.
L. Satpathy, Phys. Rev. 174 (1969).

26) D.L. Hill and J.A. Wheeler, Phys. Rev. 89 (1953) 1102.

27) i) Cohen, R.D. Lawson and S.P. Pandya, Nucl. Phys. A114 (1968) 541.

ii) S. Cohen, E.C. Halbert and S.P. Pandya, Nucl. Phys. A114 (1968) 353.

28) D.R. Kulkarni and S.P. Pandya, Nuovo Cim. 60B (1969) 100.

29) D.R. Kulkarni and S.P. Pandya, Nuovo Cim. Lett. 4 (1970) 133.

30) T.T.S. Kuo and G.E. Brown, Nucl. Phys. A114 (1968) 241.

31) D.R. Kulkarni and K.H. Bhatt to be published.

32) T.T.S. Kuo, Nucl. Phys. A103 (1967) 71.

CHAPTER II

SU_3 properties of Radial Integrals

II.1 Introduction

The calculations of Elliott[1] for 1d-2s shell nuclei based on SU_3 scheme confirmed that even in complicated nuclei, the SU_3 classification seems to be quite useful in giving a qualitative description of the spectra. The success of this scheme in turn substantiated the underlying assumption that the effective two-body interactions in 1d-2s shell is dominantly (Q.Q) in character. In the shell model studies of such nuclei, several different interactions have been used[2] and the wave functions generated by such interactions always appear to have large overlaps with exact SU_3 symmetric eigenfunctions. In other words, when the wave functions obtained by diagonalising Hamiltonian matrices are analysed in terms of orbital and SU_3 symmetries, one particular SU_3 symmetry component appears to be quite dominant. This has generally led to the conclusion that in the effective interactions valid for the 1d-2s shell, the quadrupole force is quite dominant and hence the approximate SU_3 symmetric structure of the wave functions. It may be useful to look at the origin of this SU_3 symmetry from a somewhat different view point. Cohen[3] et al. have shown that the effective interaction in 1d-2s shell can be very well parameterised in terms of radial matrix elements in relative orbital angular momentum states. These radial matrix elements are essentially the

components of central interactions. Therefore it seems necessary to study the SU_3 properties of these radial matrix elements separately so that one can explain the success of SU_3 scheme for a given interaction in terms of these radial matrix elements. This study will also enable us to predict how far this scheme will be useful in other shells.

II.2 Radial Integrals

The calculations of two-body matrix elements of a central interaction is a comparatively easy job in the harmonic oscillator basis. In this basis the two-body wave functions can be decomposed in the relative and centre-of-mass coordinates using the following transformations.

$$\vec{r} = \vec{r}_1 - \vec{r}_2 \quad , \quad \vec{R} = \frac{\vec{r}_1 + \vec{r}_2}{2} \qquad (1)$$

The decomposition is of immense value in simplifying the calculations as generally the nuclear interactions depend only on the relative distance . The transformation brackets for going to relative and centre-of-mass coordinates are given by Brody and Moshinsky[4]. The expression for two-body matrix elements of central interactions can be given as follows.

$$\langle j_1 j_2 | V | j_3 j_4 \rangle_{JT}$$

$$= N_1 N_2 \sum_{L,S,n,\ell,n'} \left[1 - (-1)^{\ell+S+T}\right] \times 2 \times A \begin{Bmatrix} \ell_1 & \frac{1}{2} & j_1 \\ \ell_2 & \frac{1}{2} & j_2 \\ L & S & J \end{Bmatrix} \times \qquad (2)$$

$$A \begin{Bmatrix} \ell_3 & \frac{1}{2} & j_3 \\ \ell_4 & \frac{1}{2} & j_4 \\ L & S & J \end{Bmatrix} \langle n\ell N\Lambda L | n_1\ell_1 n_2\ell_2 \rangle \langle n\ell N\Lambda L | n_3\ell_3 n_4\ell_4 \rangle$$

$$\langle n\ell | V(r) | n'\ell' \rangle$$

where curly brackets A denote the normalised nine-j symbols for transforming the wave functions from j-j to L-S coupled wave functions. The terms $\langle n\ell N\lambda L \mid n_1\ell_1 n_2\ell_2\rangle$ denote the Moshinsky brackets for transformation to relative and centre-of-mass coordinates where n,l and N, λ are quantum numbers describing orbital motion for relative and c.m. coordinates respectively. The quantity $\langle n\ell \mid V_c(r) \mid n'\ell\rangle$ is a radial matrix element and depends on the radial dependence of the given interaction. N_1 and N_2 are the normalisation coefficients for bra and ket sides of the matrix elements. For example N_1 is given as

$$\frac{1}{\sqrt{2(1+\delta_{j_1 j_2})}}$$

It should be noted that in the expression (2), if all the states j_1, j_2, j_3 and j_4 belong to the same major shell, the radial matrix element becomes diagonal i.e. $n = n'$. We denote these diagonal radial matrix elements as $I_{nl} = \langle n\ell \mid V_c(r) \mid n\ell\rangle$ So the expression (2) in the single major shell can be written as

$$\langle j_1 j_2 \mid V_c \mid j_3 j_4\rangle_{JT} = \sum_{n,\ell} a(n\ell, LS, JT)\, I_{n\ell} \qquad (3)$$

The coefficients a(nl, LS, JT) incorporate all the geometrical factors like nine-j symbols, Brody-Moninsky brackets and so on. In general the two-body interaction is spin-isospin dependent. Therefore the strength of the interactions is different in four

Table II.1

Various states of two body wave functions

State	S	T	Relative 'l' values.
Singlet-Even	0	1	Even
Triplet-odd	1	1	Odd
Singlet-odd	0	0	Odd
Triplet-even	1	0	Even

spin-isospin states. Table 1 gives explicity the four interactions.

The fact that interaction depends on spin and isospin makes the radial matrix elements dependent on S and T values. But the S and T values restrict the possible values of relative angular momentum l due to antisymmetrization. Therefore the radial integral is now characterised by either S or T and l value. We define the radial matrix element as

$$\langle n\ell \mid V_c(r) \mid n\ell \rangle_S = I_{n\ell S} = \int_0^\infty R^*_{n\ell}(r)\, V_S(r)\, R_{n\ell}(r)\, dr \qquad (4)$$

The expression (3) is now rewritten as

$$\langle j_1 j_2 \mid V_c(r) \mid j_3 j_4 \rangle_{JT} = \sum_{n,\ell,S} a(n\ell, LS, JT)\, I_{n\ell S} \qquad (5)$$

The expression (5) shows that the calculation of two-body matrix elements of a central interaction essentially involves the evaluation of geometrical factors a(nl, LS, JT) and the radial integrals I_{nls}. The geometrical factors for a given shell can be calculated once for all, but I_{nls} should be calculated each time for interactions with different radial dependences. It has now become clear that two-body matrix elements of a central interaction in a given major shell can be expressed as a linear combination of I_{nls}. These different I_{nls} seem to be good candidates for the parameterization of any effective interaction. Moreover physically I_{nls} show the strength of the effective interaction when the two particles are in states of relative angular momentum l and radial quantum number n. This approach also permits a built-in state dependence of the effective interaction, a flexibility that largely compensates for the restrictive assumption of a central interaction. The importance of radial integrals as the most relevent and physically significant parameters has been strongly advocated by Pandya[5]. It can also be seen that in this approach the number of empirical parameters characterising the interaction is much smaller than a complete set of two-body matrix elements. Further, the more detailed theories of nuclear structure that relate the two-body matrix elements in nuclei to realistic nuclear forces (e.g. the calculations of Kuo and Brown[6]) also calculate essentially as an intermediate step the same set of parameters and hence a direct and meaningful comparison of the empirical values derived from more fundamental theories is immediately

available

It should then be of considerable interest to examine the symmetries of the various parameters I_{nls} individually, particularly with reference to the SU_3 group. The empirical analysis of Cohen[3] et al. as well as calculations of Kuo and Brown[6] with the Hamada-Johnstone potential or those of Shakin et al.[7] with Yale potential show that the reduced matrix elements in relative 's'(l=0) states are indeed dominant and would already provide a good approximation to the level schemes of nuclei. The importance of 's' state interactions indeed reflects the fact that the nuclear forces are short-ranged. Table 2 gives different radial integrals encountered in 1p, 1d-2s and 1f-2p major shells. Table 3 gives the strength of different radial integrals for both T=0 and T=1 states obtained by Cohen et al[3] by fitting the energy levels of O and F isotopes. We study the properties of s state interactions in particular and will give a rule based on group theoretical considerations for the SU_3 properties of any radial integral in general.

II.3 SU_3 scheme for nuclei

Before Elliott[1] proposed the SU_3 scheme for 1d-2s shell nuclei, many attempts were made to classify the many-particle wave functions using group theoretical methods. The states of the configuration $(l)^k$ were classified uniquely under the group $U_{2l+1} \supset R_{2l+1} \supset R_3$. Similarly attempts[9] were also made to classify

Table II.2

Radial integrals in different shells

shell	Radial Integrals I_{nl}
1p	I_{0s}, I_{1s}, I_{0d} I_{0p}
1d-2s	I_{0s}, I_{1s}, I_{2s}, I_{0d}, I_{1d}, I_{0g} I_{0p}, I_{1p}, I_{0f}
1f-2p	I_{0s}, I_{1s}, I_{2s}, I_{3s}, I_{0d}, I_{1d}, I_{2d}, I_{0g}, I_{1g}, I_{0i} I_{0p}, I_{1p}, I_{2p}, I_{0f}, I_{1f}, I_{0h}.

Table II.3

Radial Integrals (see Cohen et al[2]) in 1d-2s shell

Parameters	T=0 (MeV)	T=1 (MeV)
$I_{0s} + I_{0g}$	-9.51	-8.89
$I_{0s} + I_{1d}$	-10.86	-8.01
$I_{0s} + I_{2s}$	-14.03	-13.33
I_{1s}	-8.12	-2.52
I_{0d}	-	0.07
$I_{0p} + I_{0f}$	-	2.21
$I_{0p} + I_{1p}$	-	-0.85

the states of the configuration $(j)^k$ under the groups $U_{2j+1} \longrightarrow {}^{S}p_{2j+1} \longrightarrow R_3$. It was observed[10] that the $(1)^k$ configuration in 1p shell gives rise to rotational spectra in L-S coupling scheme, though the rotational character is not particularly noticeable in the spectra because of low cuf-off, the effect of spin-orbit forces and the wide spacing of the levels in ^{12}C and ^{8}Be. A similar study in pure 1d shell reveals no such features but since in the realistic shell model for nuclei, 1d and 2s shells are close in energy, they are expected to mix strongly. It is therefore expected that the rotations will again appear when the configurations are mixed. But for such mixing of 2s and 1d levels, the usual scheme $U_6 \longrightarrow R_6 \longrightarrow R_3$ does not classify the states uniquely. Therefore the sub-group SU_3 was proposed. This group is useful whenever we want to consider the mixing of degenerate levels of a harmonic oscillator in a major given shell. In fact this group is intimately connected to the degeneracies of the oscillator levels and also gives rise to rotational features.

i) The generators of SU_3 scheme

It was shown by Jouch and Hill[11] that a spherical oscillator Hamiltonian in n dimensions commutes with the operators of group U_n so that the eigenvalues are labelled by the irreducible representation of U_n and there is a degeneracy of functions belonging to the same representations. Thus U_3 is the symmetry group of three-dimensional oscillator, the oscillator number N

being simply the representation lable (N, 0, 0) of U_3. The generators of this symmetry group U_3 may be expressed either in cartesian form or in spherical tensor form. We give below the generators in spherical tensor form following the notations of Banerjee and Leninson[12].

Consider a single-particle Harmonic oscillator Hamiltonian

$$H = \frac{p^2}{2m} + \frac{1}{2} m\omega^2 r^2$$

Also introduce the operators that annilitate the energy quanta

$$U_{\pm 1} = \mp \frac{1}{\sqrt{2}\,b}\left[(x \mp iy) + \frac{i}{\hbar} b^2 (p_x \mp i p_y)\right]$$

$$U_0 = \frac{1}{\sqrt{2}\,b}\left(z + \frac{i}{\hbar} b^2 p_z\right) \qquad (6)$$

Similarly the operators that create the energy quanta are just the hermitian conjugate of annililation operators. These operators, have usual commutation rules. The harmonic oscillator Hamiltonian can be written as

$$H = \frac{3}{2}\hbar\omega + \hbar\omega \sum_{\mu} U_\mu^+ U_\mu \quad \text{where} \quad \mu = \pm 1, 0$$

It can be further shown that the product operators $(U_\mu^+ U_\mu)$ generate the group U_3. Moreover since the form of the commutation rules is invariant under any linear transformation of the operators, any nine linear combinations of $(U_\mu^+ U_\mu)$ also generate the group U_3. We select as generators the following linear combinations.

$$
\begin{aligned}
H &= \tfrac{3}{2}\hbar\omega + \hbar\omega \sum_{\mu} U^{+}_{\mu} U_{\mu} \\
L_{\pm 1} &= \mp \left(U^{+}_{0} U_{\mp 1} + U^{+}_{\pm 1} U_{0} \right) \\
L_{0} &= U^{+}_{1} U_{1} - U^{+}_{-1} U_{-1} \\
Q_{\pm 2} &= -\sqrt{6}\; U^{+}_{\pm 1} U_{\mp 1} \\
Q_{\pm 1} &= -\sqrt{3} \left(U^{+}_{0} U_{\mp 1} - U^{+}_{\pm 1} U_{0} \right) \\
Q_{0} &= 2 U^{+}_{0} U_{0} - U^{+}_{1} U_{1} - U^{+}_{-1} U_{-1}
\end{aligned}
\qquad (7)
$$

The first of these nine operators is again the harmonic oscillator hamiltonian and is a scalar. It also commutes with L_μ and Q_μ since it commutes with all $(U^{+}_{\mu} U_{\mu})$. The next three operators are the components of orbital angular momentum, which also generate the group R_3. The U_3 group contains R_3 as subgroup. The five operators Q_μ are related to the quadrupole distortion.

The commutation relations of the eight operators L_μ and Q_μ show that they generate a sub-group of U_3 formed by nine generators given in expression (7). This sub-group of U_3 generated by L_μ and Q_μ is SU_3, the group of three dimensional matrices with determinant unity. An irreducible representation (IR) of this group is characterized by two numbers $(\lambda\ \mu)$.

ii) Intrinsic SU_3 states

Suppose that we have k particles in a major harmonic oscillator

shell with degenerate single particle levels. Firstly in the absence of spin-isospin dependent forces the system of k particles can be characterised by IR $[f]$ of unitary group $U_n = \sum_i (2l_i + 1)$ and l_i is the angular momentum of i^{th} single particle level in a major shell. These states are further classified by IR $(\lambda \mu)$ of SU_3. The reduction of $U_n \rightarrow SU_3$ is obtained by using the chain procedure involving the use of dimensionality arguments. This procedure is described by Harvey[12]. Further in order to distinguish those states which belong to the same $[f]$ and $(\lambda \mu)$ representations, we note that the operators Q_o and L_o commute with each other and do not join the states of different $[f]$ and $(\lambda \mu)$. Hence these operators can be simultaneously diagonalised and their eigenvalues ϵ and k used to characterize the states. At the same time it is possible to consider new linear combinations of operators $L_{\pm 1}$, $Q_{\pm 1}$, and $Q_{\pm 2}$ which act as step operators with respect to L_o and Q_o. These operators will change the simultaneous eigenvalues of L_o and Q_o. Elliott[1] has shown that one more quantum number is necessary in order to distinguish the states of same eigenvalues of both L_o and Q_o. He showed that it is possible to form a group which is like R_3 such that its generators are expressed in terms of step operators. The Casimir operator Λ^2 of this group will provide one more number to specify the state of k particles. Moreover the Casimir operator Λ^2 of this new group commutes with L_o and Q_o, and does not connect the states of different $[f]$ and $(\lambda \mu)$. Therefore the k-particle state in a major harmonic oscillator shell can be written as

$$\Phi [[f], (\lambda \mu), \epsilon, k, \Lambda]$$

The allowed values of ϵ , k and $\wedge$ for the various IR of SU_3 have been determined by Elliott[1]. For a given $(\lambda\ \mu)$, ϵ may assume the values

$$\epsilon = (2\lambda+\mu),\ (2\lambda+\mu+3)\ \text{- - - - - -},\ (-\lambda-2\mu)$$

while for each value of ϵ , $\wedge$ takes the values

$$\frac{1}{6}\left|(2\lambda-2\mu-\epsilon)\right|,\ \frac{1}{6}\left|(2\lambda-2\mu-\epsilon)\right|+1,$$

$$\text{- - - -}\ \text{Min}\left[\frac{1}{6}\left|(2\lambda+4\mu-\epsilon)\right|,\ \frac{1}{6}\left|(4\lambda+2\mu+\epsilon)\right|\right]$$

and for a given $\wedge$

$$k = 2\wedge,\ 2\wedge-2,\ \text{- - - - - - -}\ (-2\wedge)$$

The state with $(\epsilon, k) = (\epsilon_{max}, k_{max}) = (2\lambda+\mu, \mu)$ is called the state of highest weight in the irreducible representation (λ, μ).

Also a bilinear Casimir operator G for the SU_3 group can be found. The eigen-value of this Casimir operator associated with the irreducible representation $(\lambda\ \mu)$ of SU_3 can be given by an analytical expression.

$$\langle G \rangle = \frac{(\lambda+\mu)(\lambda+\mu+3)-\lambda\mu}{3} \qquad (8)$$

Once the intrinsic state of k particles is formed, one can project states of good angular momentum L from it. We know that R_3 is a sub-group of SU_3. The reduction of $SU_3 \rightarrow R_3$ can also be possible

using dimensionality arguments. Elliott[1] has shown that the allowed values of L for a given $(\lambda\ \mu)$ are just those of a series of rotational bands based on states with $L_z = k$, where k assumes all consistent values for the SU_3 IR $(\lambda\ \mu)$. That is

If $\lambda \geq \mu$

$k = \mu, \mu-2, \ldots$ ---------- 0 or 1

$L = k, k+1, k+2, \ldots$ ---------- $k \neq \lambda$ for $k \neq 0$

$L = \lambda, \lambda-2, \ldots$ ---------- 0 for $k = 0$

If $\mu > \lambda$

$k = \lambda, \lambda-2, \ldots$ ---------- 0 or 1

$L = k, k+1, \ldots$ ---------- $k \neq \mu$ if $k \neq 0$

$L = \mu, \mu-2, \ldots$ ---------- 0 or 1 if $k=0$

In order to get a complete linearly independent set of states of good angular momentum, Elliott[1] has further prescribed that for $\lambda \geq \mu$, the intrinsic state may be chosen with $\sigma = \sigma_{max}$ while for $\mu > \lambda$, it may be with $\sigma = \sigma_{min}$. It should be noted that the states of same angular momentum L with different k are not necessarily orthogonal in the LM representation.

II.4 The SU_3 wave functions of two particles in 1d-2s shell

i) The formation of intrinsic states in 1d-2s shell

A single-particle state in 1d-2s shell has SU_3 representation(20)

as N=2 is the major quantum-number of 1d-2s shell. The different single-particle states in this shell are further classified by the eigenvalues of Q_0, L_0 and Λ^2. For that one is required to diagonalise simultaneously L_0 and Q_0 in the basis states of $\chi_{2s,0}$ and $\chi_{1d,m}$

After diagonalisation, the single particle state can be designated as $\Phi\left[(20), K, \leftarrow, \Lambda\right]$

The result of diagonalisation is given below:

$$\Phi\left[(20), 0, 4, 0\right] = \Phi_0 = \frac{1}{\sqrt{3}}\left[\psi_{2s,0} - \sqrt{2}\,\psi_{1d,0}\right]$$

$$\Phi\left[(20), 1, 1, \tfrac{1}{2}\right] = \Phi_1 = \psi_{1d,1}$$

$$\Phi\left[(20), -1, 1, \tfrac{1}{2}\right] = \Phi_{-1} = \psi_{1d,-1}$$

$$\Phi\left[(20), 2, -2, 1\right] = \Phi_2 = \psi_{1d,2}$$

$$\Phi\left[(20), 0, -2, 1\right] = \Phi_0' = \frac{1}{\sqrt{3}}\left[\sqrt{2}\,\psi_{1s,0} + \psi_{1d,0}\right]$$

$$\Phi\left[(20), -2, -2, 1\right] = \Phi_{-2} = \psi_{1d,-2}$$

It is convenient to regard the states Φ_K as levels in a $K - (\leftarrow$ plane as shown in figure 1. The arrows in the diagram indicate the directions in which the step operations[2] F_4, F_1, F_5

FIG. II·1

SU_3 SINGLE PARTICAL STATES IN 1f-2p SHELL

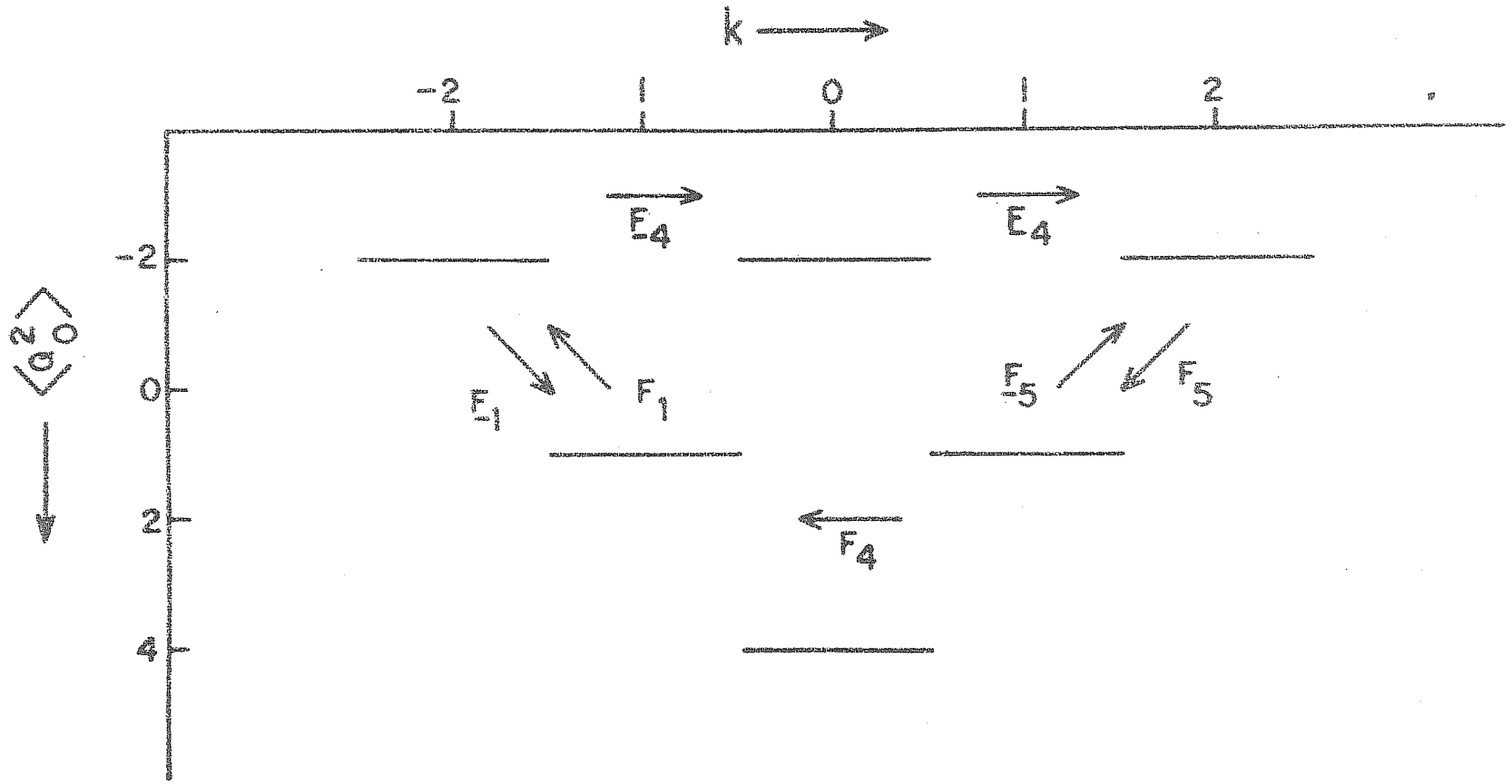

change the eigenvalues k and σ. Many particle states Ψ are constructed by filling the single particle levels in accordance with the Pauli's principle. The state will be symmetric or antisymmetric depending on to which [f] representation it belongs. It should be remembered that the state of highest weight corresponds to $\sigma = \sigma_{max}$ and $k = k_{max}$ for a given $(\lambda \mu)$. We are interested in forming the intrinsic state of 2 particles. Table 4 gives the list of various SU_3 representations possible for two particles and their L and k values. From table 4, it can be seen that there are three IR of SU_3 for two particles in 1d-2s shell. The IR (40) and (02) are symmetric in space while (21) is antisymmetr in space. Thus corresponding to these three IR of UR_3, there will be three intrinsic states. It can also be seen that the (40) representation will be lowest as it has highest eigenvalue for the Casimir operator. We will now consider how to form the intrinsic states of highest weight corresponding to these representations in details.

2. The Intrinsic state corresponding to (40), (21) and (02) representations.

The intrinsic state of highest weight corresponding to (40) will have $\sigma_{max} = 8$ units. This state can be formed by putting two-particles in the lowest state ϕ_0. As this state belongs to [2] representation of permutation group, it is symmetric in space. We demote this state as

Table II.4

SU_3 representations of two particles

Shell	Permutation symmetry	SU_3 representations	K	L	κ_{max} in units of b^2	Eigenvalue of Casimir operator
	[2]	(20)	0	2,0	4	10
1_p	[11]	(01)	0	1	1	4
	[2]	(40)	0	4,2,0	8	28
		(02)	0	2,0	2	10
1s-2d	[11]	(21)	1	3,2,1	5	16
	[2]	(60)	0	6,4,2,0	12	54
1f-2p	[2]	(22)	0	2,0	6	24
			2	4,3,2	6	24
	[11]	(41)	1	5,4,3,2,1	9	36
		(03)	0	3,1	-6	18

$$\Psi_1 = \Psi\left[(40), K=0, \kappa=8, \Lambda=0\right] = \left[\phi_0(1)\,\phi_0(2)\right]_s \qquad (11)$$

where suffix 's' indicates the symmetric combinations. Similarly the intrinsic state for (21) and (02) representations can be

written down as follows:

$$\Psi_2 = \Psi_2 \left[(21) \quad k=1, \quad \epsilon = 5, \quad \wedge = \tfrac{1}{2} \right]$$

$$= \left[\Phi_0 (1) \; \Phi_1 (2) \right]_a \qquad (12)$$

where suffix 'a' denotes the antisymmetric combination.

$$\Psi_3 = \Psi_3 \left[(02), \; k=0, \quad \epsilon = -4, \quad \wedge = 2 \right]$$

$$= a \left[\Phi_2 (1) \; \Phi_{-2} (2) \right]_s + b \left[\Phi'_0 (1) \; \Phi'_0 (2) \right]_s \qquad (13)$$

It should be noted that Ψ_3 is a linear cokbination of two possibilities in which the state $\epsilon = -4$ units can be formed. The coefficients can be determined by using step operators F_4. The operator F_4 increases k by 2 units and leaves ϵ unchanged. Hence if we operate by F_4 on Ψ_3, the resulting state will have $\wedge=2$. But $k=0$ is the maximum value of k that the state can have. Hence using expression (13) and taking into account the proper normalisation constants we get

$$F_4 \Psi_3 = -\sqrt{2}\, a \left[\Phi_2 (1) \; \Phi'_0 (2) \right]_s - \sqrt{4}\, b \left[\Phi_2 (1) \; \Phi'_0 (2) \right] = 0$$

This yields $a = \sqrt{\frac{2}{3}}$ and $b = -\sqrt{\frac{1}{3}}$, therefore

$$\Psi_3 = \sqrt{\frac{2}{3}} \left[\Phi_2 (1) \; \Phi_{-2} (2) \right]_s - \sqrt{\tfrac{1}{3}} \left[\Phi'_0 (1) \; \Phi'_0 (2) \right] \qquad (14)$$

3 The projection of good angular momentum states from Ψ_1, Ψ_2 and Ψ_3.

We now project the states of good angular momentum from these intrinsic states. The formula for projection from a two particle

intrinsic state is quite simple.

Let us first project from Ψ_1. The state Ψ_1 can also be written as

$$\Psi_1 = \sum_{\ell_1, \ell_2} a_0(\ell_1)\, a_0(\ell_2)\, |(\ell_1 \ell_2)\rangle_S$$

where $a_0(\ell_1)$ are the coefficients of single particle expansion given in expression (10). This can be also written as

$$\Psi_1 = \sum_{\ell_1, \ell_2, L} a_0(\ell_1)\, a_0(\ell_2)\, C^{\ell_1 \ell_2 L}_{0\,0\,0} \sqrt{1+\delta_{\ell_1 \ell_2}}\, |(\ell_1 \ell_2) L\rangle_S$$

where $C^{\ell_1 \ell_2 L}_{0\,0\,0}$ is a Clebsch-Gordan coefficient. In short we can write

$$\Psi_1 = \sum_{\ell_1, \ell_2, L} F((40) k=0, \ell_1 \ell_2, L)\, |(\ell_1 \ell_2) L\rangle_S$$

Now $\Phi[(40), K=0, L] = P^L_K |\Psi_1\rangle$ where P^L_K is the projection operator.

Therefore

$$\Phi[(40), K=0, L] = \sum_{\ell_1, \ell_2} F[(40) K=0, \ell_1 \ell_2, L]\, |(\ell_1 \ell_2) L\rangle_S \qquad (14)$$

Similarly the states of good angular momentum can be projected from intrinsic states Ψ_2 and Ψ_3. Tables 5 to 7 give the projected states.

Table II.5

The states of good angular momentum projected from symmetric state $\Psi_1\left[(40),\ k=0,\ \sigma_{max}=8\right]$

L	d^2	s^2	$\frac{1}{2}$ (ds+sd)	N^2
0	$\sqrt{4/9}$	$\sqrt{5/9}$		1/5
2	$\sqrt{2/9}$		$\sqrt{7/9}$	4/7
4	1	0	0	8/35

Table II.6

The states of good angular momentum projected from antisymmetric state $\Psi_2\left[(21),\ k=1,\ \sigma_{max}=5\right]$

L	d^2	s^2	$\frac{1}{2}$ (ds+sd)	N^2
1	1	0	0	2/5
2	0	0	1	1/3
3	1	0	0	4/15

Table II.7

The states of good angular momentum projected from symmetric state $\Psi_{I3}\left[(20),\ k=0,\ \sigma_{max} = -4\right]$

L	d^2	s^2	$\frac{1}{2}(ds-sd)$	N^2
0	$\sqrt{5/9}$	$-\sqrt{4/9}$	0	1/3
2	$\sqrt{7/9}$	0	$-\sqrt{2/9}$	2/3

4 Transformation matrices from j-j to SU_3 coupling

We now calculate the j-j components in shell model wave functions in terms of SU_3 components. We know that

$$|(j_1 j_2) J T\rangle = \sum_{L,S} A \begin{Bmatrix} \ell_1 & \frac{1}{2} & j_1 \\ \ell_2 & \frac{1}{2} & j_2 \\ L & S & J \end{Bmatrix} \sqrt{\frac{(1+\delta_{\ell_1 \ell_2})}{(1+\delta_{j_1 j_2})}}\ |(\ell_1 \ell_2) L S J T\rangle \qquad (15)$$

Inverting the equation (14) we get

$$|(\ell_1 \ell_2) L\rangle = \sum_{(\lambda\mu)} F\left[(\lambda\mu)k, \ell_1 \ell_2, L\right] |(\lambda\mu) k L\rangle \qquad (16)$$

Substituting the expression for $|(\ell_1 \ell_2) L\rangle$ in the equation (15) we get

$$|(j_1 j_2) J T\rangle = \sum_{L,S,(\lambda\mu)} A \begin{Bmatrix} \ell_1 & \frac{1}{2} & j_1 \\ \ell_2 & \frac{1}{2} & j_2 \\ L & S & J \end{Bmatrix} \sqrt{\frac{(1+\delta_{\ell_1 \ell_2})}{(1+\delta_{j_1 j_2})}}\ F\left[(\lambda\mu)k, \ell_1 \ell_2, L\right] |(\lambda\mu) k L S\rangle_{J T} \qquad (17)$$

Inverting the relation, we get

$$|(\lambda\mu)KLS\rangle_{JT} = \sum_{l_1,l_2,j_1,j_2} A \begin{Bmatrix} l_1 & \frac{1}{2} & j_1 \\ l_2 & \frac{1}{2} & j_2 \\ L & S & J \end{Bmatrix} \sqrt{\frac{1+\delta_{l_1,l_2}}{1+\delta_{j_1,j_2}}}\, F[(\lambda\mu)K(l_1,l_2)L]\,|(j_1,j_2)\rangle_{JT} \quad (18)$$

thus given the shell model wave functions for two particles, we can transform those wave functions into basis of SU_3 scheme. The transformation matrices are tabulated in tables 8 to 13 for J=0,2,4 for T=1 and J=1,2,3 for T=0. It may be noted that for the states T=1, J=1,3 belong to antisymmetric representation (21) while the states T=0, J=4,5 belong to symmetric representation uniquely. Also we can easily transform the two-body matrix elements in j-j representations to those in SU_3 basis by the formula.

$$\langle(\lambda,\mu)KLS|V|(\lambda',\mu')K'L'S'\rangle_{JT} = \sum_{\substack{l_1,l_2,l_3,l_4 \\ j_1,j_2,j_3,j_4}} A \begin{Bmatrix} l_1 & \frac{1}{2} & j_1 \\ l_2 & \frac{1}{2} & j_2 \\ L & S & J \end{Bmatrix} \begin{Bmatrix} l_3 & \frac{1}{2} & j_3 \\ l_4 & \frac{1}{2} & j_4 \\ L' & S' & J \end{Bmatrix} F[(\lambda\mu)K(l_1,l_2,L]$$

$$\times F[(\lambda'\mu')K(l_3,l_4,L']\langle(j_1,j_2)|V|(j_3,j_4)\rangle_{JT} \quad (19)$$

where $\langle J_1\ J_2|V|J_3\ J_4\rangle_{JT}$ is an antisymmetrized normalised two-body matrix elements in j-j representation.

II. 5 Symmetry analysis

We will now study the symmetry properties of 's' state radial integrals[13]. There are three 's' state radial integrals namely I_{0s}, I_{1s} and I_{2s}. We proceed first to construct

Table II.8

Transformation matrix from j-j to SU_3 representations for J=0, T=1.

$(\lambda\mu)_{LS}$ \ j-j	$(5/2)^2$	$(3/2)^2$	$(\ /2)^2$
$(40)_{00}$	0.5164	0.4216	0.7454
$(02)_{00}$	0.5773	0.4714	-0.6667
$(21)_{11}$	-0.6324	0.7746	0

Table II.9

Transformation matrix from j-j to SU_3 representation for J=2 , T=1.

$(\lambda\mu)_{LS}$ \ j-j	$(5/2)^2$	(5/2 3/2)	(3/2 3/2)	(5/2 1/2)	(3/2 1/2)
$(40)_{20}$	0.3266	0.2309	0.2494	0.6831	-0.5577
$(02)_{20}$	0.6110	0.4320	0.4667	-0.3651	0.2981
$(21)_{11}$	0.6693	-0.7099	-0.2191	0	0
$(21)_{21}$	0	0	0	0.6324	0.7746
$(21)_{31}$	-0.2683	-0.5059	0.8197	0	0

Table II.10

Transformation matrix from j-j to SU_3 representations for J=4, T=1.

$(\lambda\mu)_{LS}$ \ $j_1 j_2$	$(5/2)^2$	(5/2 3/2)
$(40)_{40}$	0.4472	0.8944
$(21)_{31}$	0.8944	-0.4472

Table II.11

Transformation matrix from j-j to SU_3 representations for J=1, T=0.

$(\lambda\mu)_{LS}$ \ j-j	$(5/2)^2$	$(3/2)^2$	(5/2 3/2)	(3/2 1/2)	$(1/2)^2$
$(40)_{21}$	-0.1885	0.3527	-0.2494	0.8819	0
$(02)_{21}$	-0.3527	0.6600	-0.4667	-0.4715	0
$(40)_{01}$	0.3527	-0.1885	-0.5333	0	0.7454
$(02)_{01}$	0.3945	-0.2108	-0.5963	0	-0.6667
$(21)_{10}$	0.7483	0.6000	0.2828	0	0

Table II.12

Transformation matrix from j-j to SU_3 representation for J=2, T=0.

$(\lambda\mu)_{LS}$ \ j-j	(5/2 1/2)	(3/2 1/2)	(5/2 3/2)
$(40)_{21}$	0.5577	0.6831	0.4714
$(02)_{21}$	-0.2981	-0.3651	0.8819
$(21)_{20}$	0.7745	-0.6324	0

Table II.13

Transformation matrix from j-j to SU_3 representation for J-3, T=0.

$(\lambda\mu)_{LS}$ \ j-j	$(5/2)^2$	$(3/2)^2$	(5/2 3/2)	(5/2 1/2)
$(40)_{41}$	-0.1512	0.9071	-0.3923	0
$(40)_{21}$	0.3703	-0.0617	-0.2851	0.8819
$(02)_{21}$	0.6928	-0.1155	-0.5333	-0.4714
$(21)_{30}$	0.6000	0.4000	0.6923	0

eigenfunctions of each radial integral independently. All the parameters except one of the I_{ns} are set equal to zero, so that the 68 two-body matrix elements of 1d-2s shell (in j-j coupling for convenience) are expressed in terms of only this one parameter. The resulting Hamiltonian matrices are then diagonalised and the eigenfunctions are transformed first to the LS coupling scheme to examine their orbital permutation symmetry and second, the orbital part of the wave function is analysed in terms of its SU_3 components. Note that for two particles in 1d-2s shell (see table 4) we expect orbital symmetries $[2]$ and $[11]$, the former containing SU_3 components (40) and (02) and the latter only a unique component (21). The procedure is analogous to that of Parikh and Bhatt[2]. Since initially we wish to concentrate only on the SU_3 symmetries of the interaction, we avoid the complication of the single-particle spin-orbit force and take all three orbits $d_{5/2}$, $s_{1/2}$ and $d_{3/2}$ as degenerate. Only the lowest states of each J for T=1, J=0,2,4 and for T=0, J=1,2,3 are considered. As seen before, the T=1, J=1,3 states have trivially (21) symmetry and T=0 J=4,5 have (40) symmetry only.

A: Table 14 gives the eigenfunctions for two particles in the case when the interaction is described in terms of the parameter I_{os} alone and all other radial matrix elements are set equal to zero. The decomposition of the eigenfunctions in terms of orbital and SU_3 symmetries shows, for all the states,

only a single component $[2]$ (40). Since the interaction is operative only in s-states, one expects no admixture of the $[11]$ symmetry. The occurence of only symmetry (40) is the Moszkowaski[14] result.

B: In the case when the interaction contains only the parameter I_{2s}, one finds non-zero two-body matrix elements only for T=1, J=0 and T=0, J=1 states. In fact it has already been demonstrated[15] that such a peculiar interaction exhibits a pairing property in the sense that in L-S coupling only a single L=0 state is depressed by this interaction, all other states remaining at zero excitation energy. However, the eigenfunctions for this interaction given in table 15 show that they are quite different from the usual pairing eigenfunctions. We further find that the eigenfunctions again belong to exact SU_3 symmetry.

C: On the other hand, when the interaction consists of only the parameter I_{1s}, the results obtained are shown in table 16. Now the eigenfunctions have no definite SU_3 symmetry and actually the (02) component seems to have a larger magnitude. It is this component of the interaction which is primarily responsible for the break-up of the SU_3 symmetry in the s-d shell. The effective interactions derived empirically[3], as well as from realistic two-body forces, show generally that the largest parameter is I_{0s}. Although the magnitude of I_{2s}

is smaller, it appears in the spectroscopy only in the combination $I_{os} + I_{2s}$ and hence together with I_{os} it is also a major factor in giving an approximate SU_3 symmetry to the wave functions. The SU_3 symmetry remains a good approximation in the 1d-2s shell, because although I_{1s} mixes up different SU_3 symmetries, its magnitude and overall contribution to the matrix element is generally smaller than that of I_{os} and I_{2s} [3].

D: To see the SU_3-symmetry-breaking effect of I_{1s} in a realistic way, we have calculated the two-body matrix elements with the actual values of I_{os}, I_{1s} and I_{2s} (for both T=1 and T=0 states) obtained by Cohen et al[3] from a least-squares fit to the observed low-lying states of ^{18}O, ^{19}O, ^{20}O, ^{18}F and ^{19}F. (see table 3). The eigenfunctions thus obtained (still assuming degenerate single-particle orbits) are shown in table 17 together with their decomposition into SU_3 symmetry components. It can immediately be seen that in practice (except for the state T=0, J=1)the SU_3 symmetry is well preserved, the magnitude of the (02) component is less than 5%. However, the T=0, J=1 state is strongly disturbed and contains about 20% admixture of (02).

We have also analysed the eigenfunctions obtained using the full interaction (i.e including the values of all the parameters I_{nls}) as deduced by Cohen et al[3]. For degenerate

single-particle orbits, the results are not very different from those in table 17 and hence we do not list them.

E: The effect of including the splitting of the single-particle orbits as seen in ^{17}O or ^{17}F on the symmetry of the eigenfunctions finally remains to be considered. We take the single-particle energies

$$T=1$$

$$E(d_{5/2}) = 0,\ E(S_{1/2}) = 0.87,\ E(d_{3/2}) = 5.08 \text{ MeV}$$

$$T=0$$

$$E(d_{5/2}) = 0,\ E(S_{1/2}) = 0.68,\ E(d_{3/2}) = 4.89 \text{ MeV}$$

For evaluating two-body matrix elements we take into account all the radial integrals with the values given in table 3. The resulting eigenfunctions and their symmetries are listed in table 18. Notice that now the orbital symmetry is broken to a considerable extent and the $[11]$ components have quite sizeable magnitudes. On the other hand, the mixing of (40) and (02) is actually somewhat reduced and the effect is quite appreciable in the case of T=0, J=1 state. We believe that the explanation is as follows. The wave functions generated in case C have very large components $(d_{5/2}\ d_{3/2})$ and $(d_{3/2})^2$. In fact, the wave functions are almost pure $(d)^2$. The spin-orbit splitting of $d_{5/2}$ and $d_{3/2}$ states when taken into account, reduces the $d_{3/2}$ components and to that extent weakens the symmetry-breaking effect of I_{ls}.

Table II.14

Eigenfunctions and symmetries for Case A. The intrinsic state and the overlaps between the generated and shell model wavefunctions are also shown.

	T=1			T=0		
J	0	2	4	1	2	3
$(d_{5/2})^2$	0.5163	0.3266	0.4472	0.3917		0.3071
$(d_{5/2}\ s_{1/2})$		0.6861			0.5578	0.8405
$(d_{5/2}\ d_{3/2})$		0.2310	0.8944	-0.2503	0.4714	-0.3906
$(s_{1/2})^2$	0.7453			0.5729		
$(d_{3/2}\ s_{1/2})$		-0.5577		-0.5641	0.6831	
$(d_{3/2})^2$	0.4217	0.2494		-0.3706		0.2158
[2] (40)	0.9999	0.9999	0.9999	0.9998	0.9998	0.9999
(02)	0	0	0	0	0	0
[11] (21)	0	0	0	0	0	0
Overlap	0.999	0.999	0.999	0.927	0.955	0.896

T=1, $|\tfrac{1}{2}\rangle = 0.6325\ |d_{5/2}\ 1/2\rangle - 0.5773\ |1/2\ \ 1/2\rangle - 0.5164|3/2\ 1/2\rangle$

T=0, $|\tfrac{1}{2}\rangle = 0.7000\ |5/2\ \ 1/2\rangle - 6433\ |\tfrac{1}{2}\ \tfrac{1}{2}\rangle - 0.3100\ |3/2\ \ 1/2\rangle$

Table II.15

Eigenfunctions and symmetries for Case (B)

Configuration		J=0, T=1	J=1, T=0
$(5/2)^2$		0.5163	0.3527
$(d_{5/2}\ s_{1/2})$			
$(d_{5/2}\ d_{3/2})$			-0.5333
$(s_{1/2})^2$		0.7453	0.7453
$(d_{3/2}\ s_{1/2})$			0
$(d_{3/2})^2$		0.4217	-0.1885
[3]	(40)	0.9999	0.9999
	(02)	0	0
[11]	(21)	0	0

Table II.16

Eigenfunctions and symmetries for Case C

		T=1			T=0		
J		0	2	4	1	2	3
$(d_{5/2})^2$		0.7559	0.6693	-	0.5164		0.7589
$(d_{5/2}\ s_{1/2})$			0.1999	-		0.1633	0.2581
$(d_{5/2}\ d_{3/2})$			0.4733	-	-0.7807	0.9661	-0.5842
$(s_{1/2})^2$		-0.2182		-	-0.2182		
$(d_{3/2}\ s_{1/2})$			-0.1634	-	0	0.2000	
$(d_{3/2})^2$		0.6172	0.5111	-	-0.2760		-0.1265
[2]	(40)	0.2330	0.4665	-	0.2330	0.4666	0.4665
	(02)	0.7618	0.5333	-	0.7619	0.5333	0.5333
[11]	(21)	0	0	-	0	0	0

Table II.17

Eigenfunctions and symmetries for Case D. The intrinsic state and the overlaps between the generated and the shell model eigenfunctions are also shown.

		T=1			T=0		
J		0	2	4	1	2	3
$(d_{5/2})^2$		0.5033	0.3757	0.4470	0.4904		0.5059
$(d_{5/2}\ s_{1/2})$			0.6507			0.4812	0.7609
$(d_{5/2}\ d_{3/2})$			0.2657	0.8944	-0.7417	0.6489	-0.4026
$(s_{1/2})^2$		0.6420			0.3751		
$(d_{3/2}\ s_{1/2})$			-0.5313		0.0001	0.5893	
$(d_{3/2})^2$		0.4849	0.2870	-	-0.2620		-0.0538
[2]	(40)	0.9793	0.9928	0.9993	0.8055	0.9541	0.9546
	(02)	0.0205	0.0069	0	0.1943	0.0457	0.0452
[11]	(21)	0	0	0	0	0	0
Overlap		0.996	0.997	0.999	0.904	0.998	0.917

T=1 , $|\tfrac{1}{2}\rangle = 0.6800\ |5/2\ \tfrac{1}{2}\rangle - 0.5362\ |\tfrac{1}{2}\ \tfrac{1}{2}\rangle - 0.5000\ |3/2\ \tfrac{1}{2}\rangle$

T=0 , $|\tfrac{1}{2}\rangle = 0.7500\ |5/2\ \tfrac{1}{2}\rangle - 0.3674\ |\tfrac{1}{2}\ \tfrac{1}{2}\rangle - 0.5500\ |3/2\ \tfrac{1}{2}\rangle$

Table II.18

Eigenfunctions and symmetries for Case E. The intrinsic state and the overlaps between the generated and the shell model states are shown.

	T=1			T=0		
J	0	2	4	1	2	3
$(d_{5/2})^2$	0.8046	0.6946	0.8849	0.7142		0.6001
$(d_{5/2}\ s_{1/2})$		0.6779			0.8545	0.7744
$(d_{5/2}\ d_{3/2})$		0.0818	0.4658	-0.5029	0.3856	-0.1959
$(s_{1/2})^2$	0.5700			0.4642		
$(d_{3/2}\ s_{1/2})$		-0.2120		-0.0341	0.3479	
$(d_{3/2})^2$	0.1660	0.0791		-0.1426		0.0410
[2] (40)	0.8286	0.7171	0.6598	0.8054	0.8028	0.9309
[2] (02)	0.0265	0.0345	0	0.0992	0.0017	0.0255
[11] (21)	0.1445	0.2481	0.3506	0.0950	0.1952	0.0432
Overlaps	0.992	0.987	0.989	0.960	0.999	0.980

$$\left|\tfrac{1}{2}\right\rangle = 0.8400\ \left|5/2\ \tfrac{1}{2}\right\rangle - 0.4815\ \left|\tfrac{1}{2}\ \tfrac{1}{2}\right\rangle - 0.2500\ \left|3/2\ \tfrac{1}{2}\right\rangle .$$

To conclude this section we summarise: The spectroscopy in the 1d-2s shell is largely governed by effective interactions in relative 's' states of two nucleons. Of the three parameters defining the 's' state interaction, the dominant two, viz. I_{0s} and I_{2s} are SU_3 symmetry-preserving interactions. The SU_3-symmetry-breaking property of the parameter I_{1s} is to a certain extent counter-balanced by the spin-orbit splitting of the single-particle orbits. Thus the single particle spin-orbit interactions, mainly through the mixing of orbital symmetries $[2]$ and $[11]$, turns out to be the major factor in the breaking of SU_3 symmetry of the wave function. The single particle spin-orbit force mixes orbital symmetry because it can connect symmetric and antisymmetric states in space in j-j coupled representations. Another way of looking at this is the group theoretical point of view. One knows that Wigner's supermultiplet[16] symmetry is assumed in SU_3 scheme[1]. The symmetry in spin and isospin states ultimately decides the symmetry in the orbital space due to the overall antisymmetrization of the wave function. When we have spin or isospin dependent forces, they try to violate the Wigner's supermultiplet symmetry thereby mixing the orbital symmetry also.

II.6 Intrinsic States

Recently, Hartree-Fock calculations have been used extensively in investigating the structure of the 1d-2s shell nuclei. One calculates with a suitable effective interaction the single-particle

orbits and energies in a self-consistent manner and then a Slater determinant for the orbits occupied by the nucleons is constructed. Since the orbits thus calculated do not have a spherical symmetry, a band of states of good angular momentum have to be projected out from such deformed intrinsic states. We do not perform any Hartree-Fock calculations here but instead attempt to construct empirically an intrinsic state such that wave functions projected out from it will give the best possible overlap with two-nucleon wave functions described in the previous section.

A deformed intrinsic single particle state relevent to our discussion of two nucleons in the beginning of the 1d-2s shell is $|k = \frac{1}{2}\rangle$ and can be written as

$$|\tfrac{1}{2}\rangle = \sum_j b_{j\frac{1}{2}} \; |j\tfrac{1}{2}\rangle$$

where $b_{j\frac{1}{2}}$ is the amplitude of the spherical oscillator state $|jm = \frac{1}{2}\rangle$ in the expansion of the intrinsic state. With time reversal symmetry one has for the state $|k = -\frac{1}{2}\rangle$

$$b_{j-\frac{1}{2}} = (-1)^{j-\frac{1}{2}} \; b_{j\frac{1}{2}}$$

The most simple model[17] would now be to consider for projection of T=1 states, the antisymmetrized intrinsic state $|\frac{1}{2}, -\frac{1}{2}, K=0\rangle$ and for T=0 states, the symmetric intrinsic state $|\frac{1}{2}\,\frac{1}{2}, K=1\rangle$. Parikh and Bhatt[13] have shown in this way that the lowest states of each J in ^{18}O and ^{18}F calculated by Kuo and Brown[6] can all be generated from a single axially symmetric

intrinsic state.

Our wave functions in case E are essentially similar to those obtained by Kuo and Brown[6] and hence it is not surprising that we have been able to find an intrinsic state $|\frac{1}{2}\rangle$ such that wave functions projected out from K=0 and K=1 states constructed with it have excellent overlaps with the wave functions calculated in case E. The coefficients $b_{j\frac{1}{2}}$ as well as the magnitudes of the overlaps are listed in table 13. The quality of the overlaps (particularly for T=0, J=1 states) is somewhat better than in the case of Parikh and Bhatt[2].

It is however, of interest to see if a similar state can be constructed to account for other sets of states obtained in cases A, B, C and D in the absence of the single-particle, spin-orbit force and the nature of such intrinsic orbits as well as the degree of overlaps. The result for the cases A and D are also shown in tables 14 and 17. In both cases for T=1 states (J=0,2,4) we are able to construct an intrinsic state such that the overlaps are excellent and in all cases 0.995 or better. As one might expect in these intrinsic states some of the $d_{5/2}$ strength is transferred to the $d_{3/2}$ component (in the absence of spin-orbit splitting) and the $s_{1/2}$ component is also slightly enhanced.

However, these intrinsic states (T=1 case) give rather poor overlaps when T=0 states constructed with their help are compared with the shell model wave functions calculated in A and D. In

fact, we were not able to find a single intrinsic state such that the generated wave functions and the shell model wavefunctions would have good overlaps for both T=1 and T=0 states. The intrinsic state which would give best overlaps for T=0 alone were then constructed and are also listed separately in tables 14 and 17. They differ somewhat from the T=1 intrinsic states. Even the best overlaps thus obtained for T=0 states are not satisfactory except perhaps for the J=2 states. For the states with J=1,3 we only find overlaps of about 0.900.

It appears then that in the absence of single particle spin-orbit force, it is not possible to characterize the T=0 states (particularly J=1,3) in terms of an intrinsic deformed orbit of good K. The reason may very well be that a description of these states requires K mixing. We neglected here the symmetric state $|\frac{1}{2}, -\frac{1}{2}, K=0\rangle$ from which one can project out J=1,3,5 states. It may be that the J=1,3 shell model states calculated in cases A and D contain a mixing of the K=0 and K=1 intrinsic states and hence our failure to explain them in terms of the K=1 state alone. This would suggest that in the absence of spin-orbit coupling, the T=0, J=1,3 states may have an intrinsic structure quite different from that of the T=0, J=2 states. If this argument is correct, it further appears that the single particle spin-orbit force plays a very important role in supressing the K-mixing in the T=0 states, for as we see in case E, the overlaps between projected K=1 states and shell model states are much better. Another reason why T=0

states cannot be projected from an intrinsic states perhaps lies in the fact that the I_{1s} component in total T=0 interaction is much larger than that in T=1 interaction. This component, as we have seen before, is the SU_3 - breaking component and hence does not allow a single intrinsic state which can give rise to different J states.

II.7 SU_3 symmetry properties of radial integrals:

We have studied the SU_3 symmetry properties of 's' state radial integrals and we have shown that I_{0s} and I_{2s} obey the SU_3 symmetry while I_{1s} mixes the different IRs of SU_3. The explanation of these properties will be now sought in group theoretical arguments. This explanation also enables us to understand the symmetry properties of any radial integral in general. Let us take the radial integrals I_{nl} in the shell of major quantum number N. If we have two particles in this shell, the total number of quantas are 2N. The I_{nl} denotes the strength of the interaction in the state of relative angular momentum l and radial quantum number n. We can as well say that the relative state of the particles is in the harmonic oscillator shell of major quantum number (2n+l). Naturally the centre-of-mass state of two particles must be in the harmonic oscillator shell of major quantum number (2N-2n-l) as the total number of quantas are 2N. The SU_3 representation of the state of relative motion is therefore (2n+l, 0) while that of the state of

centre-mass motion is (2N-2n-1,o). The product of these representation will yield different SU_3 representations and these are the representations that are affected by that particular radial integral I_{nl}. This argument is precisely given in the following two rules for radial integrals in symmetric and antisymmetric states in space.

1) In general any radial integral I_{nl} acting in a symmetric state in the shell bearing a major quantum number N will affect the SU_3 representations of two particle states, resulting from the product of $(2n+1,0) \otimes (2N-2n-1,0)$. This product is given as

$$(2n+1,0) \otimes (2N-2n-1,0) = (2N,0),\ (2N-4,2),\ (2N-8,4) \ldots\ldots\ldots\ldots$$
$$\ldots\ldots\ldots\ldots (2N-4x+4,\ 2(x-1))$$

where $2(x-1)$ should be equal or less than min $[(2n+1),\ (2N-2n-1)]$

2) Similar expression can be given for antisymmetric states

$$(2n+1,0) \otimes (2N-2n-1,0) = (2N-2,1),\ (2N-6,3) \ldots\ldots\ldots\ldots\ldots\ldots$$
$$\ldots\ldots\ldots\ldots (2N-4x-2,\ 2x-1)$$

where $(2x-1)$ should be equal to or less than min $[(2n+1),\ (2N-2n-1)]$

The corollary to above two rules is the fact that any radial integral I_{nl} with the exception of I_{os}, when it appears for the first time in the lowest possible major shell gives rise to a state of unique SU_3 representation. Also the radial integral I_{os} acts only in a unique SU_3 representation (2N,0) in any shell of major quantum number N. In light of these rules, we will study the symmetry properties of all radial integral in 1d-2s shell for which N=2.

Integral I_{os}: The relative state has (00) representation while the centre-of-mass state has (40) representation. The product of these representations will yield a unique SU_3 representation (40). Thus I_{os} acts only in (40) representation and hence preserves the SU_3 symmetry. In this case the angular momentum comes entirely from the centre-of-mass motion and therefore the I_{os} interaction gives rise to a degenerate set of states with L=0,2,4, belonging to (40) representation. A similar result is valid in any shell. Moszkowski[14] has also observed the same result.

Integral I_{1s}: The relative state as well as the centre-of-mass state have in this case (20) representation. The product will yield the space symmetric representations (40) and (02) and an antisymmetric representation (21). But I_{1s} acts only in symmetric representation and therefore it mixes the symmetric representations (40) and (02).

Integral I_{2s}: The relative state has (40) representation and centre-of-mass state will have (00) representation. The product gives a unique (40) representation. Therefore I_{2s} acts only in (40) representations. It should be noted that though the relative state has a representation (40) from which different l=0,2,4 can be projecte out, I_{2s} acts only in l=0 state. As a result I_{2s} acts only in total L=0 state and lowers down this state. In this way it resembles the conventional pairing interaction.

Integral I_{0d}: The relative state has (20) representation and the centre-of-mass state also has (20) representation. The product

will yield, as in the case of radial integral I_{1s}, the symmetric representation (40) and (02) and an antisymmetric representation (21). Therefore the radial integral I_{od} which acts only in symmetric states, mixes (40) and (02) representations.

Integral I_{1d}: The relative state has (40) representation and naturally the centre-of-mass motion will have (00) representation. The product will yield (40) representation only. As a result I_{1d} preserves SU_3 symmetry. Again the relative state has representation (40) from which l=0,2,4 states can be projected out but I_{1d} acts only in l=2 state. Therefore it acts only in total L=2 state.

Integral I_{og}: With similar arguments one can show that I_{og} preserves SU_3 symmetry as it acts only in (40) representation. Also this integral contributes to total L=4 state only.

For odd radial integral I_{op}, I_{1p} and I_{of} the SU_3 symmetry is trivial. These radial integrals act only in space antisymmetric SU_3 representation namely (21). Thus we conclude that all the odd radial integrals in 1d-2s shell will trivially obey the SU_3 symmetry as there is only one antisymmetric SU_3 representation available to them in that space.

1. The symmetry of radial integrals in 1p and 1f-2p shells:

We will now study the properties of radial integrals in 1p and 1f-2p shells.

1p-shell: This shell has N=1. There are in total 4 radial integrals as we can see from the table 2. The radial integrals I_{os}, I_{1s}, I_{od} act in space symmetric states while I_{op} acts in space antisymmetric state. Using the rules given above, it can be easily seen that the radial integrals I_{os}, I_{1s}, and I_{od} act only in (20) representation and hence they preserve SU_3 symmetry. Moreover the radial integral I_{1s} acts only in total L=0 state while I_{od} acts only in total L=2 state. The odd radial integral I_{op} acts only in space antisymmetric representation (01). Thus all the radial integrals obey the SU_3 symmetry. Therefore we conclude that any central interaction in 1p shell is SU_3 invariant.

1f-2p shell: The major quantum number N for this shell has value 3. There are ten even state radial integrals and 6 odd state radial integrals. The integrals I_{3s}, I_{2d}, I_{1g} and I_{oi} appear for the first time in this shell and therefore they preserve SU_3 symmetry and act only in (60) representation. Also the integrals I_{3s}, I_{2d}, I_{1g} and I_{oi} act only in total L=0, 2,4 and 6 states respectively. I_{os} also acts in a unique SU_3 representation (60) and gives rise to degenerate spectra. It can be further seen that the radial integrals I_{1s}, I_{2s}, I_{od}, I_{1d}, I_{og} mix the space symmetric representation (60) and (22).

So far as the odd state integrals are concerned, one sees

that I_{2p}, I_{1f} and I_{oh} appear for the first time in this shell and hence they preserve SU_3 symmetry and act in (41) representation only. The radial integrals I_{1p}, I_{0f} violate SU_3 symmetry by mixing the space antisymmetric SU_3 representations (41) and (03). The radial integral I_{0p} has the same property as that of I_{os}. It preserves SU_3 symmetry in any shell by acting only in (2N-2,1) representation. In 1f-2p shell it acts only in (41) representation.

To summarise, we can say that in the central interaction of 1f-2p shell there are many SU_3 mixing radial integrals. The important among them are I_{1s}, I_{2s} and I_{1p}. Therefore the central interaction in 1f-2p shell is not very much SU_3 invariant. The important, SU_3 mixing component of 1d-2s shell is I_{1s}. But the central interaction in 1p shell is exactly SU_3 invariant.

At this stage we would like to make a few remarks about the work done by Vincent and others[18]. Vincent had shown that the central interaction in 1d-2s shell can be expressed in terms of multipoles which are the irreducible representations of SU_3. To be precise any central interaction in 1d-2s shell can be expressed as the linear combinations of irreducible representations (00), (22), (44) and (60) of SU_3 group. The properties of these different representations have been studied. It was found that

(44) part of the interaction is similar to pairing-like interaction while (22) part is expected to produce rotational spectrum. The (00) part determines the centroid energy of an SU_3 multiplet. The study of the properties of these different representation in turn throws light on the overall nature of the interaction. Vincent [18] studied the 's' state interactions in this scheme and arrived at the same conclusions as ours. But we would like to stress that not only our method of analysis is simple and straightforward but also it is very general and can be applied to any radial integrals in any shell. Vincent's method of analysis is unnecessarily complicated. Given radial integrals, our analysis can immediately infer the relative merit of the given two interactions. Moreover as we have seen, any central interaction can very well be expressed in terms of diagonal radial integrals. Therefore obviously our analysis does not suffer from any other inaccuracies. The analysis of central interaction in 1d-2s shell has also been made by Banerjee and Levinson[2]. They expanded the metrix elements of central interaction in terms of 10 basis interactions. But unfortunately this set of 10 basic interactions has no simple SU_3 transformation properties and therefore their analysis is not very useful in this respect.

REFERENCES

1) i) J.P. Elliott, Proc. Roy. Soc. A245 (1958) 128, 562.

ii) M. Harvey and J.P. Elliott Proc. Roy. Soc. A272 (1963) 557

2) i) M.K. Banerjee and C.A. Levinson, Phys. Rev. 130 (1963) 1036.

ii) T. Inoue et. al. Nucl. Phys. 59 (1964) 1.

iii) J.C. Parikh and K.H. Bhatt, Nucl. Phys. A103 (1967) 496.

3) i) S. Cohen, R.D. Lawson and S.P. Pandya, Nucl. Phys. A114 (1968) 541.

ii) S. Cohen, E.C. Halbert and S.P. Pandya, Nucl. Phys. A114 (1968) 353.

4) T.A. Brody and M. Moshinsky, Tables of Transformation Brackets, Monografias del instituto de Fisica, Universidad de Mexico (1960).

5) i) S.P. Pandya, Nucl. Phys. 43 (1963) 636.

ii) S.P. Pandya and I.M. Green, Nucl. Phys. 57 (1964) 658.

6) T.T.S. Kuo and G.E. Brown, Nucl. Phys. 85 (1966) 40.

7) i) C.M. Shakin, Y.R. Waghmare and M.H. Hull, Phys. Rev. 161 (1967) 1006.

ii) C.M. Shakin, Y.R. Waghmare, M. Tomaselli and M.H.Hull, Phys. Rev. 161 (1967) 1015.

8) H.A. Jahn, Proc. Roy. Soc. A201 (1950) 516.

9) B.H. Flowers, Proc. Roy. Soc. A210 (1952) 497.

10) J.P. Elliott and B.H. Flowers, Proc. Roy. Soc. A229 (1955) 526.

11) J.M. Jouch and E.L. Hill, Phys. Rev. 57 (1940) 641.

12) M. Harvey, in "Advances in Nuclear Physics" (Plenum Press, New York, 1968), Vol. I, p. 67.

13) D.R. Kulkarni and S.P. Pandya, Nuovo Cimento, 60B (1969) 100.

14) S.A. Moszkowski, Proceedings of the International Conference on Nuclear Structure, Kingston (University of Toronto Press, Toronto, 1960) p. 502.

15) S.P. Pandya, Phys. Lett. 7 (1963) 342.

16) E.U. Wigner, Phys. Rev. 51 (1937) 106.

17) M.G. Redlich, Phys. Rev. 110 (1958) 468.

18) i) C.M. Vincent, Nucl. Phys. A106 (1968) 35.

ii) Z. Pluhar, Phys. Lett. 29B (1969) 293.

CHAPTER III

The properties of 's' state interactions in Hartree-Fock formalism.

III.1 Introduction

After the study of the symmetry properties of 's' state interactions, in this chapter we will undertake the study of the properties of these interactions in the framework of Hartree-Fock (HF) formalism[1]. The HF theory has been well established[2] in the study of deformations of light nuclei especially for those in the 1d-2s shell. The HF approximation consists of assuming that each nucleon of the nucleus is moving independently in a potential field that is the sum of the interactions of this nucleon with all other nucleons of the nucleus. The formation of such an average potential is mainly caused by the field producing components of the two-body interaction. In other words, the HF theory essentially tries to extract a one-body potential from the field-producing components of the two-body interactions. It should be noted that the HF method does not respond well to the pairing component of the interaction, and the short-range correlations produced by this component are not adequately described in the framework of the HF formalism. But the success of HF formalism appears to suggest that the field-producing component plays a dominant role in many nuclear properties in 1d-2s shell. Extensive calculations have been performed[2] for 1d-2s shell

nuclei using various effective interactions in HF formalism. Surprisingly, the results obtained with quite different types of interactions are more or less similar. An essential characteristic of all HF calculations in 1d-2s shell is that the resulting self-consistent potentials are always non-spherical and generally carry quadrupole deformation. This is usually attributed to a dominant q.q type of component in the effective interaction. We look at this problem of deformations from an entirely different point of view.

To obtain a satisfactory understanding of results it is necessary to isolate the important components of the interaction and investigate the properties of each of these components in HF framework. Fortunately we know that the effective interactions in 1d-2s shell can be reasonably well approximated[3] in terms of central forces only. Hence the study of the properties of different 's' state interactions which are the important components of this interaction, in the HF formalism seem to be the next logical step in attempting to understand the results of HF calculations in 1d-2s shell. It is with this object that we have carried out the HF calculations employing 's' state interactions for even-even nuclei in 1d-2s shells. Before we present these results, we outline in brief the HF formalism and the associated technique of projection of good angular momentum states.

III.2 Hartree-Fock theory

The main aim of the HF theory is to obtain a single-particle potential and the single-particle wave functions. We then represent the intrinsic state $|\Phi\rangle$ of the nucleus to be just a Slater determinant of single nucleon orbits $|\lambda\rangle$ in that potential field. In the notation of second quantization we write

$$|\Phi\rangle = a^{+}_{\lambda_1} a^{+}_{\lambda_2} \cdots a^{+}_{\lambda_n} |0\rangle \qquad (1)$$

where a^{+} is the fermion operator which creates a particle in the state $|\lambda\rangle$. These operators obey the usual commutation relations. The nuclear Hamiltonian in the notations of second quantization is

$$H = \sum_{\alpha,\beta} \langle \alpha | t | \beta \rangle a^{+}_{\alpha} a_{\beta} + \frac{1}{4} \sum_{\alpha,\beta,\gamma,\delta} \langle \alpha\beta | v | \gamma\delta \rangle a^{+}_{\alpha} a^{+}_{\beta} a_{\delta} a_{\gamma} \qquad (2)$$

where $\langle \alpha\beta | v | \gamma\delta \rangle = - \langle \alpha\beta | v | \delta\gamma \rangle$ is an antisymmetrized matrix element of the two-body interaction V.

To obtain the orbits $|\lambda\rangle$ of the Slater determinant $|\Phi\rangle$, we use a variational principle. These orbits are so obtained that the energy of the system described by the wave function in eqn.(1) is stationary for infinitesimal variations of the orbits λ. The energy of the system is obtained by taking the expectation value of the Hamiltonian equations (2) in the state of eq.(1).

$$E_{HF} = \langle \Phi | H | \Phi \rangle = \sum_{\lambda=1}^{A} \langle \lambda | t | \lambda \rangle + \frac{1}{2} \sum_{\lambda,\mu=1}^{A} \langle \lambda\mu | v | \lambda\mu \rangle \qquad (3)$$

where E_{HF} is called HF energy, $\langle \lambda | t | \lambda \rangle$ is the kinetic energy of the orbit λ .

It is convenient to expand the orbits on some basis j of known wave functions

$$| \lambda \rangle = \sum_{j} c_j^{\lambda} | j \rangle \qquad (4)$$

The basis j may be the set $| n \ell j m_\tau \rangle$ of shell model states in a harmonic oscillator. In fact any basis may be used to expand the orbits, provided one is able to calculate matrix elements of the interaction V with the basis states. The set of orbits λ is assumed to form an orthonormal set of wave functions

$$\sum_{j} c_j^{\lambda *} c_j^{\lambda'} = \delta_{\lambda\lambda'}, \qquad \sum_{\lambda} c_j^{\lambda *} c_{j'}^{\lambda} = \delta_{jj'} \qquad (5)$$

The wave function $| \Phi \rangle$ is determined by the coefficients c_j^{λ} which become variational parameters. The energy will be stationary with the normalisation condition (6) when

$$\frac{\partial}{\partial c_j^{\lambda *}} \left[\langle \Phi | H | \Phi \rangle - e_\lambda \sum_{j} c_j^{\lambda *} c_j^{\lambda} \right] = 0 \qquad (6)$$

Here e_λ is introduced as a Lagrange multiplier. Using the expansion (5) of the orbits, the energy $\langle \emptyset | H | \emptyset \rangle$ in eq. (6) can be expressed in terms of known matrix elements of 't' and 'v' in the basis j. The derivative (7) may then be calculated directly and one obtains

$$\sum_{j'} \left[\langle j | t | j' \rangle + \sum_{\lambda=1}^{A} \sum_{j_1 j_2} C_{j_1}^{\lambda *} C_{j_2}^{\lambda} \langle j j_1 | v | j' j_2 \rangle \right] C_{j'}^{\lambda} = e_\lambda C_j^{\lambda} \quad (7)$$

The equation has the form of an eigenvalue problem

$$\sum_{j'} \langle j | h | j' \rangle C_{j'}^{\lambda} = e_\lambda C_j^{\lambda} \quad (8)$$

where h is the HF Hamiltonian given by its matrix elements as

$$\langle j | h | j' \rangle = \langle j | t | j' \rangle + \sum_{\lambda=1}^{A} \langle j \lambda | v | j' \lambda \rangle$$

$$= \langle j | t | j' \rangle + \sum_{\lambda=1}^{A} \sum_{j_1 j_2} C_{j_1}^{\lambda *} C_{j_2}^{\lambda} \langle j j_1 | v | j' j_2 \rangle \quad (9)$$

The equations (8) and (9) are the HF equations for the orbits λ. They may be solved by well-known iteration procedure.

The iteration process is somewhat complicated by the fact that there are many local minimas of energy (3) and therefore many solutions[4] of HF equations. Various minimas may be reached by various initial guesses and therefore these are very critical inputs.

1. Single major shell Hartree-Fock calculations:-

The expansion of the HF orbit in (4) depends i) on the kind of solution one wants, and ii) on the configuration space chosen for the calculations. For our purpose we carry out the calculations in the space of a single major oscillator shell : i.e for configurations $(ds)^n$. Also it is sufficient to illustrate the points by considering nuclei only with N=Z=even. Further

we look for an axially symmetric deformed self-consistent potential. Therefore we will expand orbit λ as

$$|\lambda\rangle = \sum_j C_j^{\lambda} \; | j \; m_\lambda \; m_{\tau_\lambda} \rangle$$

where $j = 1d_{5/2}, 2s_{1/2}, 1d_{3/2}$ for 1d-2s shell

In the single major shell HF calculations, the intrinsic $|\phi\rangle$ is reqritten as

$$|\Phi\rangle = a^+_{\lambda_1} a^+_{\lambda_2} - - - a^+_{\lambda_A} |\Phi_0\rangle$$

where $|\phi_0\rangle$ state corresponds to the reference nucleus. Thus ^{16}O nucleus is used as the reference nucleus for 1d-2s shell nuclei. We assume that this reference nucleus is inert so far as the properties of nuclei are concerned. Therefore the HF self-consistency problem need be solved only for a few valence particles outside this reference nucleus (which is also called 'core'). In this restricted HF calculations, the expression for the HF energy reduces to

$$E_{HF} = E_0(c) + \sum_{\lambda=c+1}^{A} \left[\epsilon_\lambda + \frac{1}{2} \sum_{\lambda,\mu=c+1}^{A} \langle \lambda\mu | v | \lambda\mu \rangle \right] \quad (10)$$

Generally ϵ_λ are taken as the experimental s.p. energies appropriate for the core (in the 1d-2s shell, taken from ^{17}O spectrum though ideally they should be the result of the HF calculations for the core nucleus. E_0 (c) is taken as the experimental binding energy of the core. In fact, usually one only calculates the energy of the nucleus relative to the core.

$$E_{HF} - E_0(C)$$

$$= \sum_{\lambda=C+1}^{A} [\epsilon_\lambda] + \frac{1}{2} \sum_{\lambda,\mu=C+1}^{A} \langle \lambda\mu | V_A | \lambda\mu \rangle$$

$$= \frac{1}{2} \sum_{\lambda=C+1}^{A} \epsilon_\lambda + \left[\frac{1}{2} \sum_{\lambda=C+1}^{A} \epsilon_\lambda + \frac{1}{2} \sum_{\lambda,\mu=C+1}^{A} \langle \lambda\mu | V_A | \lambda\mu \rangle \right]$$

$$= \frac{1}{2} \sum_{\lambda=C+1}^{A} [\epsilon_\lambda + e_\lambda] \qquad (11)$$

It should be noted that the HF energy presented in our later results is the same as in eq. (11) and not the absolute energy of the whole nucleus.

The justification of the assumption of inert core can be given in two ways. It makes the calculations easier and faster. Secondly the work of Redlich[5], Kurath and Picman[6] had shown that the wave functions obtained from intermediate-coupling shell model calculations are very similar to those obtained by projecting states of good angular momentum from the intrinsic states obtained by the above procedure.

2. The projection of good angular momentum states.

In general the HF intrinsic state is a deformed one and does not have a good angular momentum. To relate the HF wave functions to the experimentally observed nuclear states of definite angular momentum, the projection formalism is used. There are basically

two methods used to obtain the nuclear states which have a good angular momentum from deformed HF wave functions. i) the adiabatic approximation ii) angular momentum projection. In fact it can be shown that the method of adiabatic approximation becomes equivalent to the angular momentum projection when the deformation is very large. We give here only the relevant formulae used in the angular momentum projection method which is quite standard and well-established for deformed HF solutions[2].

The angular momentum projection method was first developed by Peierls and Yoccoz[7] for the axially deformed HF solutions. They solved the Hill-Wheeler integral equation[8] by using the angle of rotation of the symmetry axis as the collective coordinate. In other words they have shown that the function of the angle of rotation of the symmetry axis to be determined variationally in the solution of Hill-Wheeler integral equation is a simple rotation matrix element. Later the results of Kurath and Picman[6] have justified the validity and usefulness of this method.

If $|\phi\rangle$ is the axially deformed HF intrinsic state, then it can be written as

$$|\Phi_K\rangle = \sum_J a_K^J \, |JK\rangle$$

In order to obtain a particular state of good angular momentum j and projection M, we write

$$|JMK\rangle = P^J_{MK} \; |\varphi_K\rangle$$

where the projection operator P^J_{MK} is defined as

$$P^J_{MK} = \frac{2J+1}{8\pi^2} \int d\Omega \; D^{J*}_{MK}(\Omega) \, R(\Omega)$$

Now we will calculate the matrix element of an operator T^k_q between the two different projection states $|J_1 \; M_1 \; K_1\rangle$ and $|J_2 \; M_2 \; K_2\rangle$. The expression can be obtained[2] easily for the axially deformed states and is written as

$$\langle \psi^{J_1}_{M_1 K_1} | T^k_q | \psi^{J_2}_{M_2 K_2} \rangle = \left(\frac{2J_2+1}{2}\right) C(J_2 M_2 K q \,|\, J_1 M_1) \times$$

$$\sum_{M\nu} C(J_2 M K \nu \,|\, J_1 K_1) \int_0^\pi d\beta \sin\beta \; d^{J_2}_{MK_2}(\beta) \langle \phi_{K_1} | T^k_\nu \, e^{-i\beta J_y} | \phi_{K_2} \rangle$$

$$\Big/ \left[N_{J_1 K_1} \cdot N_{J_2 K_2} \right]^{1/2}$$

where $N_{J_1 K_1}$ and $N_{J_2 K_2}$ are the normalization constants. They can be given as

$$N_{JK} = \frac{2J+1}{2} \int_0^\pi d\beta \sin\beta \; d^J_{KK}(\beta) \langle \phi_K | e^{-i\beta J_y} | \phi_K \rangle$$

If we take a Hamiltonian operator H which is a scalar, the above expression becomes quite simple and we get the expectation value of H in the projected states as

$$E_J = \langle \psi^J_{MK} | H | \psi^J_{MK} \rangle$$

$$= \int_0^\pi d\beta \sin\beta \; d^J_{MK}(\beta) \langle \phi_K | H e^{-i\beta J_y} | \phi_K \rangle$$

$$\Big/ \int_0^\pi d\beta \sin\beta \; d^J_{MK}(\beta) \langle \phi_K | e^{-i\beta J_y} | \phi_K \rangle$$

III.3 The HF calculations using 's' state interaction in 1d-2s shell.

In this section we present the results of axially deformed HF calculations obtained with the 's' state interactions. These calculations have been carried out for even-even N=Z nuclei in 1d-2s shell viz. ^{20}Ne, ^{24}Mg, ^{28}Si. We have also projected the states of good angular momentum and calculated their energies for these nuclei. We have further compared the HF results for ^{20}Ne with the shell model results obtained using the same interactions. In other cases shell model results are not available.

We have used the following two-body matrix elements in all calculations.

a) Two-body matrix elements calculated with I_{0s} = -10 MeV and all other radial integrals assumed to be zero.

b) Two-body matrix elements using I_{1s} = -10 MeV and all other radial integrals assumed to be zero.

c) Two-body matrix elements employing I_{2s} = -10 MeV and all other radial integrals equated to zero.

d) Two-body matrix elements using all 's' state integrals (i.e. $I_{0s} + I_{1s} + I_{2s}$). The value of each radial integrals is taken from the results of Cohen et al[4].

e) We used the two-body matrix elements obtained by using all the radial integrals whose values are determined by Cohen et al[4]. by fitting the spectra of O and F isotopes.

In cases a,b,c,d we use degenerate single-particle levels $d_{5/2}$, $s_{1/2}$ and $d_{3/2}$. Essentially we switch off l.l and l.s interactions. In case e , we use the l.l and l.s interaction so that the single particle levels are non-degenerate. The energies of these non-degenerate levels both for neutrons and protons are given below.

$\epsilon(1d_{5/2}) = 0$ MeV, $\epsilon(2s_{\frac{1}{2}}) = 0.87$ MeV, $\epsilon(1d_{3/2}) = 5.0\ 8$ MeV

Thus it should be noted that the case e) is the most realistic case so far as the interactions are concerned. Finally it should be noted that all the nuclei discussed here are even-even and have N=Z nucleons and so possess time-reversal as well as isospin invariance. Therefore each single particle orbit has four-fold degeneracy with two neutrons and two protons in it. We will now study the results obtained using different interactions listed above separately.

a) I_{Os} interaction:

This interaction acts only in singlet-even (S=0, T=1) and triplet-even (S=1, T=0) states. In order to study purely the properties of two-body interaction, we switch off the single particle spin-orbit and l.l interactions. Also to ensure the spin and isospin independence of two-body interaction, we use $I_{Os} = -10$ MeV both for singlet-even and triplet-even states.

The prolate HF solutions for ^{20}Ne, ^{24}Mg and ^{28}Si have been obtained and the states of good angular momentum are projected from

those solutions. The oblate HF solution of ^{28}Si has also been obtained but it is found to be energetically degenerate with the prolate solution. Table 1 gives the structure of the single particle wavefunctions of prolate HF solution of ^{20}Ne. The single particle orbitals for ^{24}Mg or ^{28}Si are not given separately, since we find that the structure of single particle wavefunctions is identical for all three nuclei for this interaction, although the energy of each orbital varies from nucleus to nucleus. In figure 1 we give the single particle energy spectra for prolate solutions of ^{20}Ne, ^{24}Mg and ^{28}Si and oblate solutions of ^{28}Si. Another significant feature to be noted is that the structure of the single particle wave functions is exactly the same as that for a pure quadrupole field, although the energy separations are not quite the same. Moreover the degeneracies observed in the spectrum of Q_o^2 are also present in the spectrum of I_{os}. This leads to the conclusion that in the HF orbitals of I_{os} interaction, there is maximum possible mixing of s and d states of 1d-2s shell. Since the mixing of s and d states is a measure of deformation, I_{os} interaction gives maximum possible deformation. It is also possible to describe these HF orbitals in (lm) representation (see table 1). For example in ^{20}Ne, k=0 orbital (in (lm) representation) is completely filled. In ^{24}Mg k=1 orbital is partially filled (i.e. k=3/2 is filled but k=$\frac{1}{2}$ is still empty). This partial occupancy in ^{24}Mg is reflected in the slight splitting of k=$\frac{1}{2}$ and k=3/2 levels and other unoccupied levels. But this

FIG. III · 1

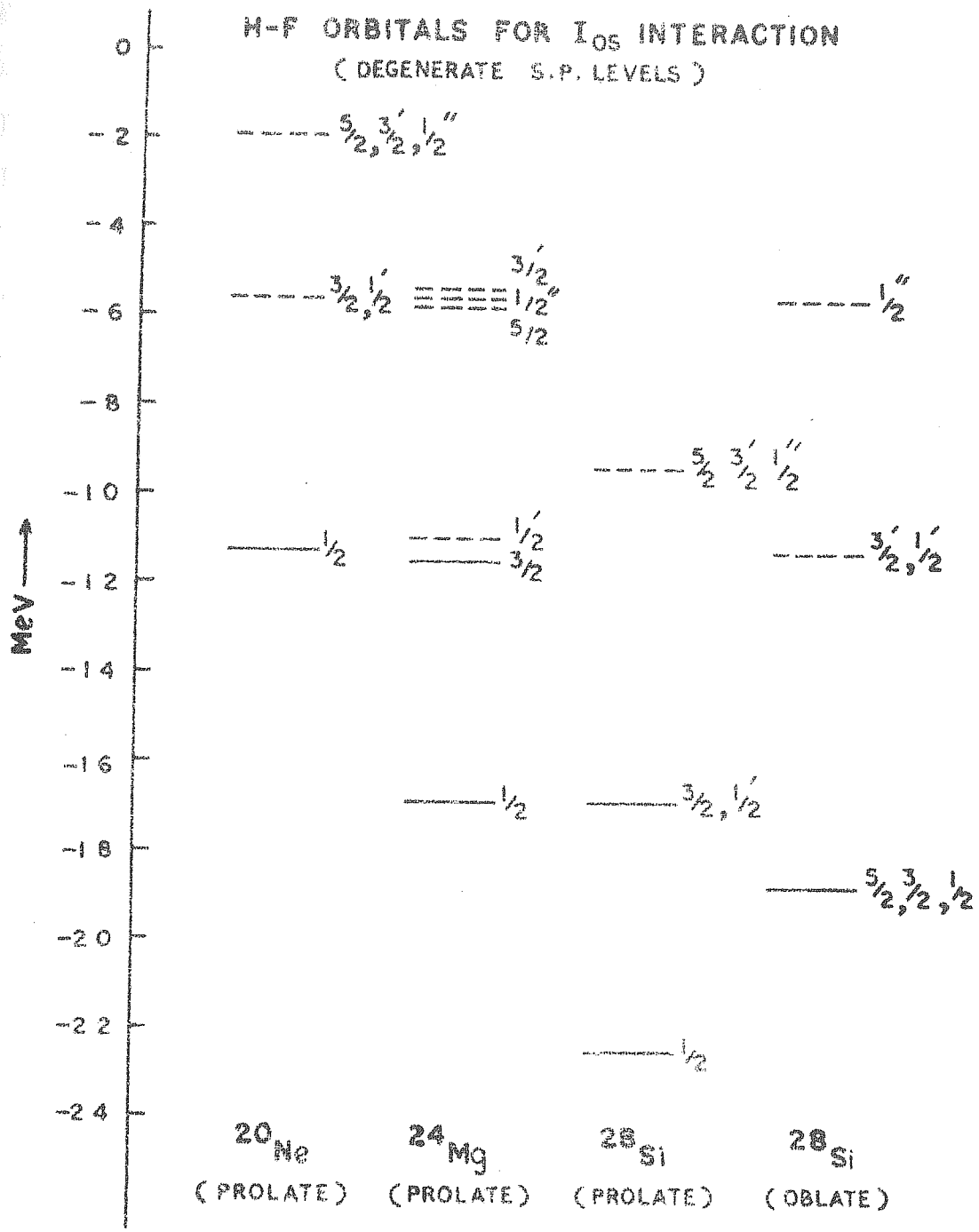
H-F ORBITALS FOR I_{OS} INTERACTION
(DEGENERATE S.P. LEVELS)
0
-2
-4
-6
-8
-10
-12
-14
-16
-18
-20
-22
-24
MeV
$5/2, 3/2', 1/2''$
$3/2, 1/2'$
$3/2''$
$1/2$
$5/2$
$1/2''$
$5/2\ 3/2'\ 1/2''$
$1/2$
$1/2'$
$3/2$
$3/2', 1/2'$
$1/2$
$3/2, 1/2'$
$5/2, 3/2, 1/2$
$1/2$
^{20}Ne (PROLATE)
^{24}Mg (PROLATE)
^{28}Si (PROLATE)
^{28}Si (OBLATE)

splitting is removed when k=½ orbital is also filled as we see in the case of ^{28}Si. In both ^{20}Ne and ^{28}Si, there is a sizable HF gap but in ^{24}Mg it is very small. Therefore the axially deformed HF ground state will not be a good representation of ^{24}Mg nucleus. This is all the more true as I_{os} is the dominant component in the total interaction. In fact it has been found[2] that the ^{24}Mg triaxial solution is lower than the axial solution. It should be noted that the oblate solution of ^{28}Si can be obtained by inverting the energy sequence of single particle orbits of prolate solution of ^{28}Si. The degeneracy of prolate and oblate solutions of ^{28}Si can be explained as follows. We have seen in chapter 2 that I_{os} gives SU_3 symmetry. From SU_3 point of view prolate HF solution of ^{28}Si has (12,0) SU_3 representation while the oblate solution has (0,12) representation. From SU_3 considerations, both the solutions are degenerate. The I_{os} interaction being SU_3 invariant retains this degeneracy.

The HF binding energy and the projected spectra of ^{20}Ne, ^{24}Mg and ^{28}Si (oblate) have been displayed in figure 2. It can be seen that the contribution to HF binding energy of I_{os} interaction is quite large. The distinguished feature of the projected spectra of all nuclei is that all J=0,2,4,6 and 8 states projected from K=0 HF intrinsic ground states are degenerate with the HF energy of the corresponding nucleus. The slight splitting observed in ^{24}Mg is attributed to the partial occupancy of the levels as we have seen before. The degeneracy of the projected spectrum is

FIG. III.2

H-F PROJETED SPECTRA
l_{OS} INTERACTION WITH DEGENERATE S.P. LEVELS

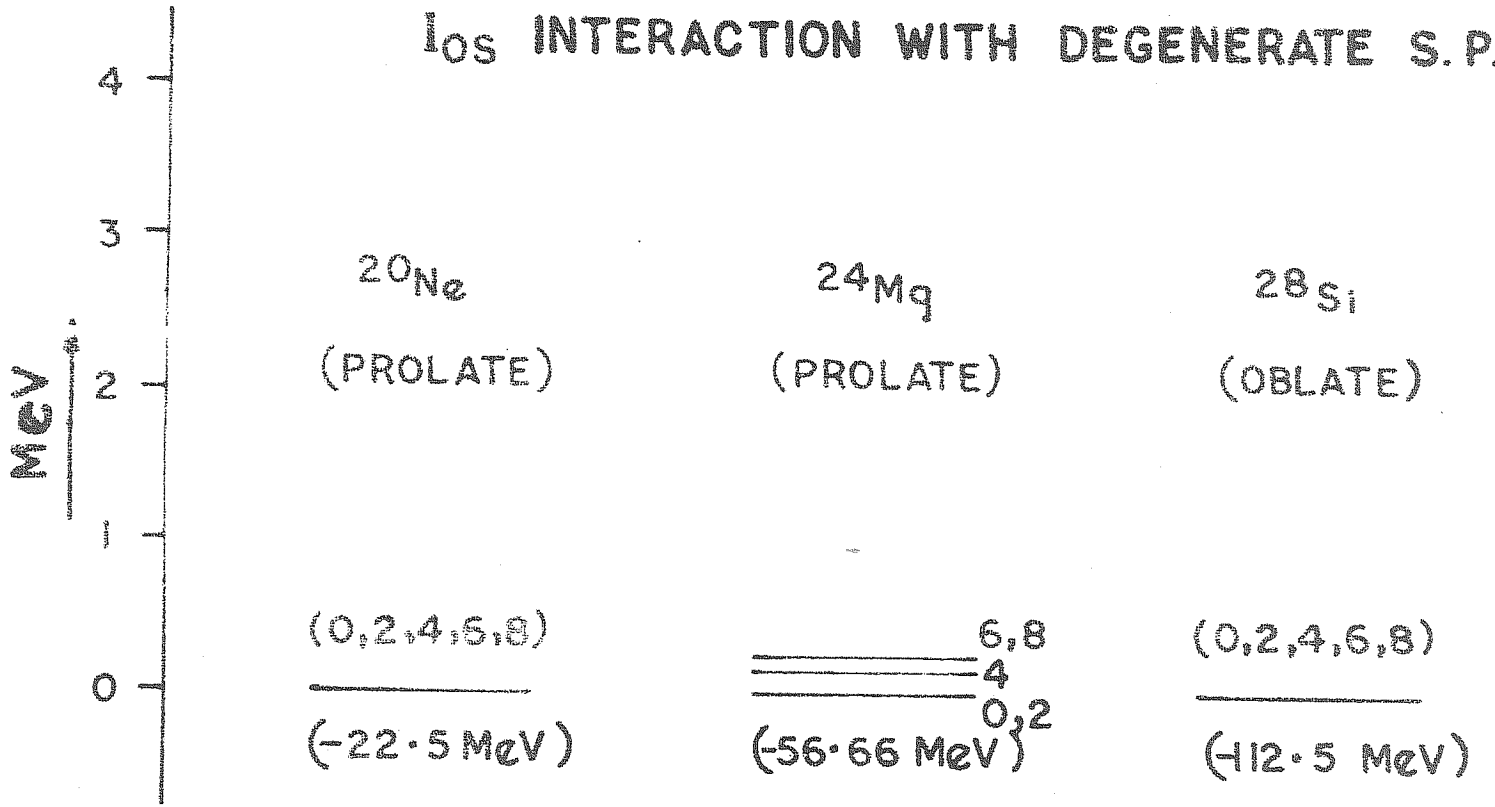

explained by the fact that I_{os} interaction can be expressed[9] as a linear combination of Casimir operator and Majorana operator. Both of these operators do not split the states of different J values.

Another effect which is characteristic of HF calculations is the effect of spin-polarization. This effect is seen quite nicely in the case of ^{24}Mg. In ^{24}Mg orbitals $k=\frac{1}{2}$ and $k=3/2$ are completely occupied. The orbital $k=\frac{1}{2}$ is the $k=0$ state in (lm) representation with spin-projection $+\frac{1}{2}$. Similarly the orbitals $k=3/2$ and $k=\frac{1}{2}'$ are obtained by coupling d_1 state with the spin angular momentum $\frac{1}{2}$, when the spin-projection is $+\frac{1}{2}$ for $k=3/2$ orbital and $-\frac{1}{2}$ for $k=\frac{1}{2}'$ orbital. The fact that we have in our calculations forced occupation of the orbital $k=3/2$ and not $k=\frac{1}{2}'$ has an effect on the ordering of unoccupied levels. In other words the orbitals with spin-projection $+\frac{1}{2}$ will be lower than those with $-\frac{1}{2}$. This explains why out of the orbitals coming from $k=2$, the orbital $k=5/2$ with spin projection $+\frac{1}{2}$ is lower than orbital $k=3/2'$ with spin-projection $-\frac{1}{2}$.

b) I_{ls} interaction

We have carried out the deformed HF calculations for the same set of nuclei using this interaction. This interaction also acts only in singlet-even and triplet-even states. As in case of I_{os} interaction, we have used degenerate single particle levels and put $I_{ls} = -10$ MeV for both singlet-even and triplet-even states.

Table III.1

Single Particle HF orbitals for Ios interaction

k	$S_{1/2}$	$d_{3/2}$	$d_{5/2}$	(lm) representation
1/2	-0.5773	-0.5164	0.6325	$\sqrt{2/3}\ d_o - \sqrt{1/3}\ s_o$
3/2	0	-0.4472	0.8944	d_1
1/2'	0	0.7746	0.6325	d_1
5/2	0	0	1.0	d_2
3/2'	0	0.8944	0.4472	d_2
1/2''	0.8165	-0.3651	0.4472	$\sqrt{1/3}\ d_o + \sqrt{2/3}\ s_o$

The HF single particle wave functions for prolate solutions ^{20}Ne, ^{24}Mg and ^{28}Si and for oblate solution of ^{28}Si are given in tables 2 to 5. The single particle energy levels for the same solutions are displayed in figure 3. It should be noted that unlike for I_{os} interaction, the oblate and prolate solutions of ^{28}Si are not degenerate. This can be explained due to non-invariant nature of I_{ls} interaction under the SU_3 transformation. Figure 4 shows the states J = 0, 2, 4, 6 and 8 projected from the

FIG. III·3

H-F ORBITALS FOR l_{ls} INTERACTION

(DEGENERATE S.P. LEVELS)

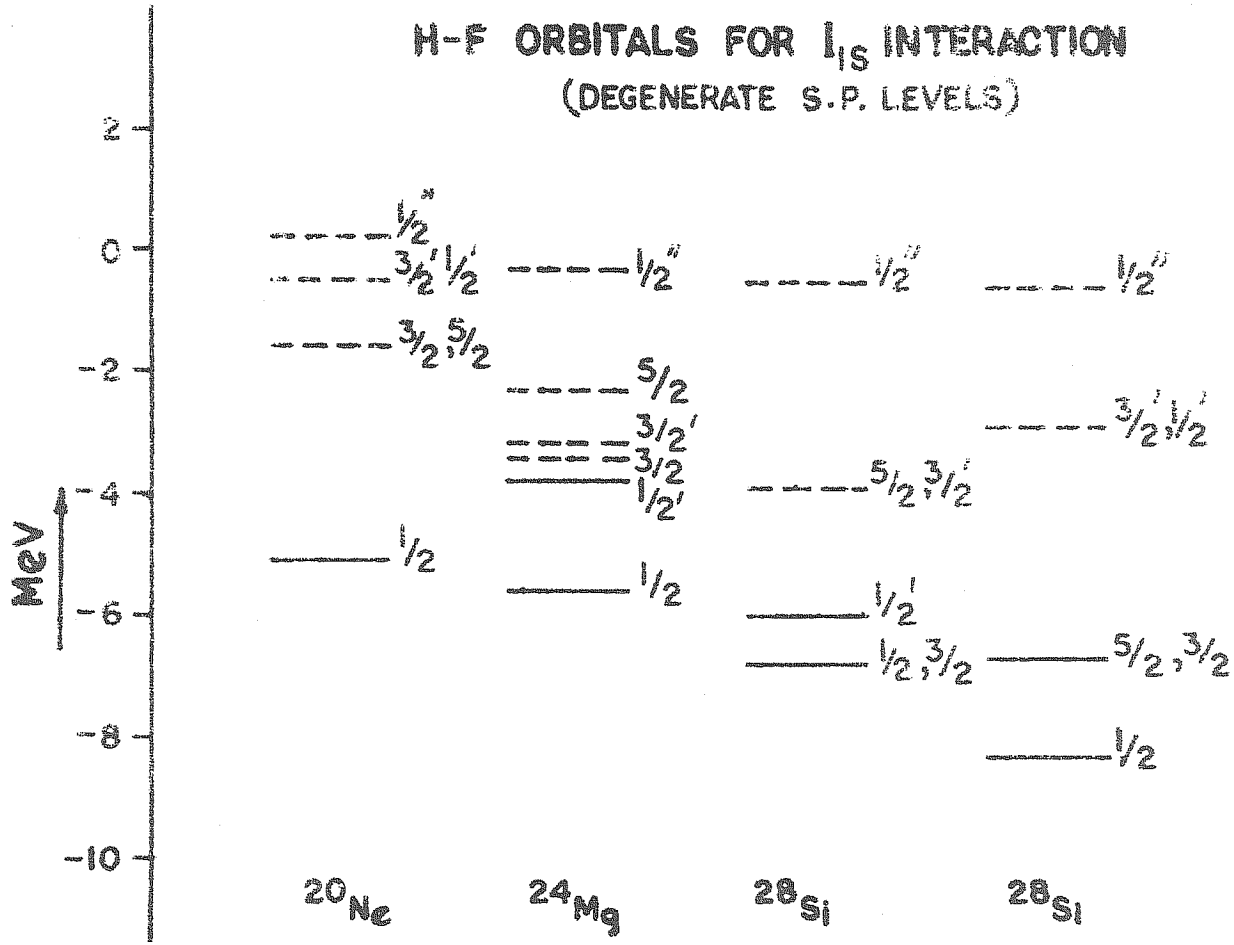

FIG. III · 4

H-F PROJECTED SPECTRA

I_{IS} INTERACTION WITH DEGENERATE S.P. LEVEL

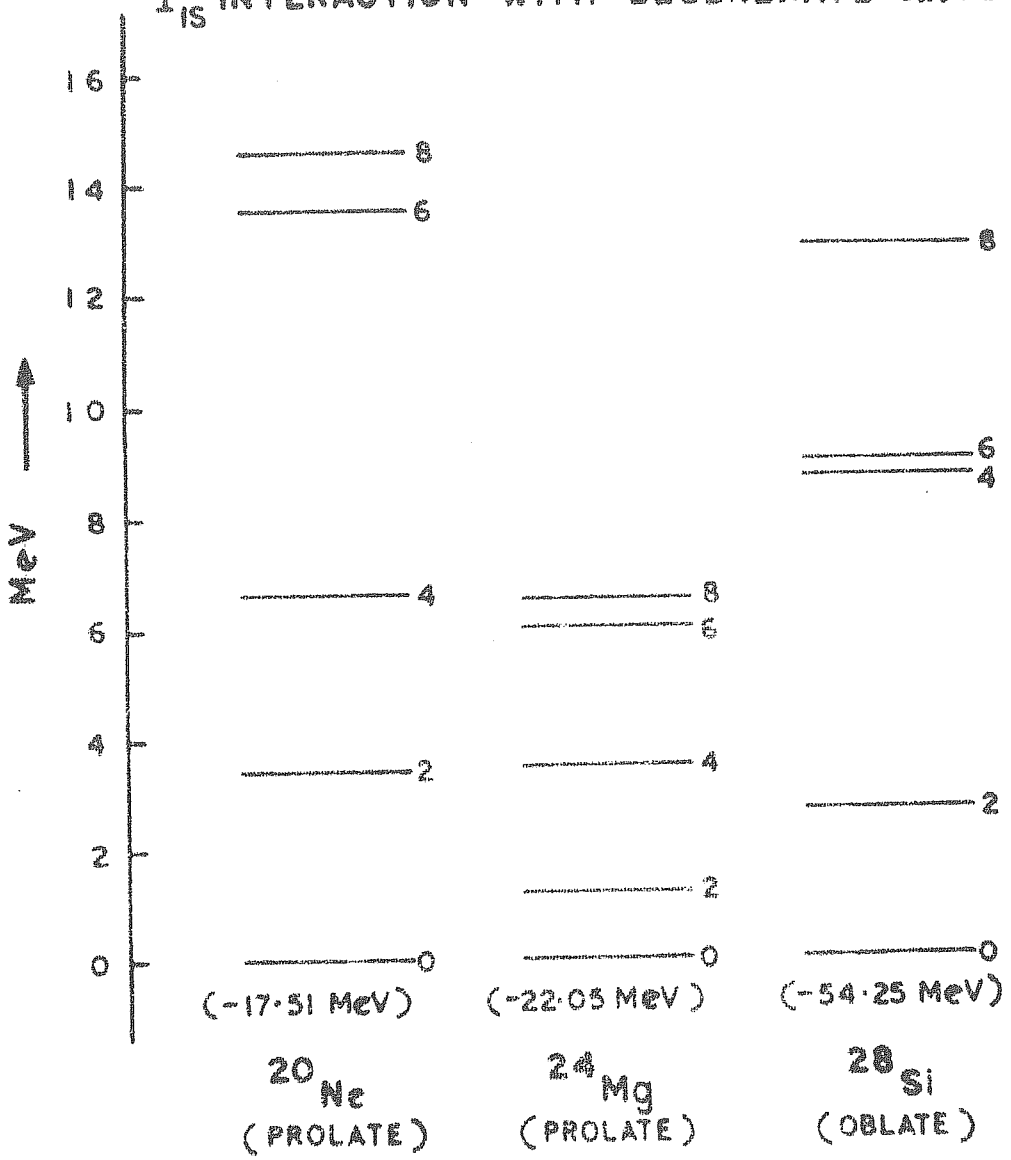

HF intrinsic ground states of ^{20}Ne (prolate), ^{24}Mg (prolate) and ^{28}Si (oblate) which is lower than the prolate solution by 4.35 MeV.

The structure of HF orbitals and their energy sequence can be qualitatively understood as follows. The interaction I_{ls} can be looked upon as the admixture of $Q^2 . Q^2$ and $Q^4 . Q^4$ interactions. We will not consider the monopole part of the interaction as it does not play any part in deciding the ordering of the HF orbitals.

Table III.2 also gives the ^{20}Ne HF orbitals in (lm) representation. It can be seen that the total quadrupole moment of ^{20}Ne intrinsic state is only 10.08 b^2 (b is harmonic oscillator constant) while the hexadecapole moment is about 18.0 b^4. Thus, the ^{20}Ne HF field in this case is dominantly a hexadecapole field and hence the ordering of levels will be mainly governed by Q_o^4 field. The observed order d_o, d_2, d_1 and S_o is consistent with this interpretation except for the position of S_o. This state in the pure hexadecapole field should have been lower than the d_1 state which has a negative Q_o^4 moment. But as we have seen above, there is also a fairly large Q_o^2 field along with the Q_o^4 field present in the HF field of ^{20}Ne. This field tries to push the level S_o above the level d_1 as the Q_o^2 moment of S_o is negative (-0.5 b^2) while that of d_1 is about 2 b^2. The observed degeneracy of levels belonging to d_2 and d_1 levels can also be explained in this way. Thus one feels that it is the competition of relative strengths of Q_o^2 and Q_o^4 multipoles that ultimately decides the ordering of levels.

Similarly the ordering of levels of ^{24}Mg can also be explained in the same way. The HF intrinsic state of ^{24}Mg has (see table 3) 14.8 units of Q_o^2 moment and the + 6 units of Q_o^4 moment. Obviously the HF field now is dominantly a Q_o^2 field. In the pure Q_o^2 field one would have expected the ordering of levels as d_o, d_1, S_o and d_2. The pure positive Q_o^4 field has following order viz. d_o, d_2, S_o and d_1. The competition between these fields will decide the order. Since Q_o^2 field is dominant, the ordering is mainly that of Q_o^2 except that the positions of S_o and d_2 are exchanged. However, the Q_o^4 moment of d_2 (0.75 b^4) is larger than that of S_o (zero), therefore the positive Q_o^4 field lowers the d_2 level. This explains the observed sequence and also shows the importance of Q_o^4 field in deciding it.

The HF orbitals of ^{28}Si (prolate) can be easily understood in a similar way. The HF intrinsic state of ^{28}Si has 19.52 units of Q_o^2 moment and - 6 units of Q_o^4 moment. The ordering of the levels will be the result of the competition between the positive Q_o^2 and negative Q_o^4 fields. The pure positive Q_o^2 field will arrange the levels in the following order, d_o, d_1, S_o and d_2. The negative Q_o^4 field will arrange the levels like d_1, S_o, d_2 and d_o. The observed sequence will be dependent on the relative strengths of Q^2 and Q^4 multipoles. The slightly higher energy of d_o with respect to d_1 may be due to the positive Q_o^4 moment of d_o level. The fact that S_o is higher than d_2 may be attributed to the fact S_o observed in this solution is really not a pure 's' state. Also

d_o obtained in this solution is also not a pure 'd' state.

Similarly a qualitative understanding of the sequence of levels for oblate solution of ^{28}Si can be obtained. For this solution the positive Q_o^4 field is dominant, hence the ordering follows the sequence of Q_o^4 field. The fact that S_o remains higher than d_1 shows the importance of Q_o^2 field also. Moreover the degeneracies observed in the solution of ^{28}Si are consistent with our interpretation.

So far as the HF binding energies are concerned I_{1s} component does not contribute much. In spite of the fact that for both I_{os} and I_{1s} components strength of the interaction is chosen the same, the contribution to the HF binding energy due to I_{1s} component is almost half of that due to I_{os} component. The states of good angular momentum are projected from these HF intrinsic states. As shown in figure 4, it is observed that this interaction gives rise to non-degenerate spectra for all the nuclei. Obviously the spectra are not expected to be rotational as there seems to be a considerable Q_o^4 component contained in this interaction. The important point to be stressed is that unlike I_{os} interaction, it gives rise to non-degenerate spectra.

The final remark about this interaction is that its contribution to the HF gaps is also smaller than that of I_{os} interaction, even though the strength of both the interactions is the same.

Table III.2

The HF orbitals of ^{20}Ne for I_{ls} interaction

(E_{HF} = -10.21 MeV)

K	$s_{1/2}$	$d_{3/2}$	$d_{5/2}$	(lm) representation
1/2	-0.0917	-0.6298	0.7713	$\approx d_0$
3/2	0	0.8944	0.4472	d_2
5/2	0	0	1	d_2
3/2'	0	-0.4472	0.8944	d_1
1/2'	0	0.7746	0.6325	d_1
1/2''	0.9958	-0.0580	0.0711	$\approx s_0$

Table III.3

The HF orbitals of ^{24}Mg for I_{ls} interaction

(E_{HF} = -18.79 MeV)

K	$s_{1/2}$	$d_{3/2}$	$d_{5/2}$	(lm) representation
1/2	-0.1315	-0.6270	0.7679	$\approx d_0$
1/2'	0	0.7746	0.6328	d_1
3/2	0	-0.4472	0.8944	d_1
3/2'	0	0.8944	0.4472	d_2
5/2	0	0	1.0	d_2
1/2''	0.9913	-0.0832	0.1019	$\approx s_0$

Table III.4

The HF orbitals of ^{28}Si (prolate) for I_{1s} interaction

(E_{HF} = -39.13 MeV)

k	$s_{1/2}$	$d_{3/2}$	$d_{5/2}$	(lm) representation
1/2	0	0.7746	0.6325	d_1
3/2	0	-0.4472	0.8944	d_1
1/2'	-0.1673	-0.6235	0.7636	$\approx d_0$
5/2	0	0	1.0	d_2
3/2'	0	0.8944	0.4472	d_2
1/2''	0.9858	-0.1061	0.1300	$\approx s_0$

Table III.5

The HF orbitals of ^{28}Si (oblate) for I_{1s} interaction

(E_{HF} = -43.48 MeV)

k	$s_{1/2}$	$d_{3/2}$	$d_{5/2}$	(lm) representation
1/2	0.0649	-0.6311	0.7730	$\approx d_0$
5/2	0	0	1.0	d_2
3/2	0	0.8944	0.4472	d_2
3/2'	0	-0.4472	0.8944	d_1
1/2'	0	0.7746	0.6325	d_1
1/2''	0.9979	0.0411	-0.0503	$\approx s_0$

c) I_{2s} interaction

We have obtained the axially deformed HF solutions for ^{20}Ne (prolate), ^{24}Mg (prolate), ^{28}Si (prolate) and ^{28}Si (oblate) using I_{2s} = -10 MeV and degenerate single particle levels. Table 6 shows the structure of the HF orbitals obtained for all these nuclei. Figure 5 shows the HF single particle spectra and figure 6 shows the projected spectra obtained for all these nuclei.

The structure of the HF orbitals is very simple and similar for all the nuclei. The lowest state is always a pure "s" state. The other states are pure "d" states and are much higher than the "s" state. Another important feature is the constant energy (-6.25 MeV) of the lowest "s" state for all the nuclei. These general features can be explained as follows:

The I_{2s} interaction acts in singlet-even and triplet-even states only. Further, it has been demonstrated[10] earlier that this interaction operates only in L=0 two-particle states (J=0, T=1 and J=1, T=0 states) and exhibits a pairing like property. It can also be seen that the j-j coupling matrix elements $\langle \frac{1}{2}\frac{1}{2} | I_{2s} | \frac{1}{2}\frac{1}{2} \rangle$ for J=0, T=1 and J=1, T=0 states are equal and the largest of all other matrix elements. Naturally the variation procedure gives the lowest state as a pure "s" state. Another conspicuous feature of this interaction is that being a pairing type interaction it can operate only when the two particles are in the time-reserved states of each other in

Table III.6

HF orbitals for I_{2s} interaction

k	$s_{1/2}$	$d_{3/2}$	$d_{5/2}$
1/2	1.0	0.0023	-0.0028
1/2'	0	-0.6325	0.7746
1/2''	0	0.7746	0.6325
3/2	0	0	1.0
3/2'	0	1.0	0
5/2	0	0	1.0

(lm) representation. For example a particle in the state d_1 interacts only with a particle in the state d_{-1}. We also know that the only non-zero matrix elements of the I_{2s} interaction will be of the three types given below.

$\langle d_{k1}\, d_{-k1} \mid V \mid d_{k2}\, d_{-k2} \rangle$, $\langle d_{k1}\, d_{-k1} \mid V \mid s^2 \rangle$ and $\langle s^2 \mid V \mid s^2 \rangle$.

But in the H-F calculations, the off-diagonal elements of the type $\langle d_{k1}\, d_{-k1} \mid V \mid s^2 \rangle$ will not appear. The matrix elements of the type $\langle d_{k1}\, d_{-k1} \mid V \mid d_{k2}\, d_{-k2} \rangle$ also

FIG. III · 5

H-F ORBITALS FOR I_{2S} INTERACTION

(DEGENERATE S.P. LEVELS)

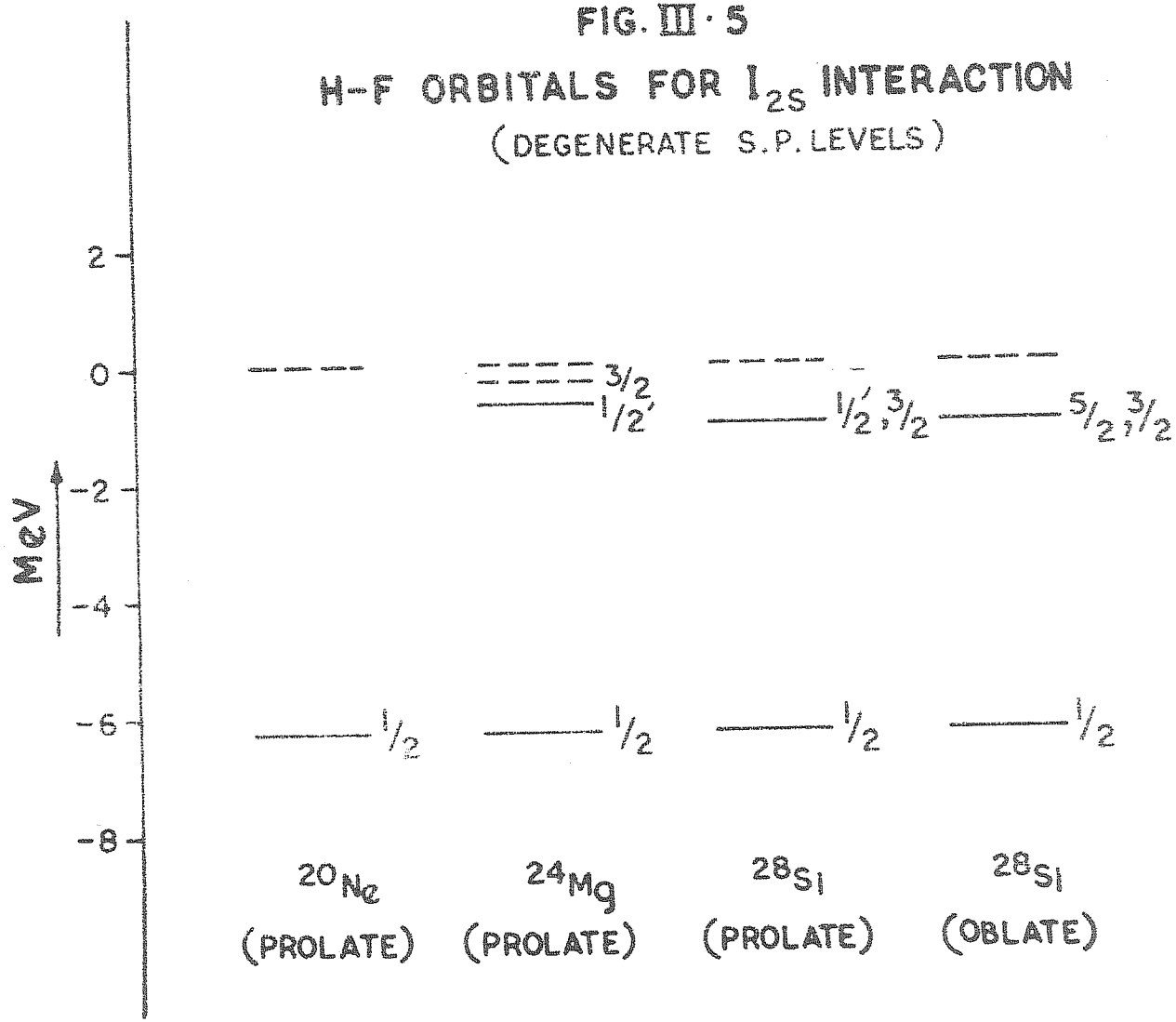

FIG · III · 6

H-F PROJECTED SPECTRA

I_{2S} INTERACTION WITH DEGENERATE S.P. LEVELS

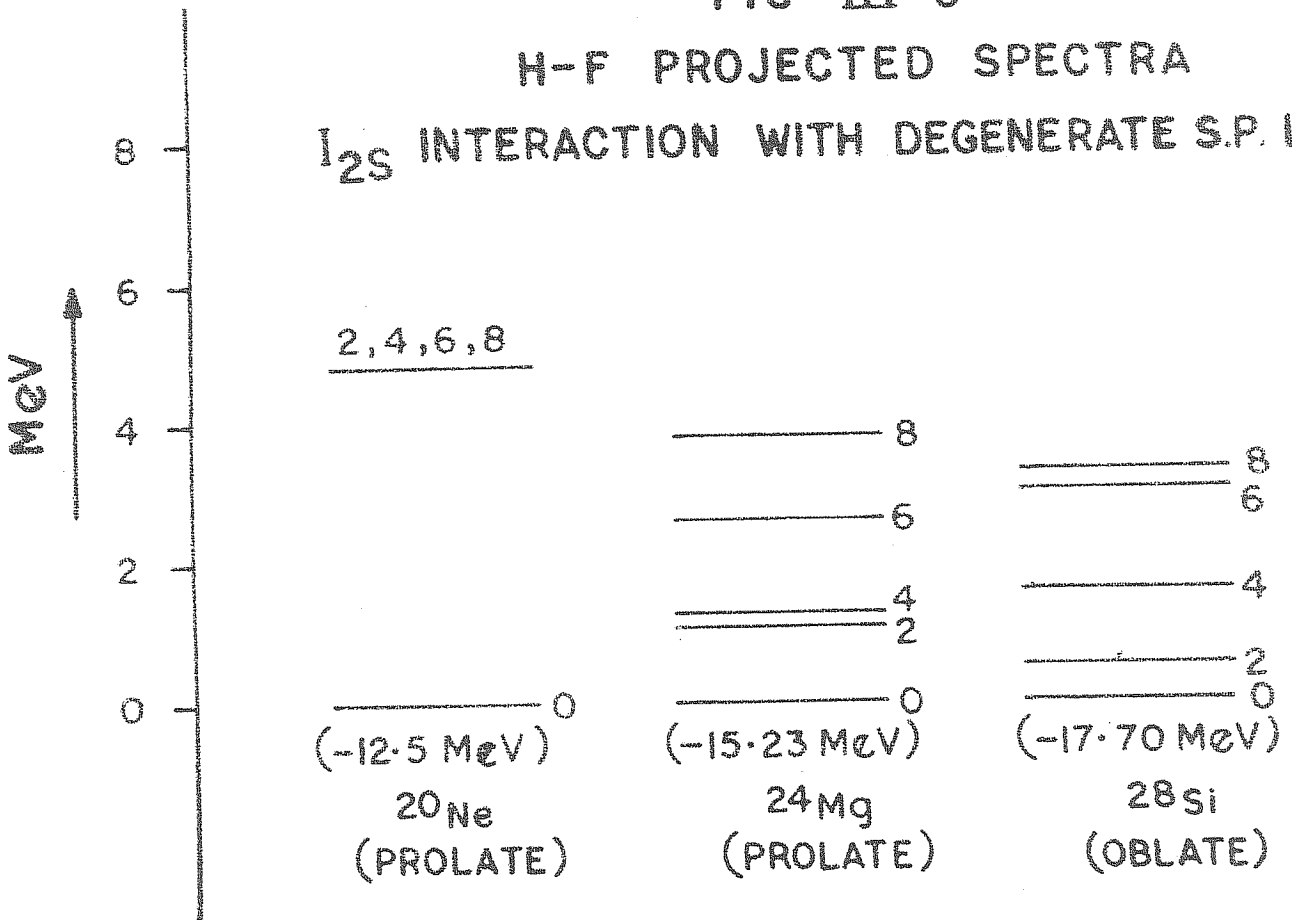

become diagonal and take the form $\langle d_{k1}\, d_{-k1} \mid V \mid d_{k1}\, d_{-k1} \rangle$. In other words the HF field of the I_{2s} interaction is due to only the diagonal matrix elements of the type $\langle s^2 \mid V \mid s^2 \rangle$ and $\langle d_{k1}\, d_{-k1} \mid V \mid d_{k1}\, d_{-k1} \rangle$. Naturally there is no interaction between different "d" and "s" single particle orbitals. This particular feature explains the constancy of the energy of the lowest "s" state.

It is obvious that in ^{20}Ne all the unoccupied "d" states are degenerate at zero energy since these states do not interact with the occupied "s" state. In ^{24}Mg the initial choice of the intrinsic (HF) state is such that the orbital $k = 3/2$ is also filled completely with four nucleons. Since the orbital $k = 3/2$ in the lm representation corresponds to the state d_1 and its time-reversal state $k = -3/2$ corresponds to the state d_{-1}, it is expected that the nucleons in the state d_1 will interact with those in the state d_{-1}. It can be further argued that since the interaction in the "d" states is quite weak compared to that in the "s" state, the energy of the d orbital is much smaller than that of the s orbitals. Surprisingly the lowest unoccupied orbital $k = 1/2'$ in ^{24}Mg is not at zero energy. This is expected because the orbital $k = 1/2'$ also comes from the state d_1. Thus the particles in the orbital $k = 3/2$ will definitely interact with those in the unoccupied orbital $k = 1/2'$. Hence the orbital $k = 1/2'$ is also slightly depressed compared to other unoccupied orbitals. In ^{28}Si (prolate) the both orbitals $k = 3/2$ and

k=1/2' are fully occupied. In other words both d_1 and d_{-1} states are fully occupied. Thus, now there will be more number of particles to interact with in this state and, therefore, the d_1 and d_{-1} states are depressed more. Consequently the orbital k=3/2 in ^{28}Si (prolate) is more depressed than in ^{24}Mg.

Another interesting consequence of this peculiar behaviour of the interaction is very well seen in ^{24}Mg. The total interaction in d_1 state is -1.0 MeV as seen in ^{28}Si. This total energy of the state d_1 is distributed between the occupied orbital k=3/2 and unoccupied orbital k=1/2' of the HF solution of ^{24}Mg.

In the ^{28}Si (oblate) solution the orbitals d_2 and d_{-2} are occupied completely. But it seems that the interaction between the particles in the d_2 and d_{-2} states is the same as that in the d_1 and d_{-1} states. This is apparent from the fact that the energy of the orbital d_2(-1.0 MeV) in the oblate solution of ^{28}Si is same as that of d_1 in the prolate solution. The essential difference between the interaction in the states d_1 and d_2 lies in the appearance of different Clebsch-Gorden coefficients corresponding to different projection values. But in this particular case they differ in sign only. Since in the actual calculations only the squares of these Clebsch-Gorden coefficients appear, the interactions in the orbitals d_1 and d_2 are essentially same. As we go from prolate to oblate solution, we find the positions of the orbitals d_1 and d_2 are exchanged. This is natural as the oblate quadrupole field will obviously prefer the d_2 state which has negative Q_0^2 moment.

So far as the HF gap is concerned, this interaction contributes to the extent how strongly the particles in the highest occupied orbitals interact with each other. In ^{20}Ne the particles in the "s" state interact very strongly and we got large HF gap. On the other hand in ^{28}Si, the interaction in 'd_1' state is quite weak and hence we got small gap. In ^{24}Mg, the particles in the occupied orbital k = 3/2 interact not only with each other but also with the unoccupied orbital k = 1/2'. As a result the total energy is divided between the orbitals k = 3/2 and k = 1/2' giving us very small HF gap.

The HF binding energy due to this interaction is slightly larger than that due to I_{1s} interaction but much smaller than that due to I_{os} interaction. For example, the HF energy of ^{20}Ne (prolate) solution is -12.49 MeV while that of ^{24}Mg (prolate) solution is -13.83 MeV. The prolate and oblate solution of ^{28}Si are degenerate to the HF energy -16.49 MeV. The projected spectra due to this interaction are shown in figure 6 for nuclei viz. ^{20}Ne, ^{24}Mg and ^{28}Si (oblate). It should be noted that the oblate and prolate solutions of ^{28}Si for this interaction are degenerate. The reason for this degeneracy is again the SU_3 symmetric nature of the I_{2s} interaction. It should be noted that the I_{2s} interaction also gives rise to non-degenerate spectra except for ^{20}Ne nucleus. For the nucleus ^{20}Ne, only J = 0 state can be projected and thus essentially this interaction depresses the J = 0 state only.

d) All 's' state integrals:

For this case we have used all the 's' state integrals viz. I_{0s}, I_{1s} and I_{2s}. The values of these radial integrals are taken from those obtained by Cohen et al[4]. These values are given in table 3 of chapter two. It should be noted that the 's' state radial integrals for singlet-even and triplet-even states are now different. Therefore, the interaction has now become spin-isospin-dependent. As in the previous cases, we have used only the degenerate single particle levels. Table 7 to 10 give the HF orbitals for different nuclei while figure 7 gives the HF single particle energy spectra. Figure 8 displays the projected spectra for ^{20}Ne, ^{24}Mg and ^{28}Si (oblate).

We note that the HF energy for the prolate solution of ^{28}Si is slightly lower than that for the oblate solution. This is most probably because of the introduction of spin-isospin dependence of the interaction. If the spin-isospin independent interaction would have been used, one would have expected oblate solution to be lower in energy than the prolate one as I_{1s} interaction prefers oblate solution while the interactions I_{0s} and I_{2s} give both the solutions degenerate.

The most remarkable feature of all the solutions is their close resemblance with the solution for I_{0s} interaction. The overlaps of these wave functions with those for the I_{0s} interaction

Table III.7

^{20}Ne HF orbitals for all 's' state radial integrals.

(E_{HF} = -25.49 MeV)

k	$s_{1/2}$	$d_{3/2}$	$d_{5/2}$
1/2	-0.5141	-0.5425	0.6644
3/2	0	-0.4472	0.8944
1/2'	0	0.7746	0.6325
1/2''	0.8577	-0.3251	0.3982
5/2	0	0	1
3/2'	0	0.3944	0.4472

Table III.8

^{24}Mg HF orbitals for all 's' state integrals.

(E_{HF} = -61.86 MeV)

k	$s_{1/2}$	$d_{3/2}$	$d_{5/2}$
1/2	-0.5287	-0.5368	0.6575
3/2	0	-0.4472	0.8944
1/2'	0	0.7746	0.6325
5/2	0	0	1.0
1/2''	0.8488	-0.3344	0.4096
3/2'	0	0.3944	0.4472

Table III.9

^{28}Si (prolate) HF orbitals for all 's' state radial integrals

(E_{HF} = -125.79 MeV)

k	$s_{1/2}$	$d_{3/2}$	$d_{5/2}$
1/2	-0.5406	-0.5321	0.6516
3/2	0	-0.4472	0.8944
1/2'	0	0.7746	0.6325
5/2	0	0	1.0
3/2'	0	0.8944	0.4472
1/2''	0.8413	-0.3419	0.4188

Table III.10

^{28}Si (oblate) HF orbitals for all 's' state radial integrals

(E_{HF} = -124.69 MeV)

k	$s_{1/2}$	$d_{3/2}$	$d_{5/2}$
5/2	0	0	1.0
3/2	0	0.8944	0.4472
1/2	0.7789	-0.3804	0.4659
3/2'	0	-0.4472	0.8944
1/2'	0	0.7746	0.6325
1/2''	-0.6015	-0.5052	0.6188

FIG. III . 7

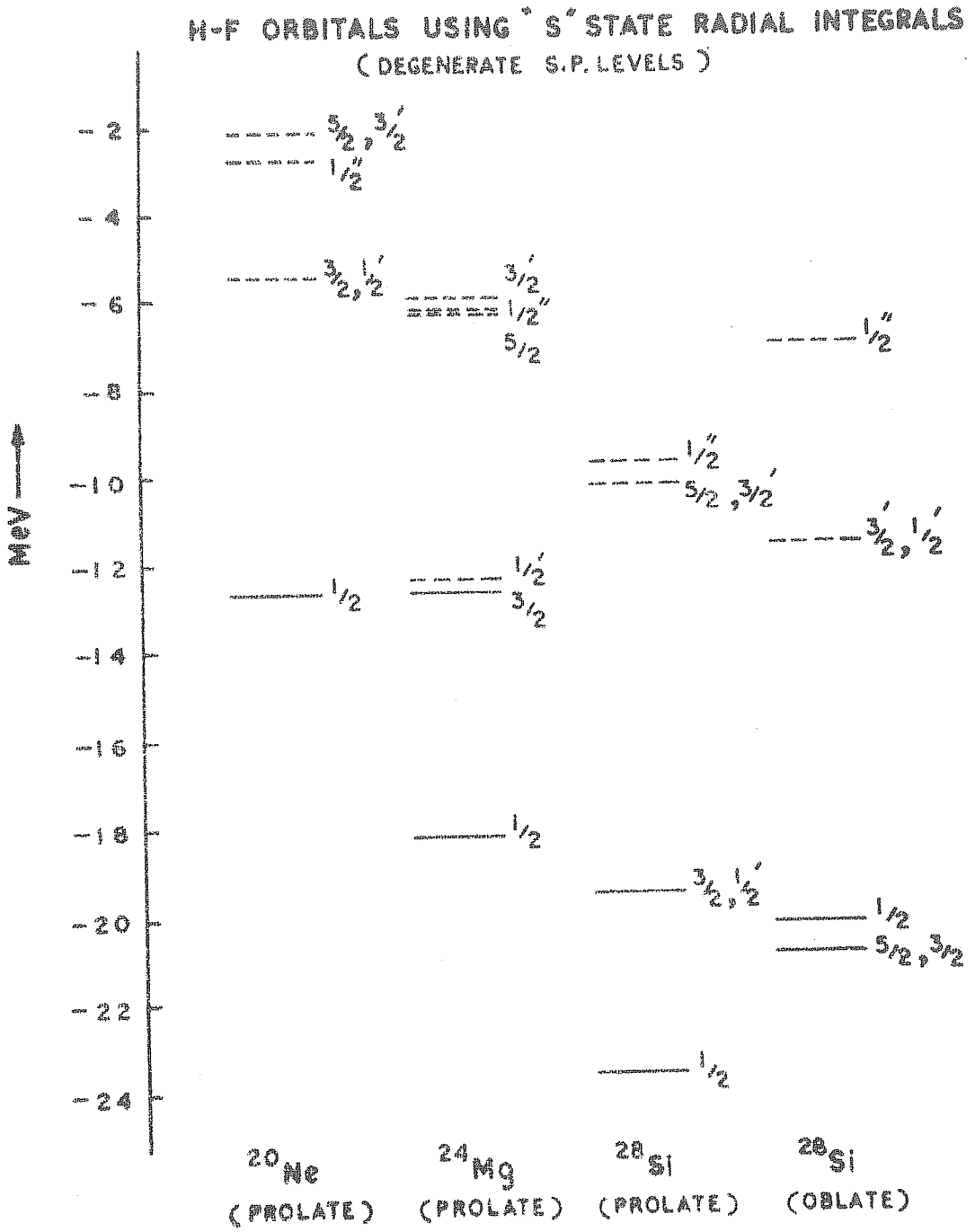
H-F ORBITALS USING "S" STATE RADIAL INTEGRALS
(DEGENERATE S.P. LEVELS)
MeV
2
4
6
8
10
12
14
16
18
20
22
24
5/2 , 3/2
1/2"
3/2 , 1/2
3/2
1/2"
5/2
1/2"
5/2 , 3/2
3/2 , 1/2
1/2
1/2
3/2
1/2
3/2 , 1/2
1/2
5/2 , 3/2
1/2
20Ne (PROLATE)
24Mg (PROLATE)
28Si (PROLATE)
28Si (OBLATE)

FIG. III·8

H-F PROJECTED SPECTRA

ALL "S" INTERACTIONS WITH DEGENERATE S.P. LEVELS

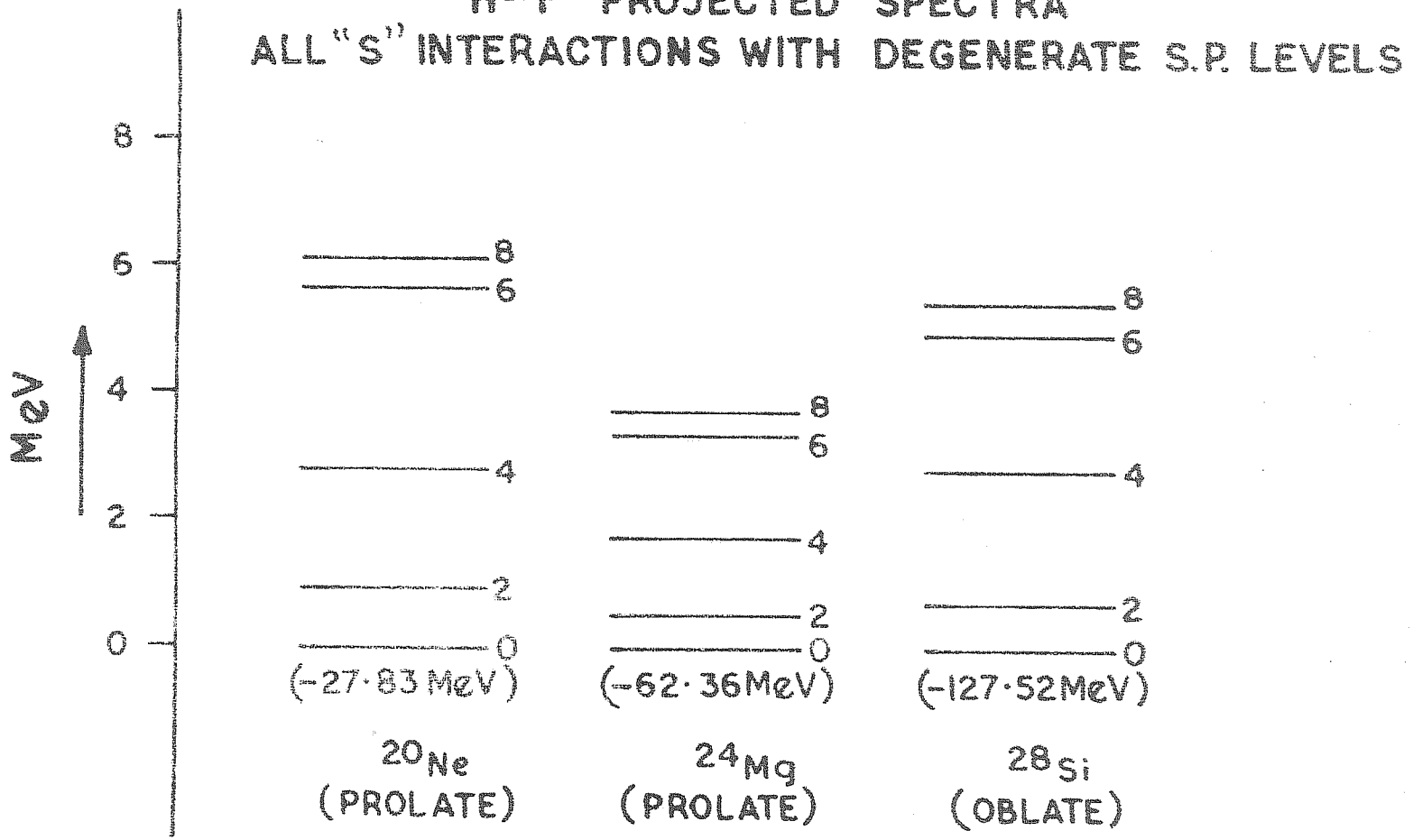

alone are very large. The reason for these almost asymptotic solutions lies in the fact that I_{0s} is the most dominant interaction among all the 's' state interactions. It is, therefore, not surprising that the ordering of HF orbitals in all the nuclei is governed by this component only. Another important point to be noted is the existence of degeneracies for the levels corresponding to d_1 (orbitals 1/2' and 3/2) and d_2 (orbitals 3/2' and 5/2) states. These degeneracies exactly correspond to that of the level scheme of Q_0^2. However, there is a slight splitting of levels corresponding to state d_2 and the orbital k=1/2". This splitting has been caused by the existence of $(Q^4.Q^4)$ force contained in the 's' state interaction. Therefore, we conclude that the 's' state interaction in 1d-2s shell contains both a dominant $Q^2.Q^2$ and a weak $Q^4.Q^4$ interaction apart from the monopole interaction.

The projected spectra in figure 8 show that the spectra are quite non-degenerate for all the nuclei. This splitting is entirely due to the components I_{1s} and I_{2s}. Also the comparison of the HF binding energy of all the nuclei for the interactions a) and d) will show that most of the binding comes from the I_{0s} component of the interaction.

e) All radial integrals (total interaction)

We have also obtained the HF solutions for the same nuclei using all the radial integrals. These integrals are obtained by fitting the spectra of Oxygen and Flourine isotopes. We have listed these integrals both for T=0 and T=1 states in Chapter two. It should be noted that the radial integrals for states T=0 and T=1 are different. Further we also now have radial integrals in relative p,d.f and g states. The radial integrals in 'd' and 'g' states are quite weak but attractive. Thus we use a complete interaction along with the single particle spectrum observed in ^{17}O. Obviously this is the most realistic situation. Tables 11 to 14 give the HF orbitals for ^{20}Ne, ^{24}Mg, ^{28}Si (prolate)and ^{28}Si (oblate) while the Figure 9 shows their HF single particle energy spectrum. Also figure 10 displays the projected spectra for ^{20}Ne, ^{24}Mg and ^{28}Si (oblate).

The inclusion of single particle l.s and l.l splitting of 's' and 'd' states has many effects on the results of HF calculations. First of all the single particle spin-orbit interaction mixes different permutation symmetries and to that extent it mixes different SU_3 representations also. In other words the simple nature of the interaction is lost. So far as the structure of HF orbitals is concerned, we observe that they cannot be described now in a simple (lm) representation. Especially we note that among the unoccupied orbitals, the orbital k=½' corresponds to pure d_1

Table III.11

^{20}Ne HF orbitals using all radial integrals

(E_{HF} = -20.59 MeV)

k	$s_{1/2}$	$d_{3/2}$	$d_{5/2}$
1/2	-0.5483	-0.3656	0.7521
3/2	0	-0.2584	0.9660
1/2'	0.5212	0.5539	0.6493
5/2	0	0	1.0
1/2''	-0.6540	0.7480	-0.1132
3/2	0	0.9660	0.2584

Table III.12

^{24}Mg HF orbitals using all radial integrals

(E_{HF} = -48.71 MeV)

k	$s_{1/2}$	$d_{3/2}$	$d_{5/2}$
1/2	-0.5104	-0.3711	0.7757
3/2	0	-0.3192	0.9977
1/2'	0.2543	0.7966	0.5484
1/2''	-0.8215	0.4772	-0.3122
5/2	0	0	1.0
3/2'	0	0.9477	0.3192

Table III.13

^{28}Si (prolate) HF orbitals using all radial integrals

(E_{HF} = -91.09 MeV)

k	$s_{1/2}$	$d_{3/2}$	$d_{5/2}$
1/2	-0.4917	-0.3425	0.8006
3/2	0	-0.3444	0.9388
1/2'	0.2363	0.8325	0.5013
1/2''	0.8351	-0.4357	0.3284
5/2	0	0	1.0
3/2'	0	0.9388	0.3444

Table III.14

^{28}Si (oblate) HF orbitals using all radial integrals

(E_{HF} = -92.46 MeV)

k	$s_{1/2}$	$d_{3/2}$	$d_{5/2}$
5/2	0	0	1.0
1/2	0.8683	-0.2412	0.4335
3/2	0	0.8006	0.5992
3/2'	0	-0.5992	0.8006
1/2'	-0.2348	0.5699	0.7875
1/2''	0.4370	0.7855	-0.4382

FIG. III·9

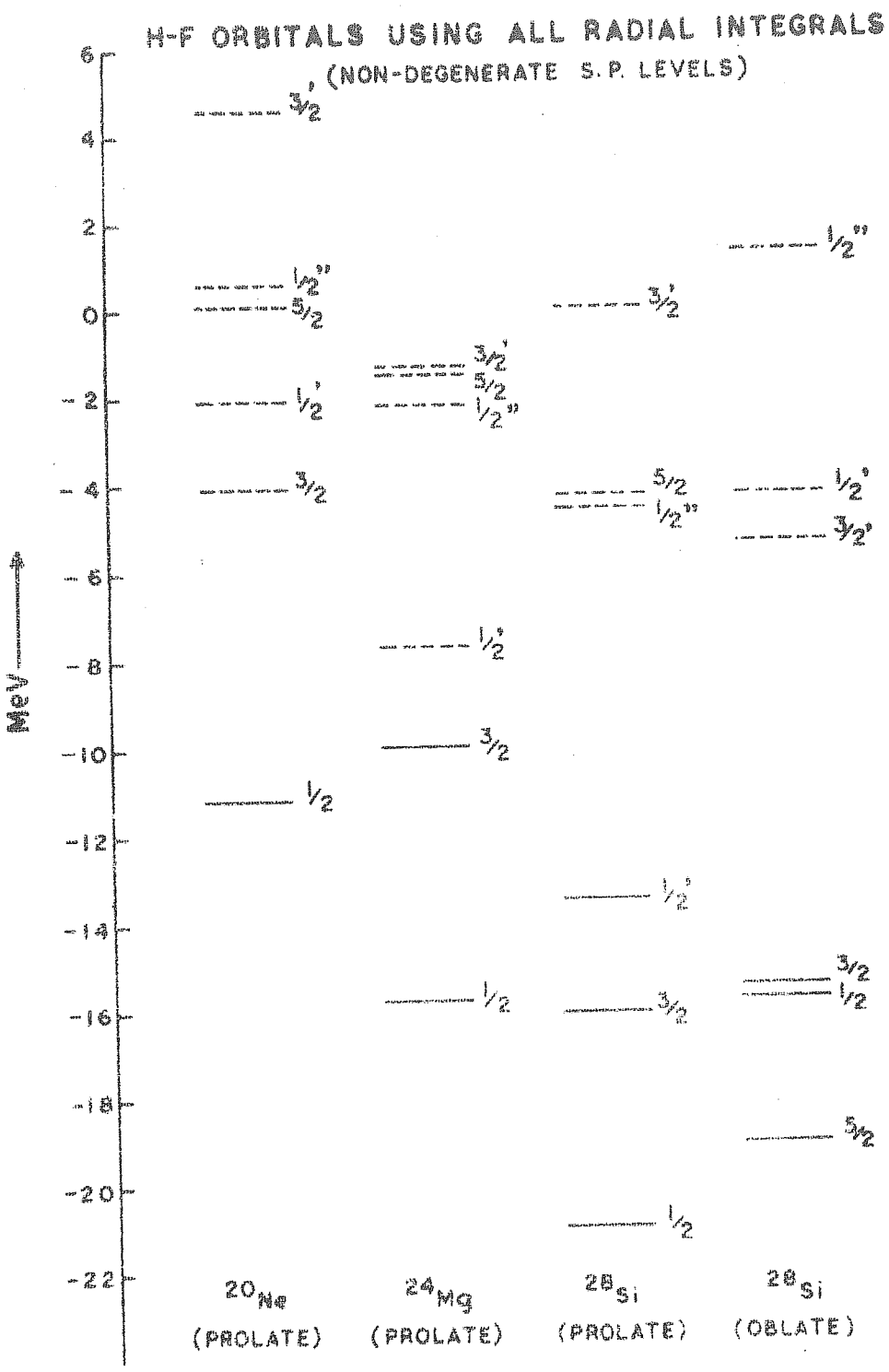
H-F ORBITALS USING ALL RADIAL INTEGRALS
(NON-DEGENERATE S.P. LEVELS)
MeV
6
4
2
0
-2
-4
-6
-8
-10
-12
-14
-16
-18
-20
-22
3/2'
1/2''
5/2
1/2'
3/2
3/2'
5/2
1/2''
1/2'
3/2
1/2
3/2'
1/2''
5/2
1/2'
3/2'
1/2'
3/2
1/2
3/2
1/2
5/2
1/2
20Ne (PROLATE)
24Mg (PROLATE)
28Si (PROLATE)
28Si (OBLATE)

FIG. III·10

H-F PROJECTED SPECTRA

ALL RADIAL INTEGRALS WITH NONDEGENERATE S.P. LEVELS

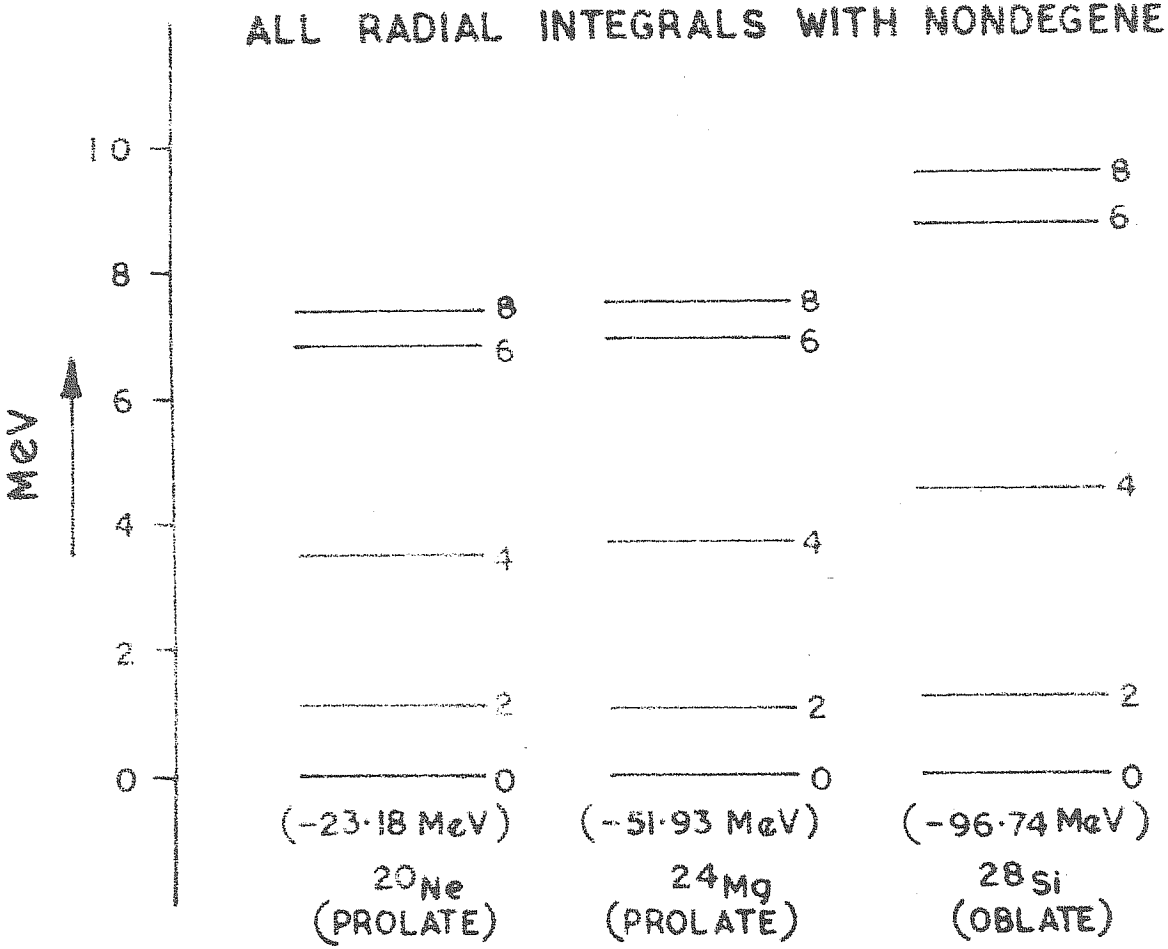

state in the absence of l-s and l-l splitting, whereas its structure changes considerably when this splitting is taken into account. This would have significant consequences on the structure of the excited k=0 bands of ^{20}Ne. Also the degeneracies that are observed in the absence of l.s interaction do not exist any more. The orbitals k=½' and k=3/2 and k=5/2 and k=3/2' get split up. It is also seen that this l.s interaction just readjusts the relative strength of $d_{5/2}$ and $d_{3/2}$ components keeping $s_{1/2}$ components intact. In general however it is clear that the structure and ordering of HF orbitals has been mainly influenced by the dominant I_{0s} component. It is also observed that the HF gap in ^{20}Ne and ^{28}Si (oblate) decreases while in ^{24}Mg and ^{28}Si (prolate) it increases. This effect may be partly because of l.s and l.l splitting of 's' and 'd' states and may be partly due to the presence of odd repulsive integrals present in the interaction.

Another important observation is that there is a reduction of HF binding energy of all the nuclei. This may be again partly because of splitting of single particle levels and partly due to the presence of repulsive odd state interactions. We also note that in this case the oblate HF solution of ^{28}Si is lower in energy than the prolate solution. However, it may be noted that the HF energies for both the solutions are quite close to each other and therefore a good description of ^{28}Si may require the mixing of these two shapes. The projected spectrum is stretched by an almost constant scale factor of 1.2 as we go from case d)

to case e). In other words the essential effect of spin-orbit splitting is to change the moment of inertia of the band.

III.4 Comparison with shell model:

In table 15 we have given the shell model spectra of ^{20}Ne obtained using interactions a), b), c) and e). It may be noted that along with the two-body interactions a), b) and c), we have used the degenerate single particle levels while the interaction e) is used along with non-degenerate single particle levels of ^{17}O. These shell model calculations have been performed for us by E.C. Halbert[11]. It is interesting to see that for I_{os} interaction the shell model and HF projected spectra agree perfectly. For I_{1s} interaction, the shell model J=0 state is 0.7 MeV below J=0 projected state. However, the overall agreement except for J=8 state is not bad. For case c, the shell model spectrum is the result of configuration mixing of $d_{5/2}$, $d_{3/2}$ and $s_{1/2}$ states while the HF projected spectra result from the sole configuration $(s_{\frac{1}{2}})^4$. Therefore the spectra are completely different. The results of shell model calculations for the interaction e) (all radial integrals with non-degenerate single particle states) and the corresponding HF results agree very well. Thus the agreement between the shell model and HF results depends critically on the interaction employed for these calculations. The I_{os} interaction which gives a maximum deformation by mixing 'd' and 's' states gives identical results for both shell model

Table III.15

^{20}Ne shell model spectra for different interactions

(energies in MeV)

	a	b	c	e
J=0	-22.5	-18.20	-14.61	-23.55
2	-22.5	-14.58	- 8.58	-22.13
4	-22.5	-12.51	- 5.81	-20.08
6	-22.5	- 5.47	- 3.08	-16.53
8	-22.5	- 0.83	-	-13.91

and HF results, while the interactions I_{1s} and I_{2s} which give pure occupied states in HF intrinsic states fail to yield results in agreement with the shell model. The HF calculations which are essentially the approximation to the shell model configuration mixing calculations can yield good results only if the interactions used allow a considerable mixing of single-particles state in the occupied orbits. In other words the interaction should have large deformation producing tendancies. The good agreement between the shell model and HF results in case e) is partly because of dominance of I_{0s} component and partly because of the spin-orbit and 1.1 interactions which make $d_{5/2}$, $s_{1/2}$ and $d_{3/2}$ state non-degenerate. This non-degeneracy of single particle states may also change the nature of the HF orbitals of the occupied levels when different 's' state interactions are used. Thus the

agreement between the shell model and HF results essentially depends on the inter-particle interaction and provides a test as to how good is the HF approximation for a given nucleus. It should be noted that almost all the effective interactions in the 1d-2s shell show the dominance of the I_{os} interaction. This explains why the axial HF formalism is equally successful in the beginning of the 1d-2s shell for all the interactions. Also the failure of axial HF formalism to explain the energy levels of ^{24}Mg and ^{28}Si is also mainly due to the dominance of the I_{os} component as we have seen before.

III.5 Summary:

It has been seen that the structure of the lowest (occupied) orbits depends very drastically on the nature of the interaction. The I_{os} interaction gives exactly the level scheme of Q_o^2 while I_{1s} contains both Q^2 and Q^4 multipoles. The I_{2s} interaction is a very peculiar interaction. It operates only when the two particles are in the time-reversed orbits of each other. In 1d-2s shell the I_{os} interaction is the most influential component and maily governs the structure of the HF orbitals of even-even nuclei. This is the component which also gives the dominant contribution to the binding of the nucleus. Further this component is mainly responsible for d-s mixing which is a measure of deformation. In fact this component gives asymptotically deformed nuclei so that [illegible] (the moment of inertia is infinite [illegible]) the projected spectrum is degenerate. However, the components I_{1s} and I_{2s} reduce the

deformation to a realistic value and thus give rise to non-generate spectrum. The spin-orbit interaction seems to reduce the HF energy and the moment of inertia with the consequent stretching of the projected spectrum.

REFERENCES

1) I. Kelson, Phys. Rev. 132 (1963) 2189.
I. Kelson and C.A. Levinson, Phys. Rev. 134 (1964) B269.
J. Bar-Tauv and I. Kelson, Phys. Rev. 138 (1965) B 1035

2) G. Ripka, Advances in Nuclear Physics, Vol. I edited by M. Baranger and E. Vogt (Plenum Press, 1968)
C.S. Warke and M.R. Gunye, Phys. Rev. 155 (1967) 1084
M.R. Gunye and C.S. Warke, Phys. Rev. 156 (1967) 1087

3) S. Cohen, R.D. Lawson and S.P. Pandya, Nucl. Phys. A114 (1968) 541.
S. Cohen, E.C. Halbert and S.P. Pandya, Nucl. Phys. A114 (1968) 353.

4) J.C. Parikh, Phys. Lett. 25B (1967) 181.

5) M. Redlich, Phys. Rev. 110 (1958) 468.

6) D. Kurath and L. Picman, Nucl. Phys. 10 (1959) 313.

7) R.E. Peierls and J. Yoccoz, Proc. Roy. Soc. 70A (1957) 381.

8) D.L. Hill and J.A. Wheeler, Phys. Rev. 89, (1953)1102.

9) S.A. Moszkowski, Proceedings of the International Conference on Nuclear Structure, Kingston (University of Toronto Press, Torongo, 1960) p. 502.
M.K. Banerjee and C.A. Levinson, Phys. Rev. 130 (1963) 1036.

10) S.P. Pandya, Phys. Lett. 7, (1963) 342.

11) E.C. Halbert, Private Communication.

CHAPTER IV

The nature of effective interaction in 1f-2p shell

IV.1 Introduction

Unlike in 1d-2s shell, nuclei in the beginning of the 1f-2p shell do not exhibit well-developed rotational spectra. This is generally attributed to the enhanced pairing correlations in the 1f-2p shell. In particular these correlations manifest themselves in showing a greater stability of Hartree-Fock-Bogolyubov (HFB) intrinsic states compared to that of Hartree-Fock (HF) intrinsic states[1]. Recently Sandhya Devi et al.[2] have also demonstrated that in the 1f-2p shell the energies of good angular momentum states projected from HFB intrinsic states are in better agreement with those of the experimental levels than the energies of states projected from HF intrinsic states. This increased importance of pairing correlations is generally attributed to a stronger pairing component in the effective two-body interaction in the 1f-2p shell than in the 1d-2s shell. However, one possible reason for the increased importance of pairing correlations in the 1f-2p shell could be the neutron excess which together with the experimental single particle energies is largelly responsible for giving rise to degeneracies at the neutron and proton fermi surfaces. This degeneracy at the fermi surface would favour pairing correlations. These correlations would then be a dynamic effect and need not be due

to any extra pairing component.

We feel that the greater instability of the HF states of the 1f-2p shell nuclei as implied by the presence of the pairing correlations is largely due to its unfavourable sequence of single particle levels rather than due to the presence of a large pairing component in the two-body interaction. In fact we shall show that the effective two-body interaction in the 1f-2p shell is predominantly quadrupole-quadrupole (q.q) type. For this purpose, we consider the two-body matrix elements calculated by Kuo and Brown[3] from Hamada-Johnston potential.

In the SU_3 model of Elliott[4], he considers a Hamiltonian which gives rotational spectra. All the levels of a rotational band belong to a unique SU_3 representation. The two-body part of this Hamiltonian is a q.q force while the single particle part is a simple l^2 interaction. The absence of well-developed rotational features in the 1f-2p shell nuclei can thus be either due to unfavourable single particle energies which do not have l(l+1) sequence or it may be due to the two-body interaction not being predominantly q.q type and the greater importance of the higher multipoles.

Our aim is to study the nature of the effective interaction in the 1f-2p shell. If it is dominantly of q.q type it should give rise to states with definite SU_3 symmetry when the single particle states are arranged in l(l+1) sequence. Keeping in mind

this criterion we try to adjust the single particle level sequence until the chosen two-body interaction gives rise to wave functions with definite SU_3 symmetry. Our exercise shows that the Kuo-Brown interaction[3] with a suitable choice of single particle energies gives rise to wave functions of good SU_3 symmetry, thus confirming its dominant q.q character, as well as the importance of single particle level scheme.

IV.2 Two-body wave functions in the SU_3 scheme

In this section we give the SU_3 representations of two particles in the 1f-2p shell. The details of SU_3 scheme are given by Elliott et al.[4] and by Banerjee and Levinson[5]. Each particle in the 1f-2p shell has three oscillator quantas and therefore it has $(\lambda \mu) = (30)$ SU_3 representation. A single particle state in the 1f-2p shell is thus written as $\phi_k[(\lambda\mu), \epsilon]$ where $\epsilon = \langle Q_o^2 \rangle$ is the quadrupole moment in units of b^2 (harmonic oscillator constant) and $k = \langle l_z \rangle$. These single particle wave functions are obtained by diagonalising the Q_o^2 operator in the basis vectors $|lk\rangle$ of different k in the 1f-2p shell. These states can be written as

$$\phi_k[(\lambda\mu), \epsilon] = \sum_l a[(\lambda\mu), k, \epsilon, l] \, |lk\rangle \quad (1)$$

the resulting eigen states of Q_o^2 and l_z are given below.

$$
\begin{aligned}
\Phi_0\left[(30),\ 6\right] &= \frac{1}{\sqrt{5}}\left[\sqrt{2}\, f_0 - \sqrt{3}\, p_0\right] \\
\Phi_{\pm 1}\left[(30),\ 3\right] &= \frac{1}{\sqrt{5}}\left[2\, f_{\pm 1} - p_{\pm 1}\right] \\
\Phi_{\pm 2}\left[(30),\ 0\right] &= f_{\pm 2} \\
\Phi'_0\left[(30),\ 0\right] &= \frac{1}{\sqrt{5}}\left[\sqrt{3}\, f_0 + \sqrt{2}\, p_0\right] \\
\Phi'_{\pm 1}\left[(30),\ -3\right] &= \frac{1}{\sqrt{5}}\left[f_{\pm 1} + 2\, p_{\pm 1}\right] \\
\Phi_{\pm 3}\left[(30),\ -3\right] &= f_{\pm 3}
\end{aligned}
\qquad (2)
$$

The eigen values and k values are shown in figure 1.

2. Two particle states in SU_3 representation

The states of two particles will have SU_3 representations resulting from the product $(30)\otimes(30)$. We have already given (see Chapter II, table 4) the various two particle SU_3 representations in the 1f-2p shell along with their k and L contents. Corresponding to these SU_3 representations, there will be five SU_3 intrinsic states. The intrinsic states of maximum weight are given below:

	$(\lambda\mu)$	ϵ	K
Ψ_1	$[(60),$	12,	$0]$
Ψ_2	$[(22),$	6,	$0]$
Ψ'_3	$[(22),$	6,	$2]$
Ψ_4	$[(41),$	9,	$1]$
Ψ_5	$[(03),$	-6,	$0]$

(3)

FIG. IV·1

SU_3 SINGLE PARTICLE STATES IN 1f – 2p SHELL

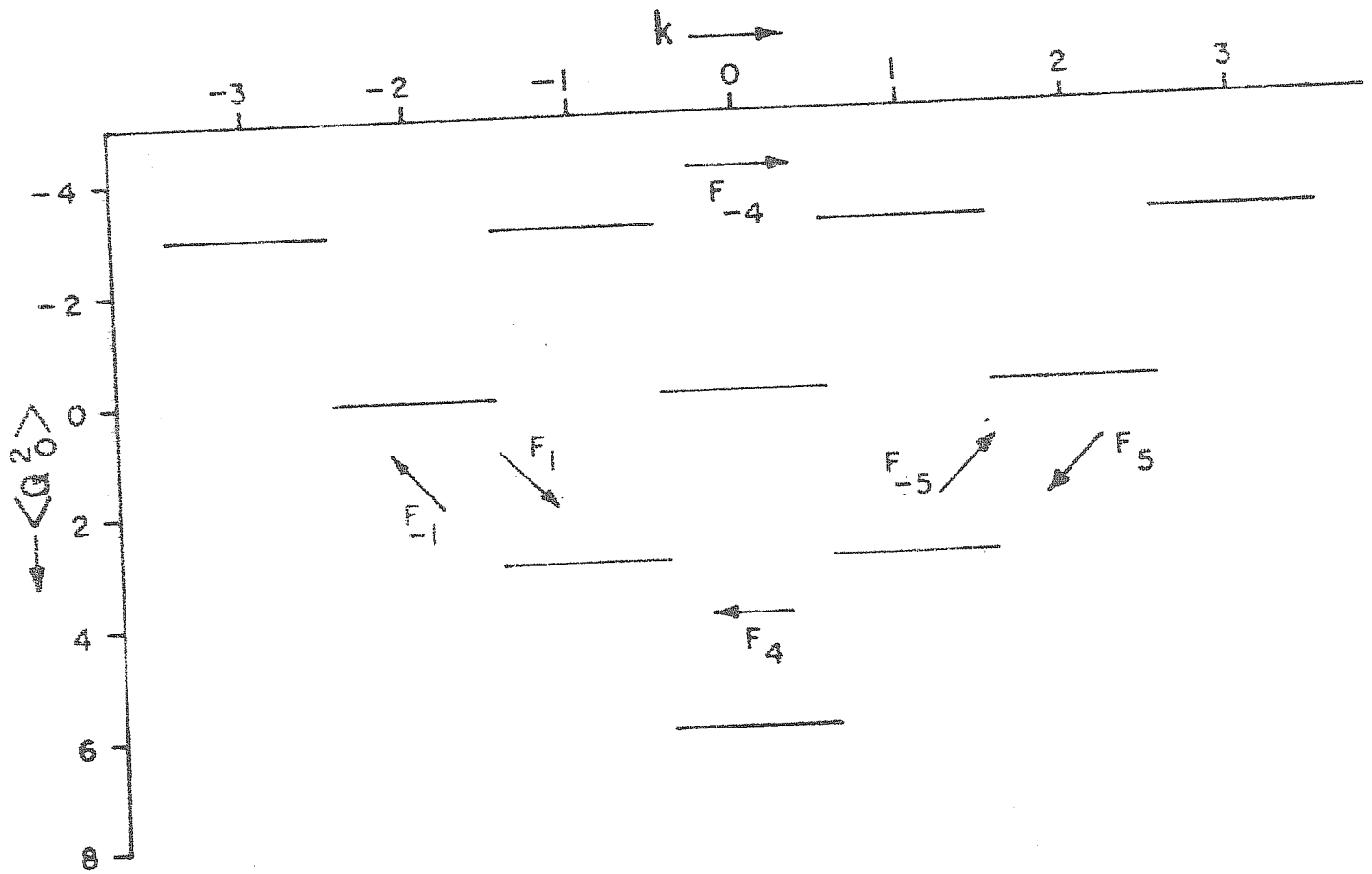

3. Construction of intrinsic states

Now we will see how various intrinsic states of two particles defined in expression (3) can be obtained. Let us take the state Ψ_1. Note that it is the symmetric state with $\epsilon = 12$ and $K = 0$. In order to make $\epsilon = 12$ and $K = 0$, we have to place both the particles in a single particle state ϕ_0 given in expressions (2). This makes

$$\Psi_1 [(60), \epsilon = 12, K = 0] = | \phi_0(1) \phi_0(2) \rangle_s \qquad (5)$$

where suffix 's' denotes a symmetric combination of the states $\phi_0(1)$ and $\phi_0(2)$. Similarly the antisymmetric Ψ_4 state with $\epsilon = 9$ and $K = 1$ can be obtained uniquely by putting one particle in the state ϕ_0 and the other in the state ϕ_1. Thus

$$\Psi_4 [(41), \epsilon = 9, K = 1] = | \phi_0(1) \phi_1(2) \rangle_a \qquad (6)$$

where suffix 'a' denotes the antisymmetric combination of states $\phi_0(1)$ and $\phi_1(2)$, defined as

$$| \phi_0(1) \phi_1(2) \rangle_a = \frac{1}{\sqrt{2}} [\phi_0(1) \phi_1(2) - \phi_0(2) \phi_1(1)] \qquad (7)$$

The intrinsic states Ψ_2 is a symmetric state with $\epsilon = 6$ and $K = 0$, and it can be formed in two ways. i) one particle in the state ϕ_0 and the other in the state ϕ_0'. ii) one particle

in the state Φ_1 and the other in the state Φ_{-1}. Therefore the state Ψ_2 can be written as a linear combination of these two possibilities as given below.

$$\Psi_2[(22), \epsilon = 6, K=0] = X \left| \phi_0(1)\, \phi_0'(2) \right\rangle_S + Y \left| \phi_1(1)\, \phi_{-1}(2) \right\rangle_S \quad (8)$$

where the mixing coefficients X and Y are to be determined such that this combination belongs to $(\lambda \mu) = (22)$ representation.

In order to determine the coefficients X and Y we will make use of the step-up operator F_1 defined as

$$F_1 = \frac{1}{\sqrt{12}} \left[Q_{-1} - \sqrt{3}\, L_{-1} \right] \quad (9)$$

This operator decreases K by one unit and increases ϵ by three units. Since $\epsilon = 6$ is the maximum possible quadrupole moment of (22) representation if we apply F_1 on Ψ_2, the result must be zero as ϵ can no longer be increased. If the linear combination on the right hand side in expression (8) is to correspond to (22) representation, then we must have

$$F_1\, \Psi_2[(22), \epsilon = 6,\ K=0] = 0 \quad (10)$$

using the normalisation condition along with the expression (10), we get

$$X = \sqrt{\frac{3}{5}} \quad \text{and} \quad Y = \sqrt{2/5}$$

Therefore the state Ψ_2 can be written as

$$\Psi_2[(22), \epsilon=6, K=0] = \sqrt{\frac{3}{5}} \left| \phi_0(1)\, \phi_0'(2) \right\rangle_S + \sqrt{\frac{2}{5}} \left| \phi_1(1)\, \phi_{-1}(2) \right\rangle_S \quad (11)$$

It should be noted that the state orthogonal to Ψ_2 belong to (60) representation. Similarly we can obtain the symmetric state Ψ_3' and anti-symmetric state Ψ_5. The results for Ψ_3' and Ψ_5 are given below.

$$\Psi_3'[(22), \epsilon=6, K=2] = \sqrt{\frac{3}{5}} \left| \phi_0(1)\, \phi_2(2) \right\rangle_S - \sqrt{\frac{2}{5}} \left| \phi_1(1)\, \phi_1(2) \right\rangle_S \quad (12)$$

and

$$\Psi_5[(03), \epsilon=-6, K=0] = \frac{1}{\sqrt{2}} \left| \phi_3(1)\, \phi_{-3}(2) \right\rangle_a - \frac{1}{\sqrt{2}} \left| \phi_1'(1)\, \phi_{-1}'(2) \right\rangle_a \quad (13)$$

4. Projection of states of good angular momenta

Having determined the exact form of the two-particle intrinsic states, our next task is to project out the good angular momentum states from them. The expression for projecting the states of good angular momentum is given in Chapter II (see expression No.14). Making use of that expression we have projected the state of good angular momentum. These projected states are given in tables 1 to 5. In these tables 5th column denotes the normalisation factor.

It may be noted that the states of angular momentum L projected from two bands K=0 and K=2 of (22) representation are

Table IV.1

The good angular momentum states of two particles projected from intrinsic state $\Psi_1 \left[(60), \quad \epsilon = 12, \quad K = 0 \right]$

L	f^2	p^2	$\frac{1}{\sqrt{2}}(fp + pf)$	N^2
0	$\sqrt{\frac{4}{25}}$	$\sqrt{\frac{21}{25}}$	0	$\frac{1}{7}$
2	$\sqrt{\frac{8}{125}}$	$\sqrt{\frac{63}{125}}$	$\sqrt{\frac{54}{125}}$	$\frac{10}{21}$
4	$\sqrt{\frac{3}{25}}$	0	$\sqrt{\frac{22}{25}}$	$\frac{24}{77}$
6	1	0	0	$\frac{16}{231}$

The notation here is that e.g.

$$\| L = 0 \rangle = \sqrt{\frac{4}{25}} \, | f^2 \rangle + \sqrt{\frac{21}{25}} \, | p^2 \rangle$$

Table IV.2

The good angular momentum states of two particles projected from the intrinsic state $\Psi_2 \left[(22), \quad \epsilon = 6, \quad K = 0 \right]$

L	f^2	p^2	$\frac{1}{\sqrt{2}}(fp + pf)$	N^2
0	$\sqrt{\frac{21}{25}}$	$-\sqrt{\frac{4}{25}}$	0	$\frac{4}{15}$
2	$-\sqrt{\frac{576}{1625}}$	$\sqrt{\frac{686}{1625}}$	$-\sqrt{\frac{363}{1625}}$	$\frac{13}{21}$

Table IV.3

The good angular momentum states of two particles projected from the intrinsic state $\Psi'_3\left[(22), \epsilon=6,\ K=2\right]$

L	f^2	p^2	$\frac{1}{\sqrt{2}}$ (fp + pf)	N^2
2	$\sqrt{\frac{972}{1375}}$	$\sqrt{\frac{42}{1375}}$	$-\sqrt{\frac{361}{1375}}$	$\frac{11}{21}$
3	0	0	-1	$\frac{1}{3}$
4	$\sqrt{\frac{22}{25}}$	0	$-\sqrt{\frac{3}{25}}$	$\frac{1}{7}$

Table IV.4

The good angular momentum states of two particles projected from the intrinsic state $\Psi'_4\left[(41\ ), \epsilon=9,\ K=1\right]$

L	f^2	p^2	$\frac{1}{\sqrt{2}}$ (fp $\mp$ pf)*	N^2
1	$\sqrt{\frac{8}{15}}$	$\sqrt{\frac{7}{15}}$	0	$\frac{9}{35}$
2	0	0	-1	1
3	$\sqrt{\frac{2}{5}}$	0	$\sqrt{\frac{3}{5}}$	$\frac{4}{15}$
4	0	0	-1	$\frac{4}{35}$
5	1	0	0	$\frac{8}{105}$

* Sign is + for even L and - for odd L

Table IV.5

The good angular momentum states of two particles projected from the intrinsic state $\Psi_5\left[(03), \epsilon=-6, K=0\right]$

L	f^2	p^2	$\frac{1}{\sqrt{2}}$ (fp + pf)	N^2
1	$\sqrt{\frac{7}{15}}$	$-\sqrt{\frac{8}{15}}$	0	$\frac{3}{5}$
3	$\sqrt{\frac{3}{5}}$	0	$-\sqrt{\frac{2}{5}}$	$\frac{2}{5}$

not orthogonal [the states of good angular momentum L projected from different representations $(\lambda\mu)$ are all orthogonal to each other.] Therefore we form a linear combination of these two states such that it will be orthogonal to the one projected from K=0. We will write the new L=2 state, for which only this difficulty arises, as

$$|\Psi_3, L=2\rangle = a|\Psi_2, L=2\rangle + b|\Psi_3', L=2\rangle \qquad (14)$$

such that $\langle \Psi_3, L=2 | \Psi_2, L=2\rangle = 0$

and $\langle \Psi_3, L=2 | \Psi_3, L=2\rangle = 1$

Using the above two conditions one can determine the values of a and b. These values are given by

$$a = \sqrt{\frac{3}{140}} \qquad \text{and} \qquad b = \sqrt{\frac{143}{140}}$$

Substituting these values of a and b and normalising we get the

new L=2 state in terms of components f^2, p^2 and fp as given below

$$|\Psi_3, L=2\rangle = 0.762\ f^2 + 0.272\ p^2 \ominus 0.587\ fp$$

In our analysis we will use this new L=2 state instead of the one projected from K=2 band of representation (22) and will call this state as belonging to representation (22)' for convenience.

Having projected the states of good angular momentum from different SU_3 intrinsic states, we calculate the transformation matrices for going from j-j to SU_3 basis for all J and T states in the 1f-2p shell using the expressions given in Chapter II (see exp. 18). However these transformation matrices have not been included in the thesis for the sake of brevity but will be available with the author. Finally it is also possible to transform the two-body matrix elements in j-j representations to SU_3 representations using the expression given in Chapter II. The two-body matrix elements in SU_3 representations are thus obtained for all values of J and T for both bare and renormalised interactions calculated by Kuo and Brown[3] from Hamada-Johnston potential. Some of the important matrix elements are tabulated in appendix I. We discuss below the salient features of these matrix elements.

IV.3 The SU_3 analysis of the effective interaction in the 1f-2p shell

1. Breaking of permutation

The two-body matrix elements in SU_3 representations

indicate that the interaction in general is more diagonal in SU_3 representations than in j-j representations. The matrix elements connecting two SU_3 representations belonging to different permutation symmetry are zero as expected for the bare interaction. In contrast to this the above mentioned matrix elements have small but non-zero values in case of renormalised interaction. Moreover this breaking seems to be more prominent in T=0 part of the interaction than in T=1 part of it. This leads to the conclusion that the procedure of renormalisation does not preserve the permutation symmetry. However this breaking of permutation symmetry is very small since the matrix elements connecting states belonging to different permutation symmetries are small compared to energy differences between these states.

2. Breaking of SU_3 symmetry.

Apart from the violation of permutation symmetry to a small extent, the interaction may be divided into two parts. i) SU_3 preserving ii) SU_3 breaking. Both the parts have central and non-central characters. The central part of the interaction is dominant over the non-central part. To see this we will examine some of the matrix elements obtained using renormalised interaction. We will classify them in the following four categories.

a) Central and SU_3 preserving:- The diagonal matrix elements belong to this category. These matrix elements are quite

large. We give some of them for illustration. (For notations see expression 19 of Chapter II)

$$\langle (60)\ 00 \mid v \mid (60)\ 00 \rangle = -3.567$$
$$\langle (22)\ 00 \mid v \mid (22)\ 00 \rangle = -2.862 \qquad J=0,\ T=1$$

$$\langle (60)\ 20 \mid v \mid (60)\ 20 \rangle = -2.344$$
$$\langle (22)\ 20 \mid v \mid (22)\ 20 \rangle = -1.141 \qquad J=2,\ T=1$$

b) Central and SU_3 breaking:- The matrix elements which are diagonal in L but not in SU_3 representation $(\lambda\mu)$ belong to this class. Some of them are given below:

$$\langle (60)\ 00 \mid v \mid (22)\ 00 \rangle = -1.617 \text{ for } J=0,\ T=1$$
$$\langle (60)\ 20 \mid v \mid (22)\ 20 \rangle = 0.719 \text{ for } J=2,\ T=1$$

These matrix elements are generally smaller than those of category (a). However it can be seen that the matrix elements connecting two different SU_3 states are larger than the energy difference of these states. This means that the interaction causes considerable mixing of different SU_3 states. Later it will be shown that this mixing will be almost eliminated by a suitable choice of single particle energies.

c) Non-central and SU_3 preserving:- The matrix elements which are diagonal in SU_3 representation but not in L are of this category. The non-central interaction contains both tensor

and spin-orbit components. The following T=0 matrix elements show the existence of tensor interaction.

$$\langle (60)\ 01 \mid v \mid (60)\ 21 \rangle = -1.105 \text{ for } J=1$$
$$\langle (22)\ 01 \mid v \mid (22)\ 21 \rangle = 0.272 \text{ for } J=1$$
$$\langle (60)\ 21 \mid v \mid (60)\ 41 \rangle = -0.478 \text{ for } J=3$$

The matrix elements in which L on bra and ket sides differs by one cannot be explicitly attributed to tensor or spin-orbit interactions as both the interactions can contribute to these matrix elements. However they are also quite small. The existence of two-body spin-orbit interaction is evident from the following T=0 matrix elements mainly because of the characteristic ordering of the levels

$$\langle (60)\ 21 \mid v \mid (60)\ 21 \rangle = -2.332 \text{ for } J=1$$
$$\langle (60)\ 21 \mid v \mid (60)\ 21 \rangle = -3.177 \text{ for } J=2$$
$$\langle (60)\ 21 \mid v \mid (60)\ 21 \rangle = -3.266 \text{ for } J=3$$

In the absence of spin-orbit interaction the states J=1,2,3 would have been degenerate.

d) Non-central and SU_3 breaking:- The matrix elements which are not diagonal in both L and $(\lambda\mu)$ come under this category. Some examples are

$$\langle (60)\ 01 \mid v \mid (22)\ 21 \rangle = 0.430 \text{ for } J=1$$
$$\langle (60)\ 21 \mid v \mid (22)\ 41 \rangle = -0.133 \text{ for } J=3 \quad T=0$$
$$\langle (60)\ 21 \mid v \mid (22)\ 41 \rangle = -0.385 \text{ for } J=5$$

It is seen that the matrix elements of category c) are comparatively larger than those of d). Thus even among non-central components, the SU_3 preserving component is dominant over the SU_3 breaking component. Similarly the matrix elements of categories a) and b) are much larger than those of c) and d). This suggests that the central part of the interaction is dominant over the non-central part.

3. General remarks

It can be observed that in general the interaction in the lowest symmetric representation is strong and attractive. The singlet-even matrix elements

$$\begin{aligned}
&\langle (60)\ 00 \mid v \mid (60)\ 00\rangle = -3.567 \text{ for } J=0 \\
&\langle (60)\ 20 \mid v \mid (60)\ 20\rangle = -2.344 \text{ for } J=2 \qquad T=1 \\
&\langle (60)\ 40 \mid v \mid (60)\ 40\rangle = -1.698 \text{ for } J=4 \\
&\langle (60)\ 60 \mid v \mid (60)\ 60\rangle = -1.233 \text{ for } J=6
\end{aligned}$$

confirm the observation. On the contrary the interaction in the lowest antisymmetric state is weak and repulsive as is seen from the following T=0, singlet-odd matrix elements.

$$\begin{aligned}
&\langle (41)\ 10 \mid v \mid (41)\ 10\rangle = 1.019 \text{ for } J=1 \\
&\langle (41)\ 20 \mid v \mid (41)\ 20\rangle = 0.852 \text{ for } J=2 \\
&\langle (41)\ 30 \mid v \mid (41)\ 30\rangle = 0.913 \text{ for } J=3 \\
&\langle (41)\ 40 \mid v \mid (41)\ 40\rangle = 0.754 \text{ for } J=4 \\
&\langle (41)\ 50 \mid v \mid (41)\ 50\rangle = 1.002 \text{ for } J=5
\end{aligned}$$

It is important to note that in the lowest symmetric representation (60), splitting of the states with different J is sizable and the order of the levels resembles the order of the spectra due to q.q interaction. In the lowest antisymmetric representation (41), the states with different J are almost degenerate. This seems to suggest that the interaction acting in lowest antisymmetric states is quite unlike a q.q interaction. This is in contrast to the simple model interaction used by Banerjee et al[5] and Harvey[6] in which the interaction apart from the Majorana part is assumed to be q.q type and of the same strength for both space symmetric and space antisymmetric states. The interaction acting in the next symmetric state (22) is similar to the one acting in (60) representation. Similarly the interaction in (03) state is also weak and repulsive.

IV.4 Quadrupole-quadrupole nature of the interaction

In the previous section, we have observed that the effective two-body interaction in the 1f-2p shell is dominantly central in character. Now we will show that this central interaction is dominantly quadrupole-quadrupole (q.q) type. To see this point explicitly, consider the Hamiltonian for two particles,

$$H = H_o - A\ (Q.Q) \qquad (6)$$

where $Q=q_1+q_2$ is the total quadrupole operator, H_o, the harmonic oscillator potential and A, the strength of the interaction.

This Hamiltonian gives rotational spectra for states belonging to a unique SU_3 representation[6]. Recalling that

$$Q.Q = C - 3L^2$$

where C is the SU_3 Casimir operator, we can write

$$H = H_o - A \sum_i C_i + 3A \sum_i l_i^2 - 2A \sum_{i<j} (q_i.q_j) \quad (7)$$

We can also write

$$H = H_o' + 3A \sum_i l_i^2 - 2A \sum_{i<j} (q_i.q_j) \quad (8)$$

Where

$$H_o' = H_o - A \sum_i C_i$$

C_i denotes the single particle SU_3 Casimir operator. The expression (8) shows that a two-body interaction of $(q.q)$ type will give rise to a rotational band of states with definite SU_3 symmetry, <u>provided</u> the single particle energies have a $l(l+1)$ sequence. In other words, for the 1f-2p shell the 2p state should be lower in energy than the 1f state. Moreover, this separation of single particle levels should be directly proportional to the strength of q.q interaction as seen from the expression (8). Hence the dominant q.q character of the Kuo-Brown interaction can be brought out by showing that when the l.s interaction is switched off and the energies of 2p and 1f orbits are properly chosen the breaking of SU_3 symmetry is eliminated.

We have obtained the two-body wave functions using the Kuo-Brown interaction[3] and the following three choices of single-particle energies: a) Experimental b) 2p and 1f orbits degenerate c) 2p orbit below 1f (no spin-orbit interaction). The experimental single particle energies used in these calculations are as follows[4].

$$1f_{7/2} = 0.0 \text{ MeV}, \qquad 2p_{3/2} = 2.1 \text{ MeV}$$
$$2p_{1/2} = 3.9 \text{ MeV}, \qquad 1f_{5/2} = 6.5 \text{ MeV}$$

The wave functions corresponding to the lowest eigenvalues are then decomposed into various SU_3 components by making use of the transformation matrices. An SU_3 decomposition of the wave functions (see tables 6 and 11) shows that in case a) all SU_3 components as well as components of different space symmetry are considerably mixed. The later admixture is almost completely eliminated in case b), showing that it is the single particle spin-orbit interaction which breaks the permutation symmetry. This admixture is greatly reduced in case c) where the separation between 2p and 1f levels is varied till maximum SU_3 symmetry is restored for all the J states simultaneously. The analysis has been carried out for both bare and renormalised interactions given by Kuo and Brown[4]. The average energy separation of levels 2p and 1f required to restore the SU_3 symmetry to about 90% for all J states is 0.8 MeV for T=1 part of the bare interaction and 1.5 MeV for that of the

renormalised interaction. The corresponding separations for T=0 part of the interaction are 1.2 MeV for the bare and 1.0 MeV for renormalised interaction. The tables 6 to 11 show the SU_3 decomposition of six different J and T states obtained with renormalised interaction. Similar results are also obtained for the other states. A similar analysis carried out by Parikh and Bhatt[7] for the effective interaction[8] in 1d-2s shell also shows the same features. We now discuss some of the features of the interaction in space symmetric and space antisymmetric states.

1. Space symmetric states.

The results in tables 6 to 11 show that the lowest eigenfunctions tend to belong to lowest symmetric representation (60) as the single particle 2p level is taken below the 1f level. Figure 2 shows the tendency of the (60) states to form a rotational sequence as the single particle 2p orbit is taken below 1f orbit. This suggests as indicated above that the interaction has a large q.q component. It is interesting to note that in the renormalised interaction the 1f-2p separation needed to restore SU_3 symmetry to T=1 states is 1.5 MeV while that for T=0 states it is only 1.0 MeV. As indicated by equation (8) the 2p-1f separation required to restore the SU_3 symmetry of the wavefunctions of q.q interaction is directly proportional to the strength of the q.q interaction. This would imply that the T=1 part of the interaction has a stronger q.q component than

Table IV.6

SU_3 decomposition of J=0, T=1 state obtained by using a) experimental single particle levels b) degenerate single particle levels c) 2p level below 1f levels with $\epsilon_f - \epsilon_p = 1.5$ MeV.

$(\lambda\mu)_{LS}$ Components	a	b	c
$(60)_{00}$	0.5345	0.7787	0.9837
$(22)_{00}$	0.6948	0.6272	0.1794
$(41)_{11}$	-0.3680	-0.0053	0.0001
$(03)_{11}$	-0.3098	-0.0128	-0.0139

Table IV.7

SU_3 decomposition of J=2, T=1 state (see the caption of Table IV.6)

$(\lambda\mu)_{LS}$ Components	a	b	c
$(60)_{20}$	0.4616	0.9012	0.9662
$(22)_{20}$	-0.4387	-0.3692	0.1429
$(22)'_{20}$	0.4324	0.1382	0.1797
$(41)_{11}$	0.4687	0.1222	0.1093
$(03)_{11}$	0.2976	0.0037	-0.0214
$(41)_{21}$	-0.1092	-0.0167	-0.0232
$(41)_{31}$	-0.2208	-0.0233	-0.0261
$(03)_{31}$	-0.1982	-0.0153	-0.0075

Table IV.8

SU_3 decomposition of J=4, T=1 state. (see the caption of table IV.6)

$(\lambda\mu)_{LS}$ Components	a	b	c
$(60)_{40}$	0.4009	0.9642	0.9974
$(22)_{40}$	0.5463	0.2585	-0.0416
$(41)_{31}$	0.5103	0.0557	0.0525
$(03)_{31}$	0.4032	0.0163	-0.0021
$(41)_{41}$	-0.0658	-0.0055	-0.0242
$(41)_{51}$	-0.1811	-0.0051	-0.0072

Table IV.9

SU_3 decomposition of J=1, T=0 state obtained by using
a) experimental single particle levels
b) degenerate single particle levels
c) 2p level below 1f levels with $\epsilon_f - \epsilon_p = 1.0$ MeV

$(\lambda\mu)_{LS}$ Component	a	b	c
$(41)_{10}$	0.3693	-0.0204	-0.0164
$(03)_{10}$	0.3038	-0.0148	-0.0100
$(60)_{01}$	0.5921	-0.7823	-0.8729
$(22)_{01}$	0.6195	-0.4992	-0.2698
$(60)_{21}$	0.0201	-0.3439	-0.3948
$(22)_{21}$	0.1104	0.1233	0.0667
$(22)'_{21}$	-0.1457	-0.0683	-0.0666

Table IV.10

SU_3 decomposition of J=3, T=0 state (see the caption of table IV.9)

$(\lambda\mu)_{LS}$ Component	a	b	c
$(41)_{30}$	0.3536	-0.0310	-0.0572
$(03)_{30}$	0.2626	0.0030	0.0320
$(60)_{21}$	0.6657	-0.7539	-0.8730
$(22)_{21}$	-0.5206	0.4085	-0.1003
$(22)'_{21}$	0.2712	-0.1481	-0.2394
$(22)_{31}$	0.0060	0.0409	0.1463
$(60)_{41}$	-0.0318	-0.4320	-0.3746
$(22)_{41}$	0.1311	-0.0878	-0.0667

Table IV.11

SU_3 decomposition of J=5, T=0 state (see the caption of table IV.9)

$(\lambda\mu)_{LS}$ Component	a	b	c
$(41)_{50}$	0.3118	0.0153	0.0177
$(60)_{41}$	0.8120	0.8995	0.9917
$(22)_{41}$	-0.4915	0.2153	0.0256
$(60)_{61}$	-0.0422	0.3799	0.1247

FIG. V·2

SPECTRUM OF SYMMETRIC REPRESENTATION (60)

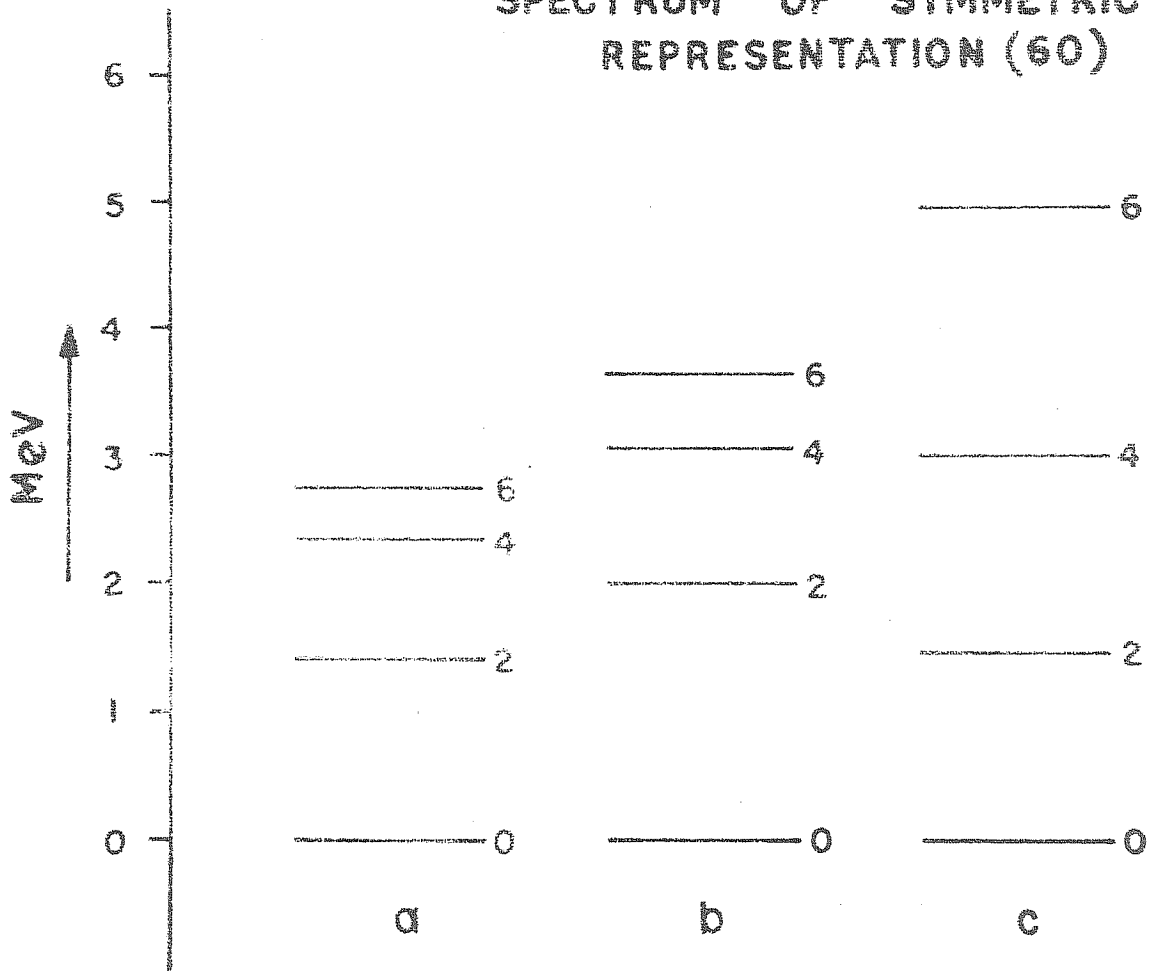

T=0 part. This conclusion may not be quite correct since the presence of higher multipoles in the interaction would also tend to increase the 1f-2p separation needed to restore SU_3 symmetry. In view of this the relevant quantity to be considered should be the spread of single particle separations required for restoring SU_3 symmetry for different ^{J} states. The larger the spread, more is the interaction different from q.q type. The spread for T=0 part of the interaction is about 0.2 MeV while that for T=1 interaction is about 0.5 MeV. However, a large part of this spread comes from the J=0 state. It should also be noted that the spread of single particle separations is small compared to the average 1f-2p separation required in both T=0 and T=1 cases. This suggests that the T=0 interaction is more q.q like than the T=1 interaction.

2. Space antisymmetric states

Attempts were made to restore the SU_3 symmetry of the lowest space antisymmetric states simultaneously. It was found that the average separation required to restore the SU_3 symmetry to about 80% simultaneously for all J states of T=0 part of the renormalised interaction is about 0.15 MeV. The spread of the single particle separations is about 0.22 MeV. Unlike in the symmetric states the spread is larger than the average 1f-2p separation. Moreover the average separation is also much smaller than is required in the symmetric states. For T=1 interaction the

optimum restoration of SU_3 symmetry to about 65% is possible when 1f and 2p are degenerate with a spread of about 1.25 MeV. These results tend to show that the interaction in the antisymmetric state is quite weak and does not have a dominant q.q character.

IV.5 Radial integral decomposition of central interaction

In section 3, we have shown that the effective interaction in 1f-2p shell is dominantly central. The two-body matrix elements of central interaction in a given major shell can be expressed as a linear combination of diagonal radial integrals[9] with relative radial quantum number n and relative orbital angular momentum l. Therefore we decompose the two-body matrix elements of this interaction in terms of various radial integrals defined as

$$I_{nl} = \int_0^\infty R_{nl}^2(r)\, V(r)\, dr \qquad (9)$$

The SU_3 symmetry of the total interaction can be understood in terms of SU_3 properties of these radial integrals discussed earlier.

In section 2, we have calculated the two-body matrix elements in SU_3 representation. In order to isolate the pure central component, we have picked up those matrix elements which have S=0 on both the sides. In other words we have

selected the matrix elements of singlet-even (S=0, T=1) and singlet-odd (S=0, T=0) components of the interaction. These matrix elements have been expressed in terms of radial integrals as follows:

$$\langle (\lambda\mu) L S \mid V \mid (\lambda'\mu') L' S' \rangle_{J T}$$

$$= \sum_{\substack{l_1 \geq l_2 \\ l_3 \geq l_4 \\ n, l}} F[(\lambda\mu) K, l_1 l_2, L]\, F[(\lambda'\mu') K, l_3 l_4, L] \times \langle n_1 l_1 n_2 l_2 \mid n l N \mathcal{L} L \rangle \langle n_3 l_3 n_4 l_4 \mid n l N \mathcal{L} L' \rangle \times \frac{1}{\sqrt{(1+\delta_{l_1 l_2})(1+\delta_{l_3 l_4})}} \times I_{nl} \qquad (10)$$

where $\langle n_1 l_1\ n_2\ l_2 \mid n l N \mathcal{L}\ L \rangle$ and $\langle n_3 l_3\ n_4 l_4 \mid n l N \mathcal{L}\ L \rangle$ denote Moshinsky brackets. The two-body matrix elements of singlet-even interactions have contributions from the following even radial integrals.

$$I_{0s},\ I_{1s},\ I_{2s},\ I_{3s},\ I_{0d},\ I_{1d},\ I_{2d},\ I_{0g},\ I_{1g},\ \text{and}\ I_{0i}$$

Similarly those of singlet-odd interaction are contributed to by the following odd radial integrals.

$$I_{0p},\ I_{1p},\ I_{2p},\ I_{0f},\ I_{1f}\ \text{and}\ I_{0h}$$

All the even integrals (except I_{0g}, I_{1g} and I_{0i} which are assumed to be zero) are obtained by a least-squares fit to the singlet-even matrix elements. Similarly all the odd radial integrals (except I_{0h} which is again assumed to be zero) are obtained from singlet-odd matrix elements. The even radial integrals

I_{0g}, I_{1g}, and I_{0i} and the odd radial integral I_{0h} were neglected in the fit since they are expected to be small. Similar fits are obtained for bare as well as renormalised interactions.

The least-squares fit to even radial integrals gives a r.m.s. deviation of 1.4 KeV for bare interaction and of 70 KeV for renormalised interaction. The fit to odd integrals is almost perfect for bare interaction and gives a r.m.s. deviation of 90 KeV for renormalised interaction. The fact that the r.m.s. deviation for the renormalised interaction is considerably larger than that for the bare interaction may indicate that the higher radial integrals I_{0g}, I_{1g}, I_{0i} and I_{0h} which were neglected in the fit, are more important in the renormalised interaction. This may imply that the renormalised interaction has a "larger range" than the bare interaction.

The values of even and odd radial integrals obtained for bare and renormalised interactions are given in tables 12 and 13 respectively. The results show that due to renormalisation the over-all strength of the singlet-even interaction is increased but that of singlet-odd interaction is slightly decreased. Later it will be shown that even the strength of triplet-even interaction decreases slightly due to renormalisation. This leads to conclusion that the renormalisation procedure decreases the overall strength of T=0 interaction slightly.

It is also of interest to obtain some estimate of the central part of the S=1 and T=0 interaction. To do this we first average over the different J states of a given LS multiplet. For example, a spin-averaged matrix element for a given L state of the $(\lambda\mu) = (60)$ multiplet can be written as

$$\langle (60)_L | V | (60)_L \rangle = \frac{\sum_J (2J+1) \langle (60)LS | V | (60)LS \rangle_J}{\sum_J (2J+1)} \qquad (11)$$

The radial integrals are fitted to all such matrix elements obtained from the renormalised interaction which are now similar to the two-body matrix elements of the singlet-even interaction. The least-squares fit gives a r.m.s. deviation of 17 KeV for these matrix elements. The resulting radial integrals are given in the 3rd column of table 12. It can be seen that these radial integrals are larger than those obtained for S=0, T=1 renormalised interaction (column 2, table 12). This shows that as far as the even states are concerned the spin-averaged T=0 interaction is stronger than T=1 interaction.

Similar results can be obtained for the odd state interaction. The singlet-odd interaction is expected to be stronger than the spin-averaged triplet-odd interaction. We have verified that if the radial integrals obtained by fitting the singlet-odd matrix elements are reduced by a factor of about 1.3, it is possible to reduce the triplet-odd matrix elements fairly well. (See table 13).

1. SU_3 properties of radial integrals

We have expressed the effective interaction in the 1f-2p shell in terms of radial integrals. As the SU_3 symmetry properties of radial integrals have been studied in chapter II, it is possible to throw some light on the SU_3 preserving properties of the total interaction.

In chapter II we have classified the various radial integrals according to their SU_3 preserving properties. It seems that the radial integrals I_{1s}, I_{2s} and I_{1p} are the important SU_3 breaking components of the effective interaction in the 1f-2p shell. The increase in radial integrals I_{1s}, I_{2s} due to renormalisation as shown in table 12 indicates that the

Table IV.12

Radial integral fit to singlet-even interaction

I_{nl}	bare	renormalised	
	T=1 (MeV)	T=1 (MeV)	Spin-averaged T=0 (MeV)
I_{0s}	-4.16	-4.39	-6.74
I_{1s}	-3.79	-5.10	-6.25
I_{2s}	-3.02	-5.37	-4.98
I_{3s}	-2.39	-3.99	-3.92
I_{0d}	-0.33	0.39	-0.53
I_{1d}	-0.41	-0.72	-0.45
I_{2d}	-0.55	-0.85	-0.63

renormalised interaction is less SU_3 preserving than the bare interaction. If we compare the radial integrals of column 2 and 3 of table 12 we see that the I_{0s} radial integral is significantly larger in T=0 interaction compared to T=1 interaction, while the SU_3 breaking components I_{1s} and I_{2s} remain almost the same. This means that the T=0 interaction is more SU_3 preserving and contributes more to the binding energy through I_{0s} [10,11].

Table IV.13

Radial integral fit to singlet-odd interaction

I_{nl}	T=0 bare (MeV)	T=0 renormalised (MeV)
I_{0p}	1.27	1.77
I_{1p}	1.75	0.85
I_{2p}	2.38	0.28
I_{0f}	0.27	0.93
I_{1f}	0.27	0.09

IV.6 Summary

The present analysis of the effective two-body interaction in the 1f-2p shell was undertaken to understand qualitatively the reason for the empirical fact that the 1f-2p shell nuclei do not exhibit rotational features clearly observed in 1d-2s shell nuclei. It is commonly felt that the increase in the

pairing character of the interaction in the 1f-2p shell is responsible for the non-occurance of rotational features.

The features of the interaction which give rise to rotational properties were brought out by expressing the interaction in SU_3 basis. It is seen that in the space symmetric states the interaction is strongly attractive and dominantly q.q type. Such an interaction will clearly give rise to rotational spectra if the single particle 2p orbit is below 1f orbit[12,13]. Since experimentally this is not the case, it seems that it is not so much the increase in the pairing character as the unfavourable sequence of single-particle levels in the 1f-2p shell which prevents the formation of rotational features.

In contrast to the interaction in the space symmetric states, the interaction in the space antisymmetric states is weak and does not have dominant q.q character. This is revealed by the near degeneracy of the multiplet of states belonging to space antisymmetric representation.

We have mentioned that the interaction in the space symmetric states is strong and have also shown that it is dominantly central. Such an interaction can give rise to non-rotational spectra if it mixes the different SU_3 states of symmetric space representation. The SU_3 breaking components of a central interaction were isolated by expressing the interaction in term of radial integrals. It was shown that the radial integrals

I_{1s}, I_{2s}, I_{0d} and I_{0g} mix the SU_3 representations (60) and (22) and would lead to the non-rotational features. It is this mixing which is considerably reduced when the single particle 2p level is kept below 1f level. A rather sophisticated group theoretical analysis of the Kuo-Brown interaction in 1f-2p shell has been carried out by Pluhar[14]. The conclusions drawn through this analysis are very much similar to ours.

REFERENCES

1) H.H. Wolter, A. Faessler and P.U. Sauer, Nucl. Phys. A116 (1968) 145.

2) K.R. Sandhya Devi, S.B. Khadkikar, J.K. Parikh and B. Banerjee, Phys. Lett. 32B (1970) 179.

3) T.T.S. Kuo and G.E. Brown, Nucl. Phys. A114 (1968) 241.

4) J.P. Elliott, Proc. Roy. Soc. A245 (1958) 128, 562.

5) i) M.K. Banerjee and C.A. Levinson, Phys. Rev. 130 (1963) 1036

ii) M.K. Banerjee, C.A. Levinson and S. Meshkov, Phys. Rev. 130 (1963) 1064.

6) M. Harvey, Advances in Nuclear Physics, Vol. I, edited by M. Baranger and E. Vogt (Plenum Press, New York, 1968).

7) J.C. Parikh and K.H. Bhatt, Nucl. Phys. A103 (1967) 496.

8) T.T.S. Kuo and G.E. Brown, Nucl. Phys. 85 (1966) 40.

9) S.P. Pandya Nucl. Phys. 43 (1963) 636
S.P. Pandya and I.M. Green, Nucl. Phys. 57 (1964) 658.

10) D.R. Kulkarni and S.P. Pandya, Nuovo Cimento, 60B(1969) 100.

11) D.R. Kulkarni and S.P. Pandya, Nuovo Cimento Lett. 4 (1970) 133.

12) K.H. Bhatt and J.B. McGrory, Phys. Rev. C3 (1971) 2293.

13) S.K. Sharma, private communication.

14) Z. Pluhar, Phys. Lett. 34B (1971) 475.

CHAPTER V

Core-Excitation effects in Hartree-Fock and SU_3 Scheme

V.1 Introduction

The explicit nature of the effective nuclear force is one of the most important ingredients of theories of nuclear structure. With the steadily improving knowledge of the interaction between free nucleons, it is now becoming increasingly relevant and necessary to carry out nuclear structure calculations with such free interactions. An important contribution to this programme was the work of Kuo and Brown[1] in which they obtained an effective interaction for A=18 nuclei (to be treated as two nucleons outside an inert closed ^{16}O core) starting from the free interaction of Hamada and Johnston[2]. They pointed out that not only must one convert the free interaction (which has a hard-core) into an effective G-matrix representing the direct (or'bare') interaction between the valence nucleons, but that it is equally important to take into account interaction of the valence nucleons via virtual excitations of the core particles i.e. in this case the particles comprising the ^{16}O core. The effective interaction which contains the core - excitation effects also is called the 'renormalised' interaction. Brown and Kuo[3] showed in a further analysis that this renormalisation introduces in the bare interaction additional multipole components as well as pairing interaction. In particular a P_2-component roughly corresponding

in magnitude to that required empirically by Kisslinger and Sorenson[4] is contributed by the renormalisation effects.

The calculation of renormalised matrix elements is done by starting with the two-body matrix elements of the bare interaction and evaluating the correction due to core excitations in each case. This is rather laborious and complicated and obviously involves some uncertainties and approximations. Since it is indeed quite important from a practical point of view to have an effective interaction which operates in a reasonably small configuration space, it seems desirable to get a good feeling for the changes in the overall nature of the effective interaction brought about by inclusion of core-excitation effects.

We propose to do the Hartree-Fock (HF) calculations for 1d-2s shell nuclei using both 'bare' and 'renormalised' interactions. The self-consistent field as obtained by the HF calculations is very sensitive to the quadrupole component of the force as shown by the very close resemblance of the spectrum of HF orbits to Nilsson orbits. On the other hand the pairing component or a higher multi-pole such as a hexadecapole component in the effective interaction may make its presence felt in the energies of the good angular momentum states projected out of the intrinsic deformed HF state. It is therefore likely that a comparison of HF calculations for 1d-2s shell nuclei carried out with bare and renormalised two-body matrix elements may give an

alternative and an interesting way to look into the nature of core-excitation effects and to the degree to which the quadrupole and other multipole components get enhanced. We have also compared the results of our calculations for ^{20}Ne with the available results of exact shell-model calculations in the 1d-2s configuration. Moreover the multi-shell HF calculations carried out in a large configuration space of first four major shells with a 'bare' interaction also provides an alternative method of taking core-excitation into account. Hence it is meaningful to compare results of such calculations with those obtained by using a renormalised interaction in 1d-2s shell. We have carried out such a comparison in the case of ^{20}Ne and have pointed out certain common features.

The relative increase in various multipoles in the 'renormalised' interaction may also be reflected in the symmetry properties of the interaction under SU_3 transformation. These multipoles would mix different SU_3 irreducible representations. As a result, the renormalised interaction may show more mixing of different SU_3 representations than the bare one. To show this explicitly we expressed both bare and renormalised interactions in the SU_3 basis. This analysis reveals the nature of the two interactions in the framework of SU_3 scheme.

In previous chapters we have studied the properties of radial integrals in both SU_3 and HF formalisms. We tried to use these

properties in examining the core-excitation effects. For that we first fitted various radial integrals in 1d-2s shell to both bare and renormalised interactions. We thus obtained two sets of radial integrals. The differences in magnitudes of different radial integrals from two sets clearly bear out the effects of core-excitation.

V.2 Brief description of calculations of two-body matrix elements

The calculations of 'renormalised' two-body matrix elements is quite tedious and a complicated task. We outline here the salient features of the procedure adopted by Kuo and Brown[1] essentially to point out the approximations made at various stages of the calculations. The procedure can be mainly divided in two parts. First part relates with the calculations of bare two-body matrix elements. Second part essentially deals with the calculations of the effects of core-excitation. It should be noted that the 'bare' two-body matrix elements go as input for the second part of the calculations.

The 'bare two-body matrix elements have been calculated using the realistic Hamada-Johnston interaction[2]. The Hamada-Johnston potential fits the nucleon-nucleon scattering data to about 330 MeV and has an infinitely repulsive hard core at small distance. The potential is a sum of a spin-dependent

central, a tensor, a spin-orbit and a quadratic spin-orbit force and approaches the one-pion-exchange potential for large relative distances. Kuo and Brown[1] investigated the structure of ^{18}O and ^{18}F nuclei on the assumption that in lowest order they could be treated as nuclei having two particles outside a doubly magic ^{16}O core. The model space in these calculations was the $(1d_{5/2}, 2s_{1/2}, 1d_{3/2})$ space. To find the effective-interaction matrix elements to be used within this model space, one must solve first the Bethe-Goldstone integral equation[5],

$$G = V + V \frac{Q}{e} G \qquad (1)$$

where e is defined as the difference in the energies of the intermediate and initial states, Q is the Pauli operator which excludes all the occupied intermediate states. G is called the Brueckner reaction matrix and represents the effective interaction in the model space derived from the realistic interaction V. In other words the nuclear structure calculations should be performed using these G matrix elements.

In evaluating the reaction matrix elements several approximations are made. In fact the reaction matrix G depends on the energy of the initial states and should be obtained using the Brueckner-Hartree-Fock Method[6] involving the double self-consistency. But this problem of self-consistency has been usually avoided by making the following two assumptions.

i The single-particle states in the model space have harmonic oscillator wave functions and those outside the model space are plane wave functions.

ii The state-dependency of the reaction matrix G is avoided and instead suitable state-independent energy denominators are used.

These assumptions simplify the calculations to a great extent. The singlet-even and triplet-even parts of the interaction are treated by Scott-Moszkowski's separation method[7]. The reaction matrix of the short-range part (G_s) of the interaction is approximately made to vanish by suitably choosing the state-independent separation d. Moreover the calculations of G_s involve only the Plane-wave intermediate states. Since these states are all unoccupied, the Pauli operator Q is approximated to one in the calculations. The long-range part V_L can be calculated very easily. The tensor interaction has an appreciable second order correction in V_L. The calculations of the second order correction for tensor is also performed using the intermediate states as plane waves and the state-independent energy denominator. The singlet-odd and triplet-odd parts of the interactions are dealt with by reference spectrum method due to Bethe, Brandow and Petschek[8]. Again the 'Q' operator is replaced by one and the state-independent energy denominator

is used. Thus it should be noted that the state-dependence is completely avoided in the original calculations of reaction matrix by Kuo and Brown[1]. Later Kuo[9] used also the state-dependence of e, especially in the calculations of G_s and the second-order correction for the long-range tensor interaction. The state dependent reaction matrices G are found to be slightly less attractive than the original Kuo-Brown G matrices. Thus there seems to be a repulsive contribution coming in due to introduction of state-dependent parameters. However the main criticism against both these calculations is the assumption that the states outside the model space are plane waves. In other words they assume that the shell-model potential vanishes for all states outside the model space. This seems to be a drastic assumption and needs to be verified critically.

Using these reaction matrices, Kuo and Brown[1] have calculated the single-particle spectrum of ^{17}O with linked-cluster perturbation formula. They have to introduce the second-order contributions such as 2p-1h, 3p-2h due to p-h (particle-hole) excitations of the core. The results thus obtained are in good agreement with the experimental levels of ^{17}O.

Further they 'renormalise' the G reaction matrices by including the effects of core excitations. The second-order term in the linked-cluster perturbation series corresponds to the process represented by the diagram containing only one bubble.

This takes into account the fact that one of the valence nucleons in the 1d-2s shell can interact with a core-nucleon to produce a particle-hole excitation, and then the particle-hole excitation can be annihilated by an interaction with the second valence nucleon. Since parity is conserved by the residual two-body force a restriction to excitation energies no greater than (2 h w) limits the one particle-hole pairs to $(2s,1s^{-1})$, $(1d,1s^{-1})$, $(2p,1p^{-1})$ and $(1f\text{-}1p^{-1})$ configurations only. There are other first order diagrams which should be included for an accurate calculation of renormalisation effects. These corrections correspond to the excitation of two valence particle to 1f-2p or the excitation of two holes in 1p shell. These contributions have also been added to bare matrix elements to get 'renormalised' two-body matrix elements. We have used the bare and renormalised sets of two-body matrix elements given by Kuo[9] for our calculations.

V.3 HF orbitals

In this section we describe the structure and the energies of the HF single particle orbitals for ^{20}Ne, ^{24}Mg and ^{28}Si obtained with the use of both bare as well as renormalised $(ds)^2$ matrix elements. The experimental levels of ^{17}O as given below are used as single particle levels in these calculations both for protons and neutrons.

$1d_{5/2}$ = 0 MeV, $1d_{3/2}$ = 5.08 MeV, $2s_{1/2}$ = 0.87 MeV

The results of these calculations are given in tables 1 to 9. It can be very well seen that the structure of the orbitals shows dramatically the almost total insensitivity of the HF calculations to any but the quadrupole component of the interactions. It is found that the overlaps of the wave functions calculated with bare and renormalised matrix elements are in all cases $\geq$ 0.995. Core-excitation apparently has li tle effect on the nature of the HF orbitals. The reason for this becomes clear if one takes the overlaps of these wavefunctions with asymptotic Nilsson orbits (i.e. orbits for very large deformation $\delta \to \infty$). These overlaps are shown in table 7 for occupied orbits and are in all cases again very close to unity. It appears then that even the 'bare' interaction yields almost exactly the asymptotic Nilsson orbits and an additional quadrupole component, if any, brought in by the renorralisation of the matrix elements due to core-excitation can produce little further change in the structure of the orbits.

The nuclear intrinsic state obtained by filling the lowest asymptotic Nilsson orbits is a state of definite SU_3 symmetry with maximum weight. Our calculations show that with both sets of matrix elements given by Kuo[9] the HF calculations also tend to yield essentially the intrinsic states of the SU_3 model. The close similarity of the HF orbits to the asymptotic Nilsson

Table V.1

^{20}Ne HF single particle orbitals (bare interaction)

k	E_k in MeV	$s_{1/2}$	$d_{3/2}$	$d_{5/2}$
1/2	-9.86	-0.5274	-0.3945	0.7525
3/2	-4.54	0	-0.1843	0.9829
1/2'	-2.66	0.6930	0.3127	0.6496
5/2	-2.25	0	0	1
1/2''	-0.23	-0.4916	0.8640	0.1085
3/2'	2.54	0	0.9829	0.1843

Table V.2

^{20}Ne HF single particle orbitals (prolate)
(renormalised interaction)

k	E_k in MeV	$s_{1/2}$	$d_{3/2}$	$d_{5/2}$
1/2	-11.63	-0.4995	-0.3973	0.7699
3/2	- 4.38	0	-0.2260	0.9741
1/2'	- 1.81	0.6860	0.3614	0.6315
5/2	- 1.10	0	0	1.0
1/2''	0.27	-0.5291	0.8436	0.0921
3/2'	3.77	0	0.9741	0.2260

Table V.3

^{24}Mg HF single-particle orbitals (prolate)
(bare interaction)

k	E_k in MeV	$s_{1/2}$	$d_{3/2}$	$d_{5/2}$
1/2	-14.75	-0.5508	-0.3386	0.7387
3/2	- 9.54	0	-0.2979	0.9546
1/2'	- 9.15	0.2912	0.7400	0.6063
5/2	- 5.51	0	0	1.0
1/2''	-4.71	0.7822	-0.5490	0.2944
3/2'	-1.93	0	0.9546	0.2979

Table V.4

^{24}Mg HF single particle orbitals (prolate)
(renormalised interaction)

k	E_k in MeV	$s_{1/2}$	$d_{3/2}$	$d_{5/2}$
1/2	-16.34	-0.5269	-0.3610	0.7695
3/2	-10.27	0	-0.3259	0.9454
1/2'	- 8.41	0.2714	0.7865	0.5548
5/2	- 3.50	0	0	1.0
1/2''	- 3.48	0.8055	-0.5011	0.3164
3/2'	0.34	0	0.9454	0.3259

Table V.5

^{28}Si HF single particle orbitals (oblate)
(bare interaction)

k	E_k in terms of MeV	$s_{1/2}$	$d_{3/2}$	$d_{5/2}$
5/2	-18.13	0	0	1.0
1/2	-17.05	0.8028	-0.2683	0.5326
3/2	-15.38	0	0.7521	0.6590
3/2'	-9.01	0	-0.6590	0.7521
1/2'	-8.66	-0.3837	0.4513	0.8057
1/2''	-4.48	0.4565	0.8511	-0.2593

Table V.6

^{28}Si HF single particle orbitals (oblate)
(renormalised interaction)

k	E_k in terms of MeV	$s_{1/2}$	$d_{3/2}$	$d_{5/2}$
5/2	-19.35	0	0	1.0
1/2	-16.93	0.8108	-0.2378	0.5348
3/2	-16.40	0	0.7536	0.6573
3/2'	-6.50	0	-0.6573	0.7536
1/2'	-6.08	-0.3640	0.5107	0.7789
1/2''	-1.31	0.4583	0.8262	-0.3275

Table V. 7

Overlaps of asymptotic Nilsson orbits with occupied HF orbitals calculated with bare interaction.

Nucleus	Overlap		
	$k=\frac{1}{2}$	$k=\frac{3}{2}$	$k=\frac{5}{2}$
^{20}Ne (prolate)	0.984	-	-
^{24}Mg (prolate)	0.986	0.987	-
^{28}Si (oblate)	0.992	0.967	1.000

Table V.8

Intrinsic quadrupole moments of ground HF states in units of b^2. The SU_3 limit values are shown in the last column, with appropriate SU_3 symmetry of the state in brackets.

Nucleus	Intrinsic quadrupole moment Q_{HF}		
	bare	renor-malised	SU_3
^{20}Ne (prolate)	15.59	15.46	16.00(8,0)
^{24}Mg (prolate)	19.35	19.23	20.00(8,4)
^{28}Si (oblate)	-23.03	-22.96	-24.00(0,12)

Table V.9

Hartree-Fock energies for intrinsic states in MeV.

Interaction	Hartree-Fock Energy E_{HF}		
	^{20}Ne (prolate)	^{24}Mg (prolate)	^{28}Si (oblate)
bare	-17.66	-45.61	-94.52
renormalised	-21.23	-50.34	-97.88

orbits can be further demonstrated by calculation of intrinsic or mass quadrupole moments for the ground states. Table 8 shows the intrinsic quadrupole moments for the HF ground states in appropriate units, and lists also values for the corresponding intrinsic states of the SU_3 model. Both bare as well as renormalised interaction give intrinsic quadrupole moments that are very close to those for the SU_3 states with maximum weight. However, an additional point of interest from our point of view is the small but systematic reduction of the intrinsic quadrupole moment given by the renormalised interaction, compared to the values given by the bare interaction in each case. This suggests that the core-excitation effects do bring in additional forces which tend to break the SU_3 symmetry of HF orbitals, even though their presence is felt only very weakly in the structure of HF orbits.

We have also plotted in fig.1 the energy level spectra of the single particle orbits for all cases. The spectra shown for ^{20}Ne and ^{24}Mg correspond to prolate deformation whereas that for ^{28}Si corresponds to oblate deformation, since the HF energy is lower for this case by about 3 MeV (-91.83 MeV for prolate deformation and -94.52 MeV for oblate deformation). It is clear that the energies of all occupied orbits are lowered, whereas those of all unoccupied orbits are raised by the core-excitation effects. Thus the renormalised interaction gives

FIG. V-1

H-F SINGLE PARTICLE SPECTRA

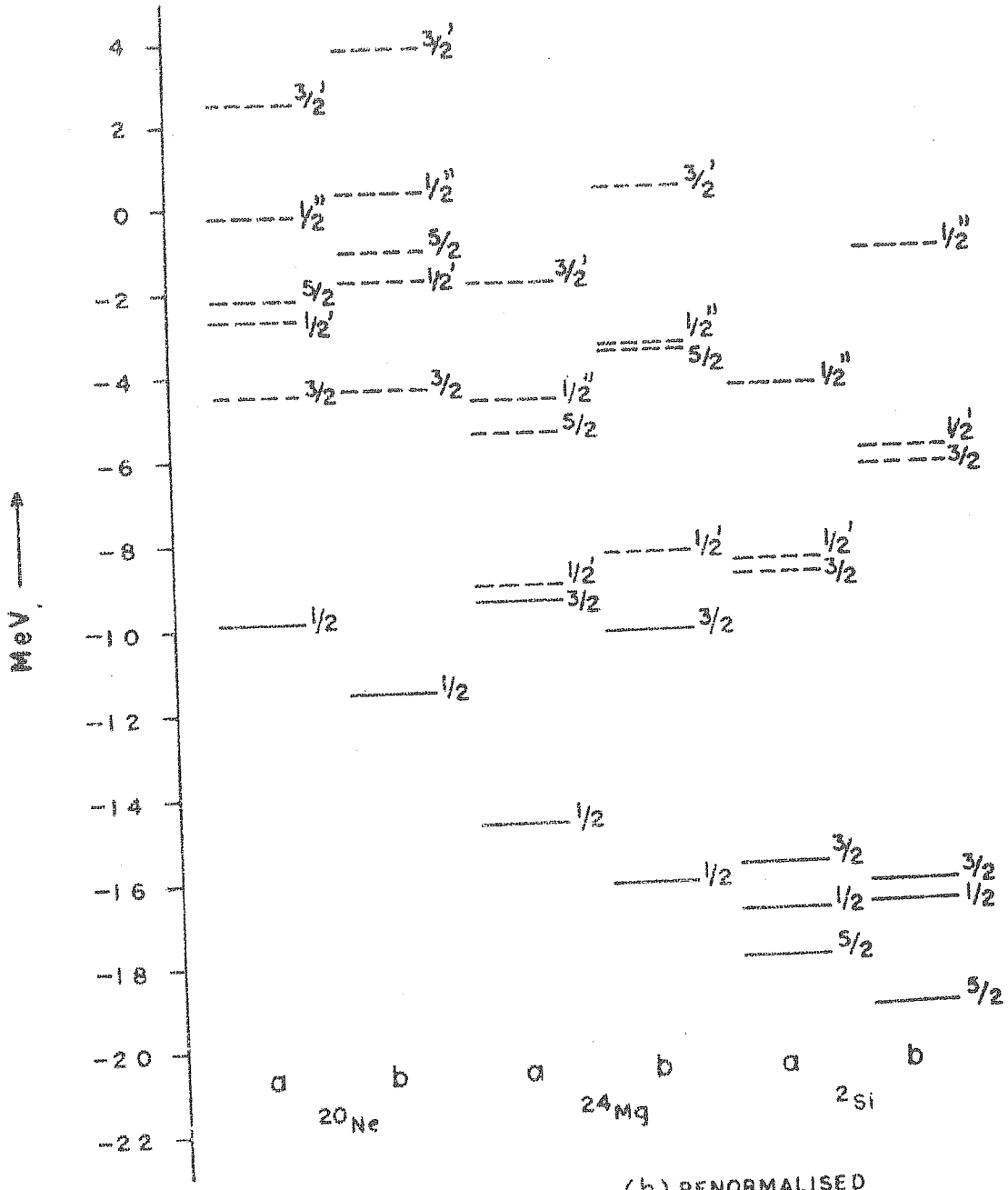

(a) BARE (b) RENORMALISED

significantly larger gaps. This is particularly so for ^{24}Mg where the bare interaction gives the occupied $k = 3/2$ orbital almost degenerate with the first unoccupied $k = \frac{1}{2}$ orbital whereas the renormalised interaction gives a gap of about 2 MeV. Since the origin of the gap is generally attributed to the Majorana component[10] of the monopole part of the nuclear interaction, one might think that it is this component that may change considerably due to core-excitation effects. Recently, Rowe[11] has attributed the presence of gap in HF spectra to any component of the effective interaction resulting in a HF field that violates some symmetry invariance of the original Hamiltonian. The gap given by the bare interaction may then be attributed to the presence of the quadrupole component of the force which violates the angular momentum conservation for the original two-body interaction, but which in turn gives near SU_3 symmetry for the eigenfunctions of HF Hamiltonian. Again then we may attribute further increase in gap to the core-excitation effects which bring in components that break the near SU_3 symmetry of the bare interaction. This would be in line with our previous observations on the intrinsic quadrupole moments.

One of the important SU_3 breaking components in the 1d-2s shell corresponds to the multipole Q^4. It is interesting to see qualitatively from the energies of HF orbitals that there is an increase in this component due to the core-excitation effects. We note that the structure of both bare and renormalised HF

orbitals is quite similar. Moreover the Q_o^2 field is dominant in both the solutions as seen from the sequence of HF energy levels. We have also seen in he third chapter that the small Q_o^4 field if it is present, will essentially lead to the splitting of degeneracies of k= ±2 and k'=0 levels of Q_o^2 field. In fact k'=0 will be depressed much more due to the Q_o^4 field than the k=±2 levels because of its large positive Q_o^4 moment. We can look for a similar effect in the HF orbitals of both the bare and renormalised interactions. However the HF orbitals obtained by using bare and renormalised interactions are not exactly SU_3 like as we use non-degenerate single particle levels. This non-degeneracy of single particle levels is mainly because of the spin-orbit interaction. We also know that the non-central interactions are not important in 1d-2s shell. We must therefore eliminate the effect of l.s interaction. The splitting of the orbitals k=3/2' and k=5/2 will give us the strength of the l.s interaction which consequently enables us to determine the position of state k=2. Further it can be seen that the l.s interaction pushes the orbital k=1/2" up. Therefore the position of k'=0 can also be obtained using the same strength of spin-orbit interaction. It was found that for ^{20}Ne nucleus the position of k=2 levels is at about -0.25 MeV while the level k'=0 is at about -2.40 MeV when the bare interaction is used. Thus the net splitting is about 2.15 MeV. If the renormalisation brings in the additional hexadecapole component in the interaction

we expect that this splitting should increase. In the case of renormalised interaction for the same nucleus, it was observed that the position of k=2 level is about 1.0 MeV while that of k'=0 level is about -1.9 MeV. As a result the splitting of these levels has been raised from 2.15 MeV to 2.90 MeV. This fact coupled with our observation that there is a slight decrease in mass Q_0^2 moment suggests that there is a large hexadecapole multipole present in the renormalised interaction as a result of core-excitation effects.

V.4 Projected Energy level spectra.

In this section we present the results of projection of good angular momentum states from HF intrinsic states of ^{20}Ne, ^{24}Mg and ^{28}Si described in section 3. The energies of the projected states both for bare and renormalised interactions are plotted in fig.2. All energies are shown relative to the projected ground state energy E(J=0), and the absolute value of this energy is shown in brackets below each spectrum. Also shown in the table 9 are the HF energies of the intrinsic states for each case. We note that these intrinsic HF energies are lowered by several MeV due to core-excitation effects, viz. by 3.56 MeV for ^{20}Ne, 4.73 MeV for ^{24}Mg and 3.36 MeV for ^{28}Si.

It can be seen from fig.2 that the spectra for renormalised interaction are much more spread out than those for the bare force.

FIG. V·2

H-F PROJECTED SPECTRA

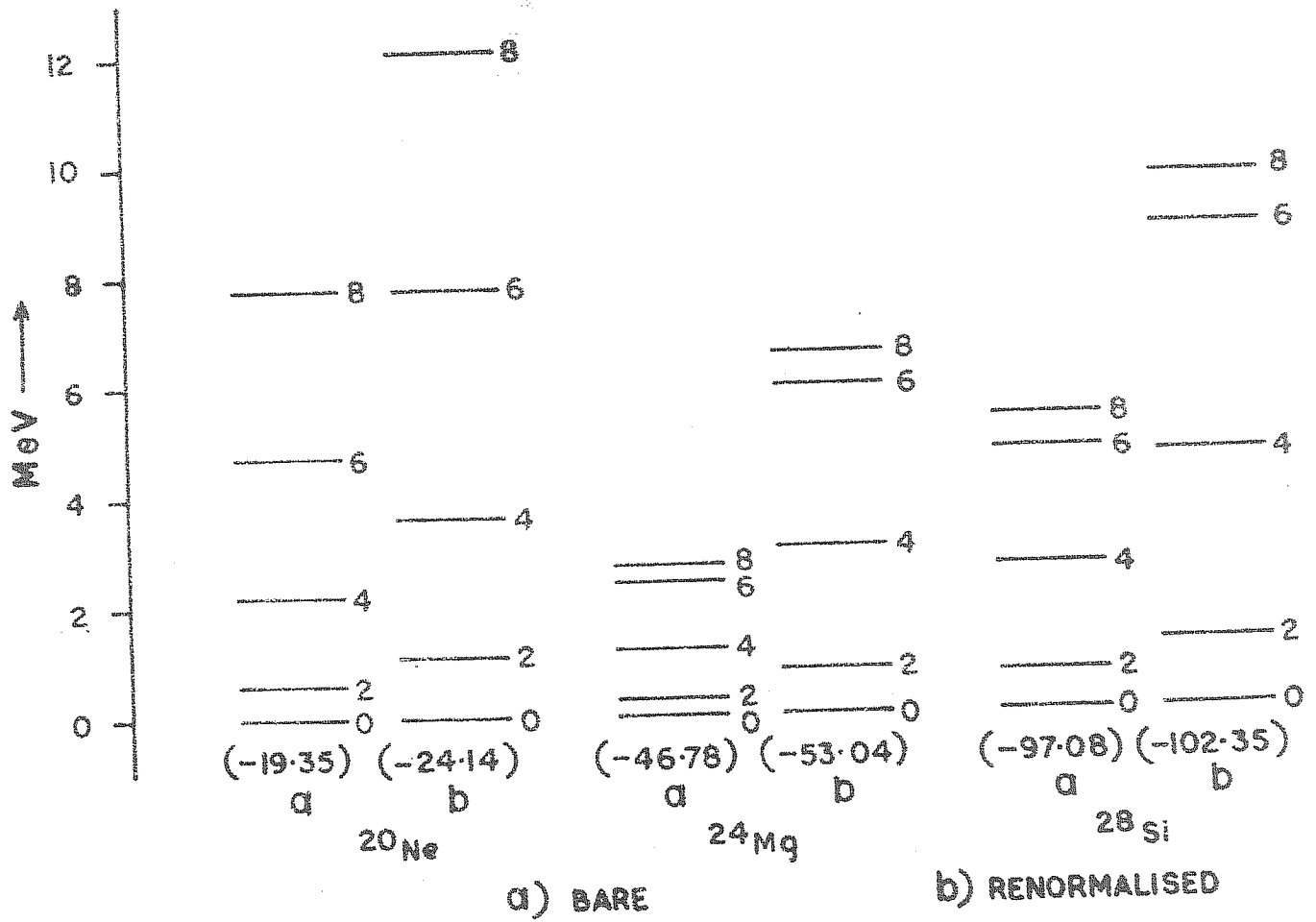

The indication then is that core-excitation effects reduce by a factor of 2 to 3 the moment of inertia of the lowest rotational band in these nuclei. This may be in part due to the increase in the gap of the single particle level spectra described earlier. We note that the relative increase in gap is the largest for ^{24}Mg and so is the reduction in moment of inertia. It is possible that both these effects are due to a strong renormalisation and enhancement of the other multipole components of the effective interaction due to inclusion of the core-excitation effects, since in a rather simple view these would be the components mainly responsible for the violation of the near SU_3 symmetry of the bare interaction.

It may be of some interest to compare the results of HF calculations for ^{20}Ne with those of exact shell model calculations of Halbert et al[12] who also use Kuo's renormalised matrix elements and the $(ds)^4$ configuration. The shell model spectrum is shown in fig.3 and the absolute value of the binding energy of the four particles relative to the ^{16}O core is also shown. We see that the shell-model energies are somewhat larger than the HF energies by about 1 MeV for the ground state J=0 and 0.5 MeV for J=2,4,6 states. We of course expect the exact shell model energies to be lower than those given by the variational calculation. However the overall agreement between two sets of energies appears to be good.

FIG. V·3

^{20}Ne SPECTRUM

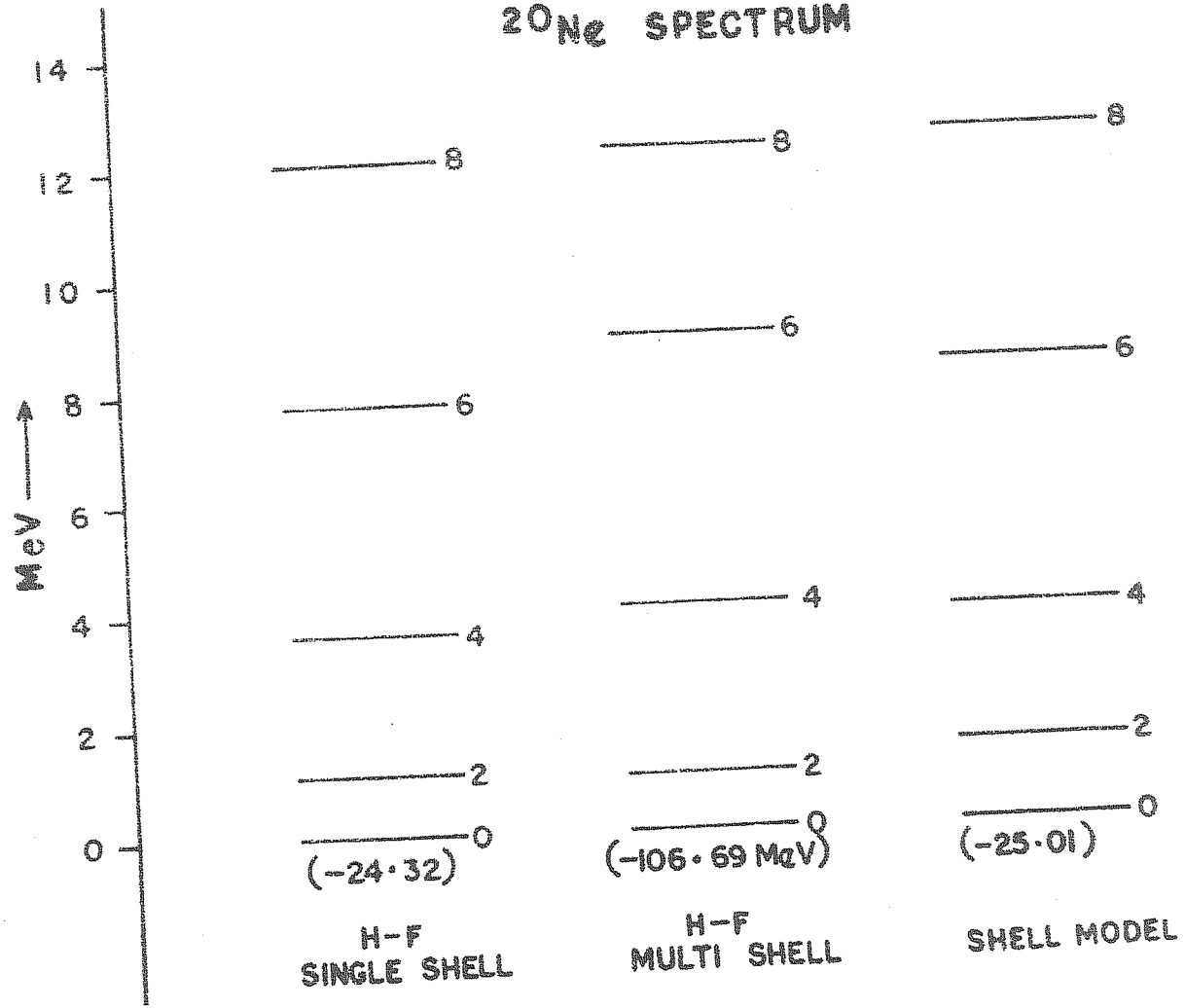

We also show in fig.3 the results of multi-shell HF calculations for ^{20}Ne. The calculations have been carried out using the full configuration space of N=0,1,2 and 3 shells treating explicitly all the twenty nucleons. The effective interaction matrix elements used are those derived by the Sussex group[13] from N-N scattering phase shifts. We have verified that these two-body matrix elements (at least for the 1d-2s shell) are very close to the bare matrix elements of Kuo[9] - the r.m.s. deviation between the two sets being only 261 KeV. Moreover it should be noted that Kuo has also considered the configuration space of only first four major shells to calculate the effects of virtual particle-hole excitations in renormalising the bare interaction. It is therefore of interest to compare these results of multi-shell HF calculations in a large configuration space with the results with renormalised interaction in a truncated configuration space. The energy levels in two cases are in fairly good agreement (see fig.3). Also the multi-shell HF calculations result in a larger gap at the Fermi surface as compared with that in the 1d-2s shell calculations with bare interaction. This increase in the gap results from additional deforming component of the HF field resulting from core-polarization.

V.5 SU_3 analysis of the interaction.

The relative enhancement of different multipoles and the

introduction of non-central components in the renormalised interaction due to the effects of core-excitation may also show up in the SU_3 analysis of both bare and renormalised interactions. The main effect of the presence of the multipoles other than the quadrupole will be reflected in the mixing of different SU_3 representations. With this view in mind, we have carried out the SU_3 analysis of these interactions by expressing the two-body matrix elements in SU_3 basis. The equation for transforming the two-body matrix elements in j-j representation to SU_3 representation has been already given in Chapter II. We have employed the same equation here to obtain the two-body matrix elements in SU_3 basis for different J and T states. The results thus obtained are given in tables 10 to 17. It should be noted that for J=4,5 and T=0 states there is only a unique SU_3 representation (40). The states (NLS) given in table 11 to 18 can be read as $|(\lambda\mu)LS\rangle$ where N denotes the different SU_3 representations as given below

$$N = 1 \equiv (40),\ N = 2 \equiv (02),\ N = 3 \equiv (21)$$

It may also be noted that for every matrix element, upper number denotes the bare interaction and the lower one the renormalised one. To be more explicit we note that (NLS) corresponds to bra state while (N'L'S') stands for ket state.

Table V.10

SU_3 decomposition of Kuo interaction in 1d-2s shell J=0, T=1

(NLS) \ (N'L'S')	(100)	(200)	(311)
(100)	-3.6134 -4.7393	-0.9311 -1.8988	-0.0368 0.0536
(200)	-0.9311 -1.8988	-2.1761 -2.7074	-0.0235 0.0073
(311)	-0.0368 0.0536	-0.0235 0.0073	2.4165 2.2517

Table V.11

SU_3 decomposition of Kuo interaction in 1d-2s shell J=1, T=1

(NLS) \ (N'L'S')	(311)	(321)
(311)	-0.3320 -0.1257	-0.1678 -0.0976
(321)	-0.1678 -0.0976	-0.3278 0.2167

Table V.12

SU_3 decomposition of Kuo interaction in 1d-2s shell J=3, T=1

(NLS) \ (N'L'S')	(321)	(331)
(321)	-0.2877 0.1723	-0.0633 -0.0892
(331)	-0.0633 -0.0892	-0.4028 0.1315

Table V.13

SU_3 decomposition of Kuo interaction in 1d-2s shell J=2, T=1

(NLS) \ (N'L'S')	(120)	(220)	(311)	(321)	(331)
(120)	-3.1707 -3.5887	-0.3855 -0.6603	0.0088 -0.1784	0.0087 -0.0781	-0.0094 0.0386
(220)	-0.3855 -0.6603	-0.9549 -0.8144	0.0041 0.0405	0.0009 0.1949	-0.0043 -0.0799
(311)	0.0088 -0.1784	0.0041 0.0405	-0.3256 -0.2350	-0.1368 -0.1853	0.1675 0.0848
(321)	0.0087 -0.0781	0.0009 0.1949	-0.1368 -0.1853	0.5966 0.8084	-0.5799 -0.5147
(331)	-0.0094 0.0386	-0.0043 -0.0799	0.1675 0.0848	-0.5799 -0.5147	0.4444 1.0525

Table V.14

SU_3 decomposition of Kuo interaction in 1d-2s shell J=4, T=1

(NLS) \ (N'L'S')	(140)	(331)
(140)	-2.5424 -2.4284	0.0072 -0.1735
(331)	0.0072 -0.1735	0.0861 0.7181

Table V.15

SU_3 decomposition of Kuo interaction in 1d-2s shell J=1, T=0

(NLS) \ (N'L'S')	(101)	(121)	(201)	(221)	(310)
(101)	-5.5277 -6.5851	-0.9775 -1.5686	-1.5064 -2.1775	-0.7507 -0.7791	0.0149 -0.2531
(121)	-0.9775 -1.5686	-3.8393 -4.3491	-0.4515 -0.7609	-0.1306 -0.3001	-0.0067 0.1503
(201)	-1.5064 -2.1775	-0.4515 -0.7609	-3.2274 -3.8015	0.6153 0.0048	0.0117 -0.1492
(221)	-0.7507 -0.7791	-0.1306 -0.3001	0.6153 0.0048	-0.6327 -0.6481	0.0020 -0.2249
(310)	0.0149 -0.2531	-0.0067 0.1503	0.0117 -0.1492	0.0020 -0.2249	2.3531 1.5973

Table V.16

SU_3 decomposition of Kuo interaction in 1d-2s shell J=2, T=0

(NLS) \ (N'L'S')	(121)	(221)	(320)
(121)	-5.3230 -5.6702	-1.1291 -1.4985	0.0084 -0.0979
(221)	-1.1291 -1.4985	-1.8906 -2.5985	-0.0001 -0.1156
(320)	0.0084 -0.0979	0.0001 -0.1156	1.5137 1.5094

Table V.17

SU_3 decomposition of Kuo interaction in 1d-2s shell J=3, T=0

(NLS) \ (N'L'S')	(121)	(141)	(221)	(330)
(121)	-4.2332 -5.0383	-0.4581 -0.6275	-0.4805 -0.5892	0.0072 -0.1412
(141)	-0.4581 -0.6275	-3.3547 -3.7750	-0.6312 -0.7682	-0.0071 0.0677
(221)	-0.4805 -0.5892	-0.6312 -0.7682	-1.0255 -1.1839	0.0017 0.0129
(330)	0.0072 -0.1412	-0.0071 0.0677	0.0017 0.0129	1.1538 1.7281

		Bare	Renormalised
J=4, T=0 $\langle(141) \mid v \mid (141)\rangle$	=	-4.1582	-4.3138
J=5, T=0 $\langle(141) \mid v \mid (141)\rangle$	=	-3.4215	-3.6640

Table V.18

The wavefunctions in SU_3 basis for T=1 states

J	(NLS) (100)	(120)	(140)	(200)	(220)	(311)	(321)	(331)
0	0.397 0.858			0.441 0.514		0.007 -0.006		
1						0.711 0.967	0.703 0.256	
2		0.986 0.975			0.167 0.218	-0.003 0.047	-0.002 0.009	0.002 -0.004
3							0.404 0.623	0.914 0.782
4			0.999 0.998					-0.003 0.055

Table V.19

The wave functions in SU_3 basis for T=0 state

J	(NLS) (101)	(121)	(141)	(201)	(221)	(310)	(320)	(330)
1	0.844 0.811	0.353 0.384		0.398 0.431	0.071	-0.002 0.023		
2		0.958 0.926			0.287 0.377		-0.001 0.017	
3		0.879 0.907	0.434 0.418		0.197 0.197			0.001 0.013

Table V.20

Radial integrals fitted to two-body interaction in 1d-2s shell

Radial integrals I_{nl} (MeV)	T=1		T=0	
	Bare	Renor-malised	Bare	Renor-malised
I_{0s}	-6.231	-6.267	-9.294	-9.972
I_{1s}	-3.360	-6.092	-6.634	-8.374
I_{2s}	-1.213	-3.255	-2.751	-3.873
I_{0d}	-0.676	0.088	-0.604	-0.575
I_{1d}	-0.657	-1.655	-0.664	-1.041
I_{0p}	-0.237	0.902	2.222	3.187
I_{1p}	1.113	0.099	3.064	0.862

In table 18 and 19, we have listed the two-particle wave-functions for T=1 and T=0 states in SU_3 basis. These states are obtained by diagonalising the different Hamiltonian matrices given in tables 10 to 17. We have presented only the wave-functions corresponding to the lowest eigenvalue. Here also the upper number denotes the components obtained with the bare interaction while the lower ones correspond to the renormalised interaction.

It can be seen from these tables that even the bare interaction has a small permutation - symmetry mixing component. It may be noted that the bare interaction in 1f-2p shell due

to Kuo and Brown[14] does not have this component as seen from our analysis of 1f-2p shell interaction in chapter IV. However the procedure adopted for calculating the "G" matrix elements by Kuo and Brown in both the 1d-2s and 1f-2p shells is exactly same. This leads us to believe that the procedure of computations of bare matrix elements adopted by Kuo[9] might have introduced this component. The comparison of the two procedures shows that the main difference lies in the fact that Kuo's bare matrix elements are state-dependent. Kuo[9] has introduced this state dependence in the calculations of short-range reaction matrix (G_s) and the second order term for the tensor force. We therefore feel that the introduction of this state-dependence might have caused very small but finite permutation -symmetry mixing in the resulting interaction.

We also note that the permutation symmetry mixing is slightly more for T=1 interaction than for T=0 interaction. Moreover this mixing increases as we go from bare to renormalised interaction. We have noticed this feature in 1f-2p shell also.

Another effect of core-excitation seems to have been reflected in the following observation. The mixing of different SU_3 representations of a given space-symmetry viz., (40) and (02) increases as we go from bare to renormalised interaction. This is also seen from the structure of the wavefunctions for both

T=0 and T=1 states. Similar result is observed in 1f-2p shell also.

It is further seen that the interaction in the symmetric state is strong and attractive while the interaction in antisymmetric states is repulsive and relatively weak. Also the effect of core-excitation seems to make in general the interaction in the symmetric state stronger while that in the antisymmetric states is made somewhat weaker.

Another interesting effect of core-excitation will be obvious if we compare the following matrix elements of symmetric and antisymmetric states.

For symmetric states, study the following T=1 matrix elements.

$$\langle (40)\ 00 \mid v \mid (40)\ 00 \rangle = \begin{matrix} -3.6131 \\ -4.7393 \end{matrix} \quad \text{for } J=0,\ T=1$$

$$\langle (40)\ 20 \mid v \mid (40)\ 20 \rangle = \begin{matrix} -3.1707 \\ -3.5839 \end{matrix} \quad \text{for } J=2,\ T=1$$

$$\langle (40)\ 40 \mid v \mid (40)\ 40 \rangle = \begin{matrix} -2.5424 \\ -2.4284 \end{matrix} \quad \text{for } J=4,\ T=1$$

For antisymmetric states, study the following T=0 matrix elements.

$$\langle (21)\ 10 \mid v \mid (21)\ 10 \rangle = \begin{matrix} 2.3531 \\ 1.5973 \end{matrix} \quad \text{for } J=1,\ T=0$$

$$\langle (21)\ 20 \mid v \mid (21)\ 20 \rangle = \begin{matrix} 1.5137 \\ 1.5094 \end{matrix} \quad \text{for } J=2,\ T=0$$

$$\langle (21)\ 30 \mid v \mid (21)\ 30 \rangle = \begin{matrix} 1.1538 \\ 1.7231 \end{matrix} \quad \text{for } J=3,\ T=0$$

It is clear from these matrix elements that in the lowest symmetric representation (40) the splitting of the states with different J values is sizable in both bare and renormalised interactions and the order of levels resembles the order of the spectra due to q.q interaction. In the antisymmetric representation (21) the states with different J are almost made degenerate due to core-excitation in the renormalised interaction. Both these observations are similar to those seen in the 1f-2p shell.

We can also see the presence of the non-central component in the interaction from studying the two-body matrix elements in SU_3 basis.

The following matrix elements in which L on both sides differ by two show the presence of SU_3 preserving tensor components.

$$\langle (40)\ 01 \mid v \mid (40)\ 21 \rangle = \begin{matrix} -0.9775 \\ -1.5686 \end{matrix} \quad \text{for } J=1,\ T=0$$

$$\langle (20)\ 01 \mid v \mid (20)\ 21 \rangle = \begin{matrix} 0.6153 \\ 0.0048 \end{matrix} \quad \text{for } J=1,\ T=0$$

$$\langle (40)\ 21 \mid v \mid (40)\ 41 \rangle = \begin{matrix} -0.4581 \\ -0.6275 \end{matrix} \quad \text{for } J=3,\ T=0$$

Also the matrix elements in which L on both the sides differ by 1 can also be attributed to tensor or spin-orbit interactions or both. It can be seen however that the most of the important matrix elements are diagonal in L and therefore the overall interaction can be approximated by a central interaction. The group theoretical analysis of the same interaction has been carried out by Pluhar[15] in a more sophisticated way. But our method and emphasis are altogether different from that of Pluhar.

V.6 Radial integral analysis

We have seen from the SU_3 analysis of the previous section that both bare and renormalised interactions can be reasonably well approximated by central interaction. Also we know that any central interaction can be expressed as a linear combination of radial matrix elements. Therefore we tried to obtain by a least-squares fit the radial integrals which best approximate to these interactions. It should be noted that we have neglected the radial integrals I_{0g} and I_{0f} from our fits as their contribution is expected to be small. Thus corresponding

to T=0 and T=1 matrix elements for a given interaction, we obtain two different sets of radial matrix elements. In table 30 we have given four sets of radial integrals corresponding to bare and renormalised interactions. The goodness of the fit can be assessed by calculating the r.m.s. deviation of calculated values from the observed ones. For T=1 states, the fit to bare interaction has given a r.m.s. deviation of 410 KeV while that for the renormalised interaction it is 370 KeV. Similarly for T=0 states, the fit to the bare interaction has given a r.m.s. deviation of 420 KeV while that for renormalised interaction it is found to be 540 KeV. Thus one notes that the fits are fairly good and the resulting radial matrix elements can well describe the salient features of both the interactions.

The values of radial integrals thus obtained lucidly show the difference between the bare and renormalised interactions. It should be noted that each integral is affected differently due to core-excitation. Thus core-excitation does not merely affect the overall strength of the interaction but also selectively introduces different components in the interaction. It is interesting to note that I_{0s} integral is hardly affected as the core-excitation effects are taken into account. The integral I_{1s} is the one which is most affected by core-excitation effects both in T=0 and T=1 states. The radial integral

I_{2s} is also affected appreciably. Other radial integrals are always small and are not much affected. Thus one concludes that the core-excitation effects mainly renormalise the 's' state interactions only.

On the basis of these results one can explain the results of HF calculations and SU_3 analysis. We know that the I_{1s} component is the only dominant component in the 1d-2s shell which mixes different SU_3 representations. The increase or decrease in the 'p' state radial integrals does not affect the SU_3 mixing as there is only one antisymmetric representation (21). The d-state matrix elements are quite small. There is some increase in the I_{1d} component which preserves SU_3 symmetry in the renormalised interaction, and a slight decrease in the I_{0d} interaction which mixes SU_3 symmetry. Therefore the additional SU_3-breaking observed in the renormalised interaction is mainly the result of the large increase (50%) of the I_{1s} component in that interaction. One can see also that the stretching of the HF projected spectra for the renormalised interaction is also the result of the large increase in I_{1s} and I_{2s} component which are found to give rise to the splitting of the ground state bands in Chapter III. The increase in HF gap for the renormalised interaction may also be probably the result of large I_{1s} and I_{2s} component in the renormalised interaction. We have shown in Chapter III

that the I_{1s} interaction does contain quite a large hexadecapole multipole. Therefore the increase in the hexadecapole component which we have qualitatively seen through the HF orbitals in section II is very well confirmed by the large increase in the I_{1s} radial integral in the renormalised interaction.

It is not very clear how the multipole structure of the interaction is connected to the components of the interaction in terms of radial integrals. But it seems almost certain that the introduction of higher multipoles will increase the importance of I_{1s} and I_{2s} components. Thus the salient features of the HF calculations and SU_3 analysis can be explained in a simple way.

V.7 Summary

To summarise, we briefly state that the effect of the core-excitation in 1d-2s shell is essentially to renormalise the 's' state interactions. The I_{0s} interaction remains largely unaffected but I_{1s} and I_{2s} components increase considerably. This explains the increased SU_3 breaking observed in the renormalised interaction. It can also explain the stretching effect in the projected spectra of various nuclei observed with renormalised interaction. These components are mainly responsible for giving rise to large energy

gap in HF single particle spectra. We also show that the projected multishell HF calculations with bare interaction produce results which are similar to those obtained by using renormalised interaction in a single shell. This implies that the projected multi-shell HF calculations using bare interaction seem to be a valid procedure for treating the core-excitations.

Before we close this chapter, we would briefly summarise some recent developments in calculating the effective interaction. Most of these efforts concentrate on the improvement of the core-excitations, leaving aside the bare reaction matrix elements which themselves are calculated using several assumptions and approximations.

In calculating the core-excitation corrections, Kuo and Brown[1] have considered only one-bubble diagram. Since this diagram gives a large contribution, one expects that higher order diagrams consisting of many-bubbles may also have an appreciable contribution to core-excitation correction. The natural course would be to calculate the third order correction in the perturbation series. However the simpler approach would be to calculate the core-excitation correction in TDA (Tamm-Dancoff approximation) or RPA (Random-phase approximation) formalisms. The TDA takes into account all the particle-hole excitations describing core-vibrations by diagonalising the particle-hole interaction. It was found that for T=0

interaction, the contribution of the TDA and the second-order perturbation term does not differ much. On the contrary for T=1 interaction, the TDA gives very large contribution compared to the perturbation term. When one takes into account the ground state correlations, one has to use the random-phase approximation. The RPA contributes quite largely to both T=0 and T=1 state interactions. In fact it was found that the RPA contribution to core-excitation is much larger than that of the second-order perturbation term. The core-excitation corrections in the RPA series has been calculated by Osnes and Warke[16] and independently by Zamick[17].

Later Barrett and Kirson[18] have explicitly calculated the third order term of the perturbation series. This term also includes some of the RPA diagrams considered in above calculations. These diagrams as seen above boosted the core-excitation corrections. But if one also takes into account some other types of diagrams called "Vertex modification" diagrams, one finds that they give repulsive contributions, thus reducing the effect of the RPA diagrams.

Recently Osnes, Kuo and Warke[19] have carried out calculations of some higher order correction in the RPA formalism. They argue that in calculating the energies and wavefunctions of the vibrational states, one should not diagonalise the bare particle-hole interaction but instead one should diagonalise

the renormalised particle-hole interaction. They find this "screening" effect cuts down the contribution from RPA so that RPA together with "screening" gives values for core-excitation corrections close to those obtained from TDA calculations with bare reaction matrix elements.

Finally Goode[20] has calculated the energies and wave-functions of the virbrational states of ^{16}O by diagonalising the bare particle-hole interaction within the full one particle-one hole and two-particle-two hole configuration space. The resultant vibrations are then coupled to the two valence nucleons of ^{18}O. When this is done, Goode finds a cancellation and his prediction of the contribution due to core-excitation is almost the same as the one particle-one hole perturbation result originally obtained by Kuo.

Very recently Kirson[21] has calculated the third order term in the perturbation series taking into account the screening effect. The self-consistent calculations of screening effect coupled with vertex modification have yielded a repulsive contribution to the core-excitation corrections. This had led to a near cancellation of the second-order term, leaving only a much smaller core-excitation effect than the simple second order corrections.

However, one should accept these results with some reservations. In fact our multi-shell HF calculations show

that there does exist some renormalisation of the bare interaction. Also the need to use effective charges to explain the transition probabilities supports the fact that there exists some renormalisation of the interaction due to core-excitation.

There are also some reasons to believe that the results Kirson[21] obtained may suffer from the following shortcomings. The "G" matrix calculations itself is an approximate one and the plane wave approximation for the states outside the model states seems to be somewhat drastic. Further the random phase approximation itself may not be valid at nuclear densities for effective interaction operators. In his calculations Kirson[21] has neglected some third order diagrams whose contributions to core-excitation is unknown. Nevertheless it is almost certain that the bare and renormalised sets of matrix elements in 1d-2s shell given by Kuo do seem to represent the most appropriate empirical set for structure calculations at least in the beginning of 1d-2s shell, even though the explicit procedure of calculating them may not be clear.

REFERENCES

1) T.T.S. Kuo and G.E. Brown, Nucl. Phys. 85 (1966) 40.

2) T. Hamada and I.D. Johnston, Nucl. Phys. 34 (1962) 382.

3) G.E. Brown and T.T.S. Kuo, Nucl. Phys. A92 (1967) 481.

4) L.S. Kisslinger and R.A. Sorenson, Mat. Phys. Medd. Dan. Vid. Selsk. 32 (1960) No.9; Rev. Mod. Phys. 35 (1963) 853.

5) i) H.A. Bethe and J. Goldstone, Proc. Roy. Soc. A238 (1957) 551.

ii) K.A. Brueckner and J.L. Gammel, Phys. Rev. 109 (1958) 1023.

iii) K.A. Brueckner, A.M. Lockett and M. Rotenberg, Phys. Rev. 121(1961) 255.

6) H.A. Bethe, Phys. Rev. 103 (1956) 1353.

7) B.L. Scott and S.A. Moszkowski, Ann. Phys. 14 (1961) 107, Nucl. Phys. 29 (1962) 665.

8) H.A. Bethe, B.H. Brandow and A.G. Petschek, Phys. Rev. 129 (1963) 225.

9) T.T.S. Kuo, Nucl. Phys. A103 (1967) 71.

10) J. Bar-Touv and C.A. Levinson, Phys. Rev. B153 (1967) 1099.

11) D.J. Rowe, Nucl. Phys. A140 (1970) 74.

12) E.C. Halbert, J.B. McGrory, B.H. Wildenthal and S.P. Pandya, in advances in Nuclear Physics, (Plenum Press, New York, 1971), Vol. 4 p. 315-442.

13) J.P. Elliott, A.D. Jackson, H.A. Mavromatis, E.A. Sanderson and B. Singh, Nucl. Phys. A121 (1968) 241.

14) T.T.S. Kuo and G.E. Brown, Nucl. Phys. A114 (1968) 241.

15) Z. Pluhar, Phys. Lett. 29B (1969) 293.

16) E. Osnes and C.S. Warke, Phys. Lett. 30B (1969) 306.

17) L. Zamick, Phys. Rev. Lett. 23 (1969) 1406.

18) i) B.R. Barrett and M.W. Kirson, Nucl. Phys. A148 (1970) 145.

ii) M.W. Kirson and L. Zamick, Ann. Phys. 60 (1970) 185.

19) E. Osnes, T.T.S. Kuo and C.S. Warke, Nucl. Phys. A168 (1971) 190.

20) P. Goode, Nucl. Phys. A172 (1971) 66.

21) i) M.W. Kirson, Theory of Effective Interactions, Nuclear Theory Course, January 13-March 12, 1971, International Centre for Theoretical Physics, Trieste.

ii) M.W. Kirson, Ann. of Phys. 66 (1971) 624.

CHAPTER VI

The generator-coordinate method for ^{20}Ne

VI.1 Introduction

The generator-coordinate formalism[1,2] is basically intended to study the collective motion of the nucleons in a nucleus. This is a microscopic formalism based on the variational principle. This formalism is quite general in its scope and can handle any kind of collective excitations in the nucleus. In fact it has been shown[3] that the generator coordinate method under some approximation yields the equations corresponding to the random phase approximation. which is essentially developed to study the vibrational motion of the spherical nuclei. Also the theory of pairing vibrations can be obtained[4] in the framework of this method. Further it is known that the study of the rotational motion of the deformed nuclei can be very well made using the projected Hartree-Fock (PHF) formalism which does not use the adiabatic approximation of the unified model. Peierls and Yoccoz[5] were the first to show that the formalism of angular momentum projection could be obtained by using the angle of rotation as the generator coordinate. This method can be generalised by incorporating additional generator coordinates besides the angle of rotation to obtain many excited states not belonging to ground band. We will illustrate this method by presenting calculations for ^{20}Ne spectrum.

Thus in the framework of this method, different kinds of collective motions can be studied by choosing different generator coordinates. The suitable choice of the generator coordinates to describe the collective excitations is the crux of the method.

VI.2 Theory of generator coordinate method

We will now discuss in brief the theory of generator coordinate method. The theory has been first developed by Wheeler with Hill[1] and Wheeler with Griffin[2]. Later Jancovici and Schiff[3] and also Brink and Weiguny[6] have studied in detail the integral equation and the various aspects of its solutions. In this theory one avoids defining collective variables explicitly in terms of the single particle variables. To start with, one constructs a many-body wavefunction of the nucleus as a function of the collective variables. The trial wavefunction is an integral over the collective variables with unspecified amplitudes which are to be varied to obtain an approximate eigenstate of the nucleus. In the process we replace the actual Hamiltonian by a new Hamiltonian as a function of the generator coordinate α, by which we choose to describe the collective motion of the nucleus.

Let $\Phi(x, \alpha)$ be a nuclear A-particle wavefunction depending on nuclear coordinates $x = (x_1, x_2, \ldots\ldots x_A)$

and on variables (generator coordinates) $\alpha = (\alpha_1, \alpha_2, \ldots \alpha_m)$. The trial wavefunction for the given nucleus can be constructed as a superposition of the wavefunction $\Phi(x, \alpha)$ with the weight function $f(\alpha)$

$$\Psi(x) = \int \Phi(x, \alpha) f(\alpha) \, d\alpha \tag{1}$$

where the right hand side of Eq. (1) is an m-diamensional integral over the space of parameters $\alpha_1, \alpha_2, \ldots \alpha_m$. The quantities α's are called "generator coordinates" as they serve to generate the wavefunction of the system. It may be noted that this generator coordinate is not expressed as a function of the coordinates $(x_1, x_2, \ldots x_A)$. Also the final many-body wavefunction does not explicitly depend on α. We next determine the generator wavefunction $f(\alpha)$ from the variational principle. In other words we require that the expectation value of the Hamiltonian of the A-particle system shall be an extremum with respect to the variation of the generator wavefunction $f(\alpha)$ subject to the normalisation condition.

$$\frac{\partial}{\partial f^*(\alpha)} \left[\langle \Psi | H | \Psi \rangle - E \langle \Psi | \Psi \rangle \right] = 0 \tag{2}$$

Writing explicitly we get

$$\langle \Psi | H | \Psi \rangle = \int\int f^{*}(\alpha_1) f(\alpha_2) \langle \Phi(x,\alpha_1) | H | \Phi(x,\alpha_2) \rangle d\alpha_1 d\alpha_2$$

$$= \int\int f^{*}(\alpha_1) f(\alpha_2) H(\alpha_1,\alpha_2) d\alpha_1 d\alpha_2 \qquad (3)$$

where

$$H(\alpha_1,\alpha_2) = \langle \Phi(x,\alpha_1) | H | \Phi(x,\alpha_2) \rangle \qquad (4)$$

Also we define

$$\langle \Psi | \Psi \rangle = \int\int f^{*}(\alpha_1) f(\alpha_2) I(\alpha_1,\alpha_2) d\alpha_1 d\alpha_2 \qquad (5)$$

where $$I(\alpha_1,\alpha_2) = \langle \Phi(x,\alpha_1) | \Phi(x,\alpha_2) \rangle \qquad (6)$$

Substituting the eq. (3) and (5) in the eq. (2) and differentiating with respect to $f^{*}(\alpha_1)$, we get

$$\int [H(\alpha_1,\alpha_2) - E\, I(\alpha_1,\alpha_2)] f(\alpha_2) d\alpha_2 = 0 \qquad (7)$$

The equation (7) represents the famous Hill-Wheeler integral equation. Note that the quantity $H(\alpha_1,\alpha_2)$ is generally referred to as "energy kernel" while the quantity $I(\alpha_1,\alpha_2)$ is referred to as "overlap kernel" The overlap kernel is always positive and less than or equal to unity. It is clear that both the kernels are hermitian by definition.

The Hill-Wheeler integral equation (7) can be interpreted[7] as a Schrodinger equation for the collective motion in the non-orthonomal basis with $f(\alpha)$ as the associated collective wavefunction. For every weight function $f(\alpha)$, there is a corresponding many-particle wave function $\Psi(\alpha)$ defined by eq. (1). The set of states $\Psi(\alpha)$ generated by the Hill-Wheeler integral equation forms a subspace N_Φ of the complete Hilbert space N of wavefunctions of the original many-body system. Solving the integral equation (7) is equivalent to diagonalizing the complete Hamiltonian H of the system in the subspace N_Φ of N. The generator coordinate method would give an exact solution of the original problem if all A-particle states could be generated by the integral (1), i.e. $N_\Phi = N$. In other cases the method gives approximate eigenfunctions and eigenvalues and the accuracy of the method depends on the extent to which the low eigenstates of H can be approximated by states in N_Φ. This in turn depends on the choice of the generating function $\Phi(x, \alpha)$ and on the generator coordinate α. It is obvious now that the lowest eigenvalue of eq. (7) should give an approximation to the ground state energy of the system and higher values to the excited states.

Recently Brink and Weiguny[6] have suggested another procedure for solving the Hill-Wheeler integral equation. The procedure consists of choosing a subspace N_g such that it is connected to the subspace N_Φ by a unitary

transformation. In this new subspace N_g, the Hamiltonian operator H may have relatively simple form, viz. h. Thus diagonalising the Hamiltonian operator H in the subspace N_Φ is made equivalent to diagonalizing the new Hamiltonian operator h in the subspace of N_g. It is obvious that this procedure is useful only if the equivalent Hamiltonian h is relatively simple. This approach is very useful in solving Hill-Wheeler integral equation when the Gaussian overlap approximation (GOA) is used. In GOA, we assume that the overlap kernel has a Gaussian form and the ratio of energy kernel to overlap kernel is a slowly ranging function of generator coordinates. Though there is no theoretical justification for this assumption, it was found that the GOA is a good approximation when i) the number of particles is very large, and ii) the nuclear wave function is well represented by a Slater determinant. Under the GOA, the equivalent Hamiltonian h is just a set of 'm' coupled oscillators. Therefore the eigenvalue problem in the subspace of N_g can be easily solved. It was shown that the solution of this eigenvalue problem leads to a set of RPA-like equations.

So far we have implicitly assumed that the generator coordinates are real numbers. However Brink and Weigung[6] have pointed out some problems for which a generalization to complex parameters seems necessary.

VI.3 Generalisation of the projection theory to two generator coordinates

As stated in the section 1, if one uses the additional generator coordinates besides the angle of rotation, one also gets the excited states not belonging to the ground band. With this view in mind, we have used one more generator coordinate λ besides of course Ω, the angle of rotation. We will denote both these coordinates by $\alpha = (\lambda, \Omega)$. If $\Phi(\quad)$ denotes the generating function, then our trial wavefunction can be given as

$$\Psi(x) = \int \Phi(x,\alpha) f(\alpha) \, d\alpha \tag{8}$$

Now for simplicity we assume that

$$f(\alpha) = g(\lambda) h(\Omega)$$

Hence

$$\Psi(x) = \int\int \Phi(x,\lambda,\Omega) g(\lambda) h(\Omega) \, d\lambda \, d\Omega \tag{9}$$

We will now determine the functions $g(\lambda)$ and $h(\Omega)$ by the usual variational method. The condition that

$$\frac{\partial}{\partial g^*(\lambda')} \frac{\partial}{\partial h^*(\Omega')} \left[\langle \Psi | H | \Psi \rangle - E \langle \Psi | \Psi \rangle \right] = 0 \qquad (10)$$

yields the Hill-Wheeler integral equation for both g and h. Substituting eq. (9) in eq. (10) and differentiating w.r. to $g^*(\lambda')$ and $h^*(\Omega')$ we get

$$\int\int \left[\langle \Psi(x,\lambda',\Omega') | H | \Psi(x,\lambda,\Omega) \rangle - E \langle \Psi(x,\lambda',\Omega') | \Psi(x,\lambda,\Omega) \rangle \right] \times g(\lambda) h(\Omega) \, d\lambda \, d\Omega = 0 \qquad (11)$$

Following Yoccoz and Peierls we make the ansatz that

$$\Psi(x,\lambda,\Omega) = R(\Omega) \Psi(x,\lambda) \qquad (12)$$

Also we may expand $h(\Omega)$ in terms of rotation matrices $D^J_{MK}(\Omega)$ as they form a complete set. Therefore we write

$$h(\Omega) = \sum_{J,M,K} a^J_{MK} D^J_{MK}(\Omega) \qquad (13)$$

Substituting eq. (12) and eq. (13) in eq. (11) and remembering that Hamiltonian in invariant under rotation we get

$$\int\int \left[\langle \Psi(x,\lambda') | H \bar{R}^{-1}(\Omega') R(\Omega) | \Psi(x,\lambda) \rangle - E \langle \Psi(x,\lambda') | \bar{R}^{-1}(\Omega') R(\Omega) | \Psi(x,\lambda) \rangle \right] \times \left(\sum_{J,M,K} a^J_{MK} D^J_{MK}(\Omega) \right) d\lambda \, d\Omega = 0 \qquad (14)$$

Now define the rotation (Ω'') such that

$$R(\Omega'') = R^{-1}(\Omega') R(\Omega) \tag{15}$$

then we have

$$D^{J}_{MK}(\Omega) = \sum_{K'} D^{J}_{MK'}(\Omega') D^{J}_{K'K}(\Omega'') \tag{16}$$

Substituting eq. (15) and eq. (16) in eq. (14) we get

$$\int\int \left[\langle \phi(x,\lambda') | H R(\Omega'') | \phi(x,\lambda) \rangle - E \langle \phi(x,\lambda') | R(\Omega'') | \phi(x,\lambda) \rangle \right] \times \left(\sum_{J,M,K} a^{J}_{MK} \sum_{K'} D^{J}_{MK'}(\Omega') D^{J}_{K'K}(\Omega'') \right) g(\lambda)\, d\lambda\, d\Omega'' = 0$$

Using the property of the orthogonality of the rotation matrices we get the following expression for the axially symmetric case for which summation over K does not exist.

$$\int \left[H^{J}(x,\lambda',\lambda) - E^{J} I^{J}(x,\lambda',\lambda) \right] g(\lambda)\, d\lambda = 0 \tag{17}$$

where

$$H^{J}(x,\lambda',\lambda) = \int \langle \phi(x,\lambda') | H | \phi(x,\lambda) \rangle D^{J}_{MK}(\Omega'')\, d\Omega''$$

and $I^{J}(\alpha, \alpha', \lambda) = \int \langle \Psi(\alpha, \lambda') \mid \Psi(\alpha, \lambda) \rangle D^{J}_{MK}(\Omega'') \, d\Omega''$

the equation 17 is the modified Hill-Wheeler integral equation which can be solved by various suitable approximations. In our calculations we have used the strength of the external quadrupole field as another generator coordinate (λ). The details of the solution of the equation (17) are given in the next section.

VI.4 Application to ^{20}Ne nucleus:

After the established success of the PHF method[8] to obtain the ground state bands of nuclei, it is natural to look for a generalisation based on this method to obtain higher bands of levels in the nuclear spectra. The validity of such a generalisation has to be assessed by comparison with exact shell model calculations. In this section we have shown that the generator coordinate calculations with constrained axial HF states as basis do provide such a generalization which is simpler and computationally less involved than the alternative formalism of projecting the states from particle-hole excited intrinsic states[9]. Such calculations may also give some insight into the physical nature of the excited states in the shell model spectra.

It may be noted that the generator coordinate calculations with Nilsson's states as basis is able to explain[10] the

ground state band of ^{20}Ne. However it is wellknown that PHF method is equally successful and much simpler. Hence one would look for the natural unification of the generator coordinate method and PHF method by using constrained HF solutions in projection formalism.

We have employed the effective interaction matrix elements of Kuo[11] derived from the Hamada-Johnston potential, renormalised for the 1d-2s configuration space used in these calculations along with the experimental single particle energies of ^{17}O as given below both for protons and neutrons.

$$d_{5/2} = 0 \text{ MeV}, \qquad d_{3/2} = 5.08 \text{ MeV}, \qquad s_{1/2} = 0.87 \text{ MeV}.$$

We have used the " λ " the strength of the quadrupole interaction as the generator coordinate and constructed the new Hamiltonian which will depend on the value of λ , as given below.

$$H = H - \lambda Q_0^2$$

We have employed the HF formalism to get the single particle wavefunctions for this new Hamiltonian. In other words we minimised the free energy $E_F = \langle \Phi_\lambda | H - \lambda Q_0^2 | \Phi_\lambda \rangle$ in the HF procedure to obtain the states Φ_λ for different values of λ . The different solutions Φ_λ are called the constrained HF solutions. However it has been shown[12] that the constrained

HF solutions are multivalued functions of generator coordinate λ or equivalently of the expectation value of quadrupole moment $\langle \Phi_\lambda | Q_0^2 | \Phi_\lambda \rangle$. This is expected due to the multiplicity of the existing HF solutions[13]. To get rid of this problem we used the following procedure. We started with the lowest prolate HF solution corresponding to $\lambda = 0$, and then picked out that branch of the solution which is generated, as smoothly as possible out of this lowest HF solution. This is achieved by using the HF solution Φ_λ as the starting point for the iteration of the solution $\Phi_{\lambda + d\lambda}$ where $d\lambda$ is a small increment in the strength of the external quadrupole field. The curves of energy E_F V_s λ and the quadrupole moment $\langle Q_0^2 \rangle$ V_s λ are plotted in the fig.1 in different arbitrary units. It may be noted that the constrained HF solutions obtained for different values of λ are connected to each other by quadrupole interaction. Also the fact that we minimise the energy for each value of λ indicates that we get the lowest solution for that value of λ, which can be connected by quadrupole interaction. This procedure therefore, in a way ensures that the low-lying states of ^{20}Ne will be well described by the resulting wavefunctions.

Once the different constrained HF solutions are obtained, next task is to project out the good-J states from these HF solutions. In fact it is in the basis of these good-J states

FIG. VI · 1

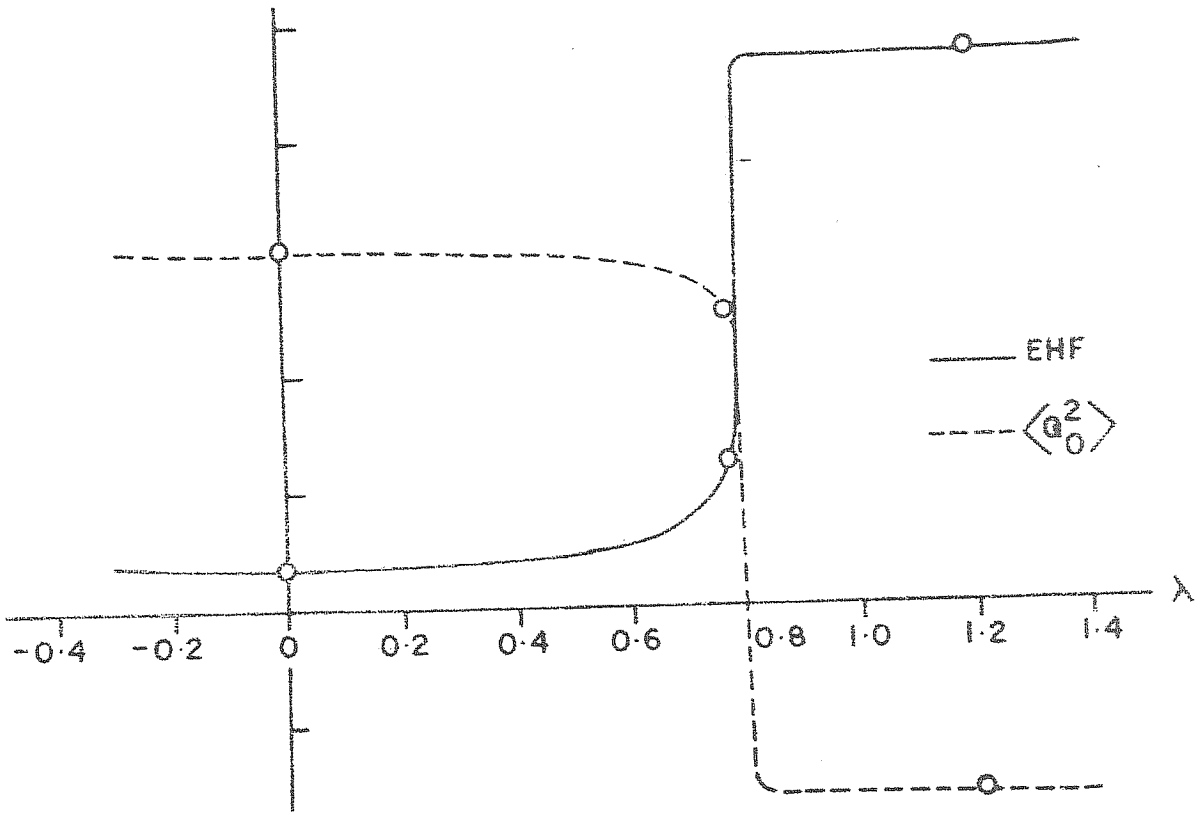

that we will construct the trial wavefunction for variation. We will therefore solve the Hill-Wheeler integral eq. (17) in the basis of these states for different J states.

$$\int \left[H^J(\lambda,\lambda') - E^J I^J(\lambda,\lambda') \right] f(\lambda')\, d\lambda' = 0$$

where $$H^J(\lambda,\lambda') = \langle \phi_\lambda | H P^J_{00} | \phi_{\lambda'} \rangle$$
$$I^J(\lambda,\lambda') = \langle \phi_\lambda | P^J_{00} | \phi_{\lambda'} \rangle$$

where P^J_{00} is the wellknown projection operator[8].

One would expect that these Hill-Wheeler integral equations may be solved by using the famous Gaussian overlap approximation. But as the number of particles involved is very small, it is possible that the Gaussian overlaps approximation will not be valid. Alternatively one sees that the curves of energy V_s λ and quadrupole moment $\langle Q_o^2 \rangle$ V_s λ (fig.1) are quite flat due to the stiffness of ^{20}Ne HF solution around prolate as well as oblate deformation. This suggests the possibility that we can as well approximate the Hill-Wheeler integral equation itself by descretising the coordinates λ as follows

$$\sum_m (H^J_{nm} - E^J I^J_{nm}) f_m = 0 \qquad (18)$$

In other words it is enough to take a few points with sufficiently different deformation as otherwise the Hilbert space ϕ^J_λ is over complete. In our calculations we have used

three suitable points to carry out the calculations. In table 1, 2 and 3 we have given the constrained HF solutions corresponding to these three points. Thus it can be seen that the problem of solving the Hill-Wheeler integral equation is reduced to diagonalising the Hamiltonian matrix in the basis of good-J states projected from the constrained HF solutions at three different values of λ. It is obvious, therefore, that for each J one has to diagonalise a (3x3) matrix after properly taking account of non-orthonormality (see appendix 2). The results of diagonalisation for J=0, 2, 4, 6 and 8 are given in tables 4 to 8. It may be noted that there are three eigenvalues and corresponding eigenfunctions representing three states for all J except for J=8. For J=8, there are only two eigenvalues. The reason lies in the fact that one of the eigenvalues of the overlap matrix is very small and hence the corresponding state has to be dropped as explained in the appendix 2. All the states below 18 MeV are shown in the fig.2 (GC). We have also shown the ^{20}Ne spectrum (see fig.2 (1p-1h)) obtained by diagonalising the Hamiltonian in the space of good-J states projected from the prolate HF as well as the K=0, T=0 states obtained by one particle-one hole (1p-1h) excitations. The results of the generator-coordinate calculations along with the above results are compared with the result of the exact shell model[14] (fig.2, (S-M)) and the experimental spectrum (fig.2 (exp)) for T=0 states of ^{20}Ne. The shell model

Table VI.1

^{20}Ne HF orbitals for the ground state (λ =0)
(Solution Φ_1)

E_{HF} = -21.23 MeV Q_{HF} = 15.45 b^2

k	ε_k in MeV	$s_{1/2}$	$d_{3/2}$	$d_{5/2}$
1/2	-11.63	-0.4985	-0.3976	0.7703
3/2	-4.38	0	-0.2259	0.9742
1/2'	-1.80	0.6869	0.3610	0.6308
5/2	-1.10	0	0	1.0
1/2''	0.27	-0.5289	0.8435	0.0932
3/2'	3.76	0	0.9742	0.2259

Table VI.2

^{20}Ne HF orbitals for the ground state (λ = 0.77)
(Solution Φ_2)

E_{HF} = -19.54 MeV Q_{HF} = 12.69 b^2

k	ε_k in MeV	$s_{1/2}$	$d_{3/2}$	$d_{5/2}$
1/2	-8.244	-0.2563	-0.4118	0.8745
3/2	-3.568	0	-0.1075	0.9942
5/2	-3.034	0	0	1
1/2'	-2.555	0.9656	-0.0678	0.2511
1/2''	0.420	-0.0441	0.9087	0.4150
3/2'	1.576	0	0.9942	0.1075

Table VI.3

^{20}Ne HF orbitals for the oblate solution (λ =1-2)
(solution Φ_3)

E_{HF} = -12.57 MeV Q_{HF} = -7.80 b^2

k	ε_k in MeV	$s_{1/2}$	$d_{3/2}$	$d_{5/2}$
1/2	-9.56	0.8361	-0.2526	0.4870
5/2	-7.36	0	0	1.0
3/2	-4.47	0	0.5482	0.8364
1/2'	0.50	-0.3658	0.4047	0.8381
3/2'	0.82	0	0.8364	-0.5482
1/2''	6.28	0.4033	0.8789	-0.2460

Table VI.4

J=0, T=0 states of ^{20}Ne obtained by generator coordinate method

E in MeV.	Φ_1	Φ_2	Φ_3
-24.44	0.7769	-0.1384	0.6142
-17.61	0.4533	0.7093	-0.3939
-11.62	-0.4364	0.5843	0.6838

Table VI.5

J=2, T=0 states of ^{20}Ne obtained by generator coordinate method

E in MeV	Φ_1	Φ_2	Φ_3
-23.24	0.9200	-0.1732	0.3514
-14.47	-0.0706	0.8090	0.5835
- 9.91	-0.3854	-0.5617	0.7321

Table VI.6

$J=4$, $T=0$ states of ^{20}Ne obtained by generator coordinate method.

E in MeV	Φ_1	Φ_2	Φ_3
-20.88	0.0772	0.9970	0.0019
-13.75	0.8272	-0.0651	0.5581
-3.55	-0.5565	0.0415	0.8297

Table VI.7

$J=6$, $T=0$ states of ^{20}Ne obtained by generator coordinate method.

E in MeV.	Φ_1	Φ_2	Φ_3
-16.64	-0.0522	0.9898	-0.1325
-8.68	-0.3962	0.1013	0.9125
-6.18	0.9167	0.1001	0.3869

Table VI.8

$J=8$, $T=0$ states of ^{20}Ne obtained by generator coordinate method.

E in MeV.	Φ_1	Φ_2
-12.82	0.1257	0.9921
-8.96	0.9921	-0.1257

FIG. XI . 2

^{20}Ne SPECTRUM

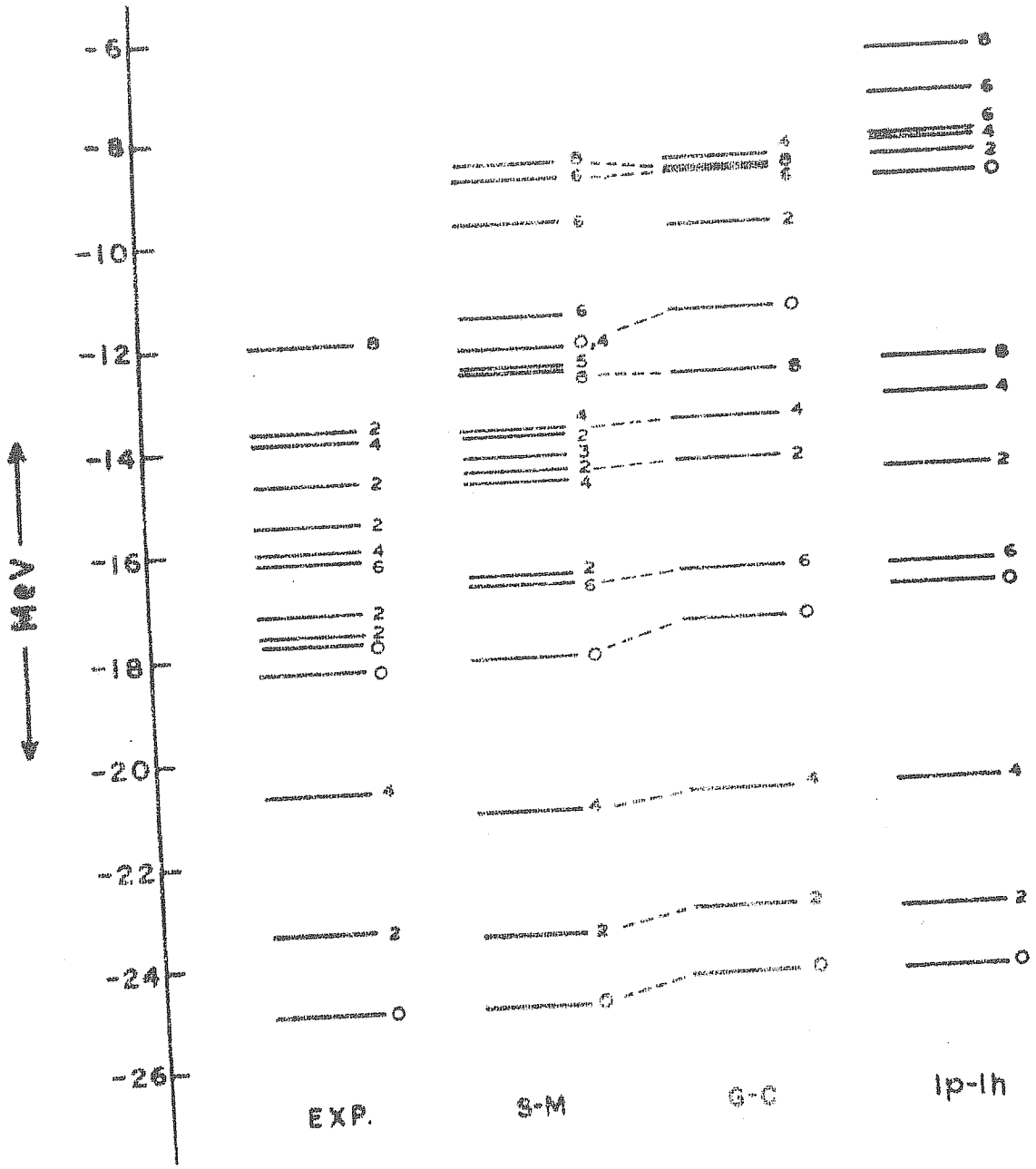

calculations using the Kuo's two-body matrix elements have been done by McGrory for us. We have plotted all the energy levels in absolute scale to facilitate a meaningful comparison of different methods.

VI.5 Discussion

From fig.2 it can be seen that the agreement between the generator coordinate spectrum and the corresponding T=0 levels in shell model spectrum is quite good. We have been able to identify[15] 11 levels in the shell model spectrum which are generated in these axially symmetric generator coordinate calculations. For the highest levels in the generator coordinate spectrum with an angular momentum 2 and 4, we do not have the corresponding results of exact shell model calculations to compare with, while there are several levels in the shell model spectrum at excitations of 8 to 10 MeV, which are not obtained in the axial generator coordinate calculations. Otherwise the generator coordinate results are consistently better in agreement with the exact shell model results than those obtained through 1p-1h projection calculations. Also note that the ground band is slightly improved in the generator coordinate calculations. In short the states calculated by the generator coordinate method give an excellent agreement with a major part of the shell model spectrum below 13 MeV. We have seen from separate calculations that there is a K=2 band at about

8 to 10 MeV. This band is very likely to mix with other states from K=0 intrinsic states. This seems to suggest that it may be possible to reproduce all T=0 shell model levels below 18 MeV excitation through addition of non-axial deformations in the generator-coordinate method. In the experimental spectrum (fig.2 (exp.)), however, there are many levels which presumably arise from the core-excitations.

It is interesting to see what really gives such an excellent agreement with the shell model calculations. Even the most elaborate and complete calculations by Macfarlane and Shukla[9] did not yield such an overall good results. If we look at the three solutions which we have taken for calculations, one sees that the last solution Φ_3 is the oblate solution. This suggests that the shape-mixing is necessary. But the oblate solution we have used is different from the usual ^{20}Ne oblate solution where the orbital k=5/2 is occupied. In our oblate solution the orbital k=1/2 is occupied. Also the middle point corresponding to solution Φ_2 is unique in the sense that it cannot be obtained in any other way. Thus our procedure of using constrained HF solutions as basis for the calculation seems to be responsible for the good agreement with the shell model results. In other words " λ " the strength of the quadrupole interaction proves to be a very useful and appropriate generator coordinate in the calculations of ^{20}Ne spectrum.

It would be interesting to see how this method with this procedure works in other 1d-2s shell nuclei. Also the study of the correlations between the generation of states and the corresponding transition probabilities will be of great interest. Finally it may be worth studying the connection between the important shape mixing effects present in the neutron excess nuclei[15] and the corresponding generator coordinate calculations.

REFERENCES

1) D.L. Hill and J.A. Wheeler, Phys. Rev. 89 (1953) 1102

2) J.J. Griffin and J.A. Wheeler, Phys. Rev. 108 (1957) 311.

3) B.J. Jancovici and D.H. Schiff, Nucl. Phys. 58 (1967) 678.

4) R. Padjen and G. Ripka, Nucl. Phys. A132 (1969) 489.

5) R.E. Peierls and J. Yoccoz, Proc. Roy. Soc. A70 (1957) 381.

6) D.M. Brink and A. Weiguny, Nucl. Phys. A120 (1968) 59.

7) C.W. Wong, Nucl. Phys. A147 (1970) 545.

8) G. Ripka, "Advances in Nuclear Physics" Vol. I, edited by M. Baranger and E.Vogt (Plenum Press, New York, 1968)

9) i) S.N. Tewari, Phys. Letts. 29B (1969) 5.

ii) L. Satpathy, Phys. Rev. 174 (1968) 1324.

iii) M.H. Macfarlane and A.P. Shukla, Phys. Letts. 35B (1971) 11.

10) M.V. Mihailovic, T. Kujawski and J. Lesjak, Nucl. Phys. A161 (1971) 252.

11) T.T.S. Kuo, Nucl. Phys. A103 (1967) 71.

12) B. Girand, J. Le. Tourneux, and S.K.M. Wong, Phys. Lett. 32B (1970) 23.

13) J.C. Parikh, Phys. Lett. 25B (1967) 181.

14) J.B. McGrory, Private Communication.

15) S.B. Khadkikar and D.R. Kulkarni, Proceeding of the Nuclear Physics and Solid State Physics Symposium 1972, Bombay.

16) S.B. Khadkikar, S.C.K. Nair and S.P. Pandya, Phys. Lett. 36B (1971) 290.

APPENDIX I

The two-body matrix elements of Kuo and Brown in the 1f-2p shell in SU_3 basis.

In this appendix we have listed the two-body matrix elements of Kuo and Brown in the 1f-2p shell in SU_3 basis. The notations used in the following tables are given below:

The number N can have six values viz. 1, 2, 3, 4, 5, and 6 standing for SU_3 representations (60), $(22)_{k=0}$, $(22)_{k=2}$, (22)', (41) and (03) respectively. Also note that the representation (22)' corresponding to the state Ψ_3 is used only in J=2, T=1, J=1 , T=0 and J=3, T=0 states. Thus the state (NLS) corresponds to SU_3 representation N having total angular momentum L and total spin S.

For example $(421) \equiv |(22)', L=2, S=1\rangle$

$(141) \equiv |(40) , L=4, S=1\rangle$

Also in tables, there are two values for each matrix elements. The upper one corresponds to the bare interaction while the lower one in the bracket corresponds to the renormalised interaction.

TABLE 1

J=0, T=1

(NLS) \ (N'L'S')	(100)	(200)	(511)	(611)
(100)	-2.719 (-3.567)	-0.927 (-1.617)	0 (0.018)	0 (0.072)
(200)	-0.927 (-1.617)	-1.991 (-2.862)	0 (0.037)	0 (0.033)
(511)	0 (0.018)	0 (0.037)	1.528 (1.358)	0.399 (0.327)
(611)	0 (0.072)	1.528 (0.033)	0.399 (0.327)	1.019 (0.948)

TABLE 2

J=1, T=1

NLS) \ (N'L'S')	(511)	(521)	(611)
(511)	-0.212 (-0.161)	0.151 (0.065)	-0.059 (-0.214)
(521)	0.151 (0.065)	-0.234 (-0.032)	0 -0.018
(611)	-0.059 (-0.214)	0 (-0.018)	-0.182 (0.026)

TABLE 3

J=2, T=1

(NLS) \ (N'L'S')	(120)	(220)	(420)	(511)	(521)	(531)	(611)	(631)
(120)	-2.004 (-2.344)	0.428 (0.719)	-0.197 (-0.304)	0 (-0.115)	0 (0.092)	0 (0.049)	0 (-0.060)	0 (-0.003)
(220)	0.423 (0.719)	-1.043 (-1.141)	-0.005 (0.041)	0 (0.017)	0 (0.035)	0 (0.041)	0 (0.063)	0 (-0.056)
(420)	-0.197 (-0.304)	0.145 (0.041)	-0.666 (-0.665)	0 (0.016)	0 (-0.085)	0 (-0.049)	0 (0.045)	0 (-0.042)
(511)	0 (-0.115)	0 (0.017)	0 (0.016)	-0.201 (-0.288)	0.139 (0.164)	0.130 (0.109)	-0.074 (-0.237)	0.074 (-0.012)
(521)	0 (0.092)	0 (0.035)	0 (-0.085)	0.139 (0.164)	0.422 (0.371)	0.342 (0.275)	0 (-0.011)	0.255 (0.198)
(531)	0 (0.049)	0 (0.041)	0 (-0.049)	0.130 (0.109)	0.342 (0.275)	0.279 (0.612)	0.057 (0.024)	0.080 (0.051)
(611)	0 (-0.060)	0 (0.063)	0 (0.045)	-0.074 (-0.237)	0 (-0.011)	0.057 (0.024)	-0.122 (-0.033)	0.002 (0.022)
(631)	0 (-0.003)	0 (-0.056)	0 (-0.042)	0.074 (-0.012)	0.225 (0.198)	0.080 (0.051)	0.002 (0.022)	0.107 (0.541)

TABLE 4

J=3, T=1

(NLS) \ (N'L'S')	(330)	(521)	(531)	(541)	(631)
(330)	-0.243	0	0	0	0
	(-0.032)	(0.013)	(0.009)	(0.031)	(-0.030)
(521)	0	-0.211	0.044	0.024	0.024
	(0.013)	(-0.099)	(0.090)	(-0.030)	(0.056)
(531)	0	0.044	-0.266	0.051	-0.079
	(0.009)	(0.090)	(0.004)	(0.019)	(-0.150)
(541)	0	0.024	0.051	-0.133	-0.069
	(0.031)	(-0.030)	(0.019)	(0.197)	(-0.046)
(631)	0	0.024	-0.079	-0.069	-0.057
	(-0.030)	(0.056)	(-0.150)	(-0.046)	(0.278)

TABLE 5

J=4, T=1

(NLS) \ (N'L'S')	(140)	(340)	(531)	(541)	(551)	(631)
(140)	-1.582	-0.245	0	0	0	0
	(-1.698)	(-0.388)	(-0.126)	(0.040)	(0.029)	(-0.027)
(340)	-0.245	-0.519	0	0	0	0
	(-0.388)	(-0.368)	(0.015)	(-0.120)	(-0.058)	(-0.030)
(531)	0	0	0.063	-0.008	0.039	-0.003
	(-0.126)	(0.015)	(0.320)	(0.028)	(0.008)	(-0.039)
(541)	0	0	-0.008	0.245	0.257	0.209
	(0.040)	(-0.120)	(0.028)	(0.311)	(0.228)	(0.202)
(551)	0	0	0.039	0.257	0.187	0.068
	(0.029)	(-0.058)	(0.008)	(0.228)	(0.662)	(0.008)
(631)	0	0	-0.003	0.187	0.068	0.003
	(-0.027)	(-0.030)	(-0.039)	(0.202)	(0.008)	(0.450)

TABLE 6

J=5, T=1

(N'L'S') / (NLS)	(541)	(551)
(541)	-0.119 (0.145)	-0.016 (0.010)
(551)	-0.016 (0.010)	-0.236 (0.156)

TABLE 7

J=6, T=1

(N'L'S') / (NLS)	(160)	(551)
(160)	-1.352 (-1.235)	0 (-0.119)
(551)	0 (-0.119)	0.085 (0.567)

TABLE 3

J=1, T=0

(NLS) \ (N'L'S')	(101)	(121)	(201)	(221)	(421)	(510)	(610)
(101)	-4.857 (-4.415)	-1.148 (-1.105)	-1.794 (-1.593)	0.538 (0.430)	-0.698 (-0.500)	0 (-0.150)	0 (-0.106)
(121)	-1.148 (-1.105	-2.993 (-2.832)	-0.527 (-0.369)	0.538 (0.446)	0.038 (-0.039)	0 (0.112)	0 (0 095)
(201)	-1.794 (-1.593)	-0.527 (-0.369)	-3.534 (-3.200)	0.176 (0.272)	0.307 (-0.055	0 (-0.129)	0 (-0.097)
(221))	0.538 (0.430)	0.538 (0.446)	0.176 (0.272)	-1.124 (-1.220)	-0.306 (-0.458)	0 (-0.044)	0 (0.018)
(421)	-0.698 (-0.500)	0.033 (-0.039)	0.307 (-0.055)	-0.306 (-0.458)	-0.439 (-0.485)	-0 (-0.117)	0 (-0.045)
(510)	0 (-0.150)	0 (0.112)	0 (-0.129)	0 (-0.044)	0 (-0.117)	1.212 (1.019)	0.369 (0.114)
(610)	0 (-0.106)	0 (0.095)	0 (-0.097)	0 (0.018)	0 (-0.045)	0.369 (0.114)	1.061 0.807

TABLE 9

J=2, T=0

(NLS) \ (N'L'S')	(121)	(221)	(421)	(331)	(520)
(121)	-3.683	1.028	-0.849	0.078	0
	(-3.177)	(0.879)	(-0.726)	(0.004)	(0.118)
(221)	1.028	-2.340	0.208	-0.155	0
	(0.879)	(-2.010)	(0.391)	(-0.449)	(-0.037)
(421)	-0.849	0.208	-1.633	-0.167	0
	(-0.726)	(0.391)	(-1.573)	(-0.276)	(0.051)
(331)	0.078	-0.155	-0.167	-0.271	0
	(0.004)	(-0.449)	(-0.276)	(-0.330)	(-0.022)
(520)	0	0	0	0	1.150
	(0.118)	(-0.037)	(0.051)	(-0.022)	(0.852)

TABLE 10

J=3, T=0

(NLS) \ (N'L'S')	(121)	(141)	(221)	(421)	(331)	(341)	(530)	(630)
(121)	-3.183 (-3.266)	-0.523 (-0.478)	0.700 (0.722)	-0.287 (-0.221)	-0.042 (-0.044)	-0.199 (-0.133)	0 (-0.120)	0 (-0.027)
(141)	-0.523 (-0.478)	-2.481 (-2.375)	0.305 (0.194)	-0.480 (-0.425)	0.118 (0.121)	-0.284 (-0.262)	0 (0.092)	0 (0.039)
(221)	0.700 (0.722)	0.305 (0.194)	-1.538 (-1.558)	-0.136 (-0.120)	0.103 (0.212)	-0.274 (-0.092)	0 (0.050)	0 (0.035)
(421)	-0.287 (-0.221)	-0.480 (-0.425)	-0.136 (-0.120)	-0.839 (-0.895)	0.097 (0.196)	-0.487 (-0.382)	0 (0.030)	0 (-0.036)
(331)	-0.042 (-0.044)	0.118 (0.121)	0.103 (0.212)	0.097 (0.196)	-0.263 (-0.268)	0.263 (0.279)	0 (-0.028)	0 (-0.027)
(341)	-0.199 (-0.133)	-0.284 (-0.262)	-0.274 (-0.092)	-0.487 (-0.382)	0.263 (0.279)	-0.506 (-0.543)	0 (0.035)	0 (-0.031)
(530)	0 (-0.120)	0 (0.092)	0 (0.050)	0 (0.030)	0 (-0.028)	0 (-0.035)	0.759 (0.913)	0.181 (0.063)
(630)	0 (-0.027)	0 (0.039)	0 (0.035)	0 (-0.036)	0 (-0.027)	0 (-0.031)	0.181 (0.063)	0.567 (0.996)

TABLE 11

J=4, T=0

(NLS) \ (N'L'S')	(141)	(331)	(341)	(540)
(141)	-2.364 (-2.528)	-0.075 (-0.109)	-0.683 (-0.605)	0 (0.049)
(331)	-0.075 (-0.109)	-0.251 (-0.392)	-0.189 (-0.174)	0 (0.028)
(341)	-0.683 (-0.605)	-0.199 (-0.174)	-1.286 (-1.352)	0 (0.037)
(540)	0 (0.049)	0 (0.028)	0 (0.037)	0.750 (0.754)

TABLE 12

J=5, T=0

(NLS) \ (N'L'S')	(141)	(161)	(341)	(550)
(141)	-2.537 (-2.629)	-0.194 (-0.153)	-0.363 (-0.349)	0 (-0.084)
(161)	-0.194 (-0.153)	-2.154 (-2.183)	-0.430 (-0.385)	0 (0.039)
(341)	-0.363 (-0.349)	-0.430 (-0.385)	-0.655 (-0.651)	0 (0.023)
(550)	0 (-0.084)	0 (0.039)	0 (0.023)	0.546 (1.002)

		Bare	Renormalised
J=6, T=0, $\langle (161) \mid v \mid (161) \rangle$	=	-2.432	-2.217
J=7, T=0, $\langle (161) \mid v \mid (161) \rangle$	=	-2.185	-2.199

APPENDIX II

The orthonormalisation of the basis states

In this appendix we discuss how to take into account the non-orthonormality of the basis states in which the Hamiltonian kernel is formed. In general one first orthonormalises the discrete basis states by Schmidt's procedure and then constructs the Hamiltonian matrix in those basis. But this procedure is somewhat tedious especially when the number of basis states is quite large. We have used here an equivalent but simpler procedure.

Let H^J denote the Hamiltonian kernel for a given J in the basis of discrete non-orthonormal basis.

N^J denotes the overlap kernel for the state J in the same basis. It may be noted that in the case of orthonormal basis, the overlap matrix will be unity. In the non-orthonormal basis the Schrodinger equation can be written as

$$(H^J - \epsilon_J^n N^J) \; C_J^n = 0 \qquad (1)$$

where C_J^n is the column vector denoting the eigenstate of the Hamiltonian in the non-orthonormal basis.

When N^J is unit matrix, the solution of this equation is obtained just by diagonalising the matrix H^J. Otherwise to

get the usual form, we must perform the following transformation. First multiply the equation by $(N^J)^{-\frac{1}{2}}$ from L.H.S. This gives

$$\left[(N^J)^{-\frac{1}{2}} \quad H^J \quad - \quad \epsilon_J^n \quad (N^J)^{\frac{1}{2}} \right] C_j^n = 0$$

We can also write

$$\left[(N^J)^{-\frac{1}{2}} \quad H^J \quad (N^J)^{-\frac{1}{2}} \; (N^J)^{\frac{1}{2}} \quad - \quad {}_J^n \; (N^J)^{\frac{1}{2}} \right] C_j^n = 0$$

Therefore

$$\left[(N^J)^{-\frac{1}{2}} \quad H^J \quad (N^J)^{-\frac{1}{2}} \quad - \quad \epsilon_J^n \right] \quad (N^J)^{\frac{1}{2}} \quad C_J^n \quad = \quad 0 \qquad (2)$$

where $(N^J)^{\frac{1}{2}}$ is defined as

$$(N^J) \quad = \quad (N^J)^{\frac{1}{2}} \quad x \quad (N^J)^{\frac{1}{2}}$$

To find $(N^J)^{\frac{1}{2}}$ we follow the procedure given below. First we diagonalise the overlap matrix N^J. In other words we find the unitary transformation matrix U such that

$$(U \quad N^J \quad U^{-1}) \quad = \quad n^J$$

where n^J is the diagonal matrix

We can also write

$$N^J \quad = \quad (U^{-1} \quad n^J \quad U)$$

Therefore

$$(N^J)^{-\frac{1}{2}} = (U^{-1} \quad (n^J)^{-\frac{1}{2}} \quad U) \tag{3}$$

Substituting for $(N^J)^{-\frac{1}{2}}$ in the expression (2), we get

$$\left[U^{-1} (n^J)^{-\frac{1}{2}} U \; H^J \; U^{-1} \; (n^J)^{-\frac{1}{2}} \; U - \varepsilon_J^n \right] U^{-1} (n^J)^{-\frac{1}{2}} U \; C_J^n = 0$$

Multiplying by U from L.H.S., we get

$$\left[(n^J)^{-\frac{1}{2}} U \; H^J U^{-1} \; (n^J)^{-\frac{1}{2}} U \; U^{-1} - \varepsilon_J^n U \; U^{-1} \right] (n^J)^{-\frac{1}{2}} U \; C_J^n = 0$$

$$\left[(n^J)^{-\frac{1}{2}} U \; H^J U^{-1} \; (n^J)^{-\frac{1}{2}} - \varepsilon_J^n \right] (n^J)^{-\frac{1}{2}} U \; C_J^n = 0$$

Denote $$\mathcal{H}^J = (n^J)^{-\frac{1}{2}} U \; H^J \; U^{-1} \; (n^J)^{-\frac{1}{2}} \tag{4}$$

$$W_n^J = (n^J)^{-\frac{1}{2}} U \; C_J^n \tag{5}$$

Therefore we write

$$(\mathcal{H}^J - \varepsilon_J^n) \; W_J^n = 0 \tag{6}$$

Note that the matrix $\mathcal{H}^J$ is symmetric and Hermitian. Also it may be pointed out that U is the orthogonal matrix and hence

$$U^{-1} = \tilde{U} \quad \text{(transpose)}$$

It may be noted that the quantity $(n^J)^{-\frac{1}{2}}$ will exist, only if the inverse of the matrix (n^J) exists. This means the determinant of the matrix n^J should be non-zero. In other words no eigenvalue of the overlap matrix N^J should be zero. If one of the eigenvalues is zero, the state which is dominant

in the corresponding eigenvector should be omitted. Physically it means that this state does not exist.

Thus we obtained the equation (6) which is of standard form. The Hamiltonian matrix H^J is constructed in the orthonormal basis W_n^J. The diagonalisation of the matrix H^J will give us different W_n^J. In order to get the real mixing of different non-orthonormal basis, we will have to inverse the equation (5) to get

$$C_J^n = U^{-1} (n^J)^{\frac{1}{2}} W_J^n .$$

where C_J^n indicates the real mixing of the non-orthonormal basis states.